Negative microfilm 63–432
received from university

PLUTA, Philip Richard, 1935–
AN ANALYSIS OF NUCLEAR REACTOR FLUCTUATIONS BY METHODS OF STOCHASTIC PROCESSES.

University of Michigan, Ph.D., 1962
Engineering, electrical

University Microfilms, Inc., Ann Arbor, Michigan

AN ANALYSIS OF NUCLEAR REACTOR FLUCTUATIONS BY METHODS OF STOCHASTIC PROCESSES

Philip Richard Pluta

A dissertation submitted in partial fulfillment
of the requirements for the degree of
Doctor of Philosophy in the
University of Michigan
1962

Doctoral Committee:

Professor William Kerr, Chairman
Professor Donald A. Darling
Assistant Professor Geza L. Gyorey
Professor John S. King
Professor Richard K. Osborn

ACKNOWLEDGEMENTS

Equipment was built and reactor fluctuation data was taken at the Phoenix Memorial Laboratory. Norman Barnett lent the tape recorder used to record and analyze the pulse data. The Chrysler Corporation and, specifically, Bruce Van Duesen, allowed the use of their analog computer data reduction facility for the calculation of autocovariance and power spectral density functions. Mr. Van Deusen gave freely of his time and practical experience, which is greatly appreciated. The use of the University's IBM 709 was helpful in the general analysis.

Stimulating discussions with Dr. William Kerr, Dr. Richard Osborn, and Richard Nicholson on theoretical aspects of the problem are appreciated.

The author is grateful for the continuous financial support given by the Atomic Energy Commission and the Ford Foundation, and for the opportunity to teach in the nuclear engineering department.

The assistance of the Industry Program of the College of Engineering in the final preparation and reproduction of the manuscript is acknowledged.

TABLE OF CONTENTS

		Page
ACKNOWLEDGEMENTS		ii
LIST OF TABLES		v
LIST OF FIGURES		vi
LIST OF APPENDICES		viii
ABSTRACT		x
Chapter		
I	INTRODUCTION	1
	A. General Remarks	1
	B. Background	1
II	THEORY	8
	A. Prelude	8
	B. General Time Dependent Moment Equations Using a BF_3 Detector	10
	C. Steady State Moment Equations	20
	D. Transfer Function Approach	23
III	THE EXPERIMENT	30
	A. Condition of the Reactor	30
	B. Core Loading	30
	C. Control Rod Calibration	33
	D. Calibration of the Reactor Oscillator	34
	E. Reactivity Associated With the Equipment	40
	F. Experimental Procedure	41
	G. Experimental Difficulties	42
IV	EQUIPMENT	46
	A. Neutron Detection System	46
	B. Oscillator System	52
V	EXPERIMENTAL RESULTS	64
	A. Moments	64
	B. Autocovariance Function	64
	C. Power Spectral Density Function	64

Page

VI DATA ANALYSIS..... 80

A. Manipulation of Pulse Data..... 80
B. Comparison of Experiment and Theory..... 89

VII CONCLUSIONS..... 108

A. Theory..... 108
B. Experiment..... 110
C. Future Research..... 112

BIBLIOGRAPHY..... 114

APPENDICES..... 117

LIST OF TABLES

Table		Page
III.1	Control Rod Calibration for Loading I.....	35
III.2	Integrated Control Rod Worth for Different Core Loading.....	36
III.3	Calibration of Cadmium Disk-Loading I.....	36
III.4	Cadmium Disk Worth at $\Theta = 180°$ for Different Loadings.....	40
VI.1	6 Delay Group Parameters.....	93
VI.2	2 Delay Group Parameters.....	93
VI.3	Roots of the 6 Group Inhour Equation and Solutions of (2.82), A_k, for Keepin (Upper) and Effective (Lower) Delay Parameters.....	95
VI.4	Roots of the 2 Group Inhour Equation and Solutions of (2.82), for Keepin (Upper) and Effective (Lower) Delay Parameters.....	96
VI.5	Theoretical Autocorrelation Function for Different Delay Times, τ, Using Keepin (Upper) and Effective (Lower) 6 Group Constants with ℓ and k as Parameters.....	98
VI.6	Theoretical Autocorrelation Function for Different Delay Times, τ, Using Keepin (Upper) and Effective (Lower) 2 Group Constants with ℓ and k as Parameters.....	99
VI.7	Corrected Normalized Autocovariance Function as a Function of Delay Time, τ.....	102
VI.8	Measured Power Spectral Density Functions Normalized to 15 c.p.s.	103
VI.9	Theoretical Power Spectral Density Functions Normalized to 15 c.p.s. Using Keepin (Upper) and Effective (Lower) 6 or 2 Group Constants, with ℓ and k as Parameters.....	105

LIST OF FIGURES

Figure		Page
3.1	Core Loading I	31
3.2	Core Loading II	31
3.3	Core Loading III	32
3.4	Core Loading IV	32
3.5	Core Loading V	32
3.6	Control Rod Differential Worth, Loading I	37
3.7	Integrated Control Rod Worth, Loading I	38
3.8	Worth of Cadmium Disk Compared to Sinusoid Normalized at $\theta = 123°$	39
3.9	Discriminator Traverse for BF_3 Detector, Loading I	45
4.1A	Neutron Detection-Conversion Block Diagram	47
4.1B	Oscillator System Block Diagram	48
4.2	Preamplifier - A	49
4.3	Filter - H. V. Decoupler	51
4.4	Oscillator Mount	53
4.5	Reactor Grade Graphite Fillers	54
4.6	Oscillator Container	55
4.7	Oscillator Container Handling Piece and Seal	56
4.8	Phototube - Schmidt Trigger	61
5.1	Ratio of the Variance to the Mean vs. Gate Time, Loading I - Noise	65
5.2	Ratio of the Variance to the Mean vs. Gate Time, Loading I - 1/2 c/s	66
5.3	Ratio of the Variance to the Mean vs. Gate Time, Loading I - 10 c/s	67

Figure		Page
5.4	Ratio of the Variance to the Mean vs. Gate Time, Loading IV - Noise.....	68
5.5	Ratio of the Variance to the Mean vs. Gate Time, Loading V - Noise.....	69
5.6	Autocovariance Function, Loading I - Noise.....	70
5.7	Autocovariance Function, Loading I - 10 c/s.....	71
5.8	Autocovariance Function, Loading V - Noise.....	72
5.9	Autocovariance Function, Loading BF_3 - 1.....	73
5.10	Power Spectral Density Function, Loading I - Noise.....	74
5.11	Power Spectral Density Function, Loading I - 1/2 c/s.....	75
5.12	Power Spectral Density Function, Loading I - 1/2 c/s.....	76
5.13	Power Spectral Density Function, Loading I - 10 c/s.....	77
5.14	Power Spectral Density Function, Loading V - Noise.....	78
5.15	Power Spectral Density Function, Loading BF_3 - 1.....	79
6.1	Block Diagram for Conversion of Pulse Data to a Frequency Modulated Recorded Signal.....	82
6.2	Signal Demodulation.....	84
6.3	Measured and Theoretical Autocorrelation Functions.....	101
6.4	Measured and Theoretical Power Spectral Density Functions	106
A.1	Explanation of Disk Notation and Geometry.....	118
A.2	Shape of Exposed Surface.....	120
D.1	Data Reduction Schematic.....	125

LIST OF APPENDICES

Appendix		Page
A.	A Surface Whose Partially Exposed Area Varies Sinusoidally With Angular Frequency and Application.....	118
B.	Neutron - Neutron and Reactivity - Neutron Transfer Functions.....	121
C.	Flux Harmonics Due to Small Sinusoidal Changes in Reactivity.....	123
D.	The Effect of a Sinusoidal Function, Superimposed on the Fluctuation Data from the Reactor, on the Calculated Ratio of the Variance to Mean Number of Detections as a Function of Detection Time.....	125
E.	A Derivation of the Relationship Between the Ratio of the Variance to the Mean of the Detections as a Function of Counting Time and Autocovariance Function.....	129
F.	Reduced Pulse Data.....	131
G.	Digital Computer Programs.....	141
	1. VAROMEAN - WESTERVELT Computes the ratio of the variance to mean for a given gate length.....	142
	2. ROOT 6 Computes the 7 roots of the 6 delay group inhour equation.....	143
	3. ROOT 2 Computes the 3 roots of the 2 delay group inhour equation.....	145
	4. CORR 6 Computes the 6 group autocorrelation function, given the roots of the inhour equations.....	146
	5. TWO GROUP Computes the effective 2 group delay constants from 6 group data using the method of Skinner and Cohen..	151
	6. TWO GROUP COEFFICIENTS Computes the coefficients needed to calculate the 2 group autocorrelation function.....	152

Page

7. CORRELATION 7
Computes the 2 group autocorrelation function given the roots of the 2 group inhour equation and the results of program 6..... 154

8. TRANSFER 6
Computes the 6 group transfer function in d.b., phase angle and power spectral density for a white noise input..... 155

ABSTRACT

Although the average neutron density in a nuclear reactor operating at steady state does not change with time, the instantaneous neutron density fluctuates about the average value. This study investigates the fluctuations in a steady state subcritical reactor.

Goals of the investigation were,

1. A theoretical description of the fluctuations, which could be related directly to an experiment.
2. Experimental validation of the theoretical model.
3. Experimental determination of the effect of an external reactivity perturbation on the measured fluctuation data.
4. Experimental study of the dependence of the fluctuations on the relative position of the neutron detector to the maximum neutron density in the reactor.

The results of this study can be classified broadly in terms of the above goals.

1. Using a model of the reactor which ignores spatial effects, a time dependent description of the variance and of the mean of the neutrons detected by a pulse type BF_3 chamber, as a function of the detection time, is developed. A detailed probability balance making use of probability generating functions is employed. The time dependent results are specialized to the steady state, to obtain an expression for the ratio of the variance to the mean number of detections, as a function of the detection time. A relationship

between the ratio of the variance to the mean number of counts as a function of counting time, and the autocovariance function associated with the detected neutrons is derived. Expressions relating the power spectral density function and the autocovariance function are used to derive the expression for the ratio of the variance to mean number of detected neutrons, by assuming that the reactor is driven by white noise and that the reactor transfer function is known. This latter expression contains less information about the reactor fluctuations, but describes steady state behavior adequately.

2. The neutron fluctuations in the Ford reactor were recorded on magnetic tape, using a BF_3 pulse detection system, for k = 0.997 at steady state. From the basic pulse data, three quantities, described below, were computed.

   a. The ratio of the variance to the mean number of counts or detections as a function of counting times from 0.001 to 9.999 seconds was calculated.

   b. The pulse data was converted to an "equivalent" continuous signal proportional to the detection rate. This was accomplished by measuring the inverse time between pulses and recording a proportional voltage. The exponentially weighted autocovariance function of this rate was determined for delay times from 0.0 to 0.33 seconds, using an analog computer. Time compensation and frequency modulation were employed to improve accuracy.

   c. An exponentially weighted power spectral density function was determined from the continuous signal using the analog computer, from 5 to 60 cycles per second.

3. An external reactivity perturbation of approximately 10^{-4} sin (ωt) was introduced with frequencies of 0.5, 1.0, 10 and 30 cycles per second. The presence of this perturbation did not change the observed values of the quantities described in 2.

4. The position of the BF_3 detector relative to the perturber and the fissionable core material was varied. In all observed instances, the position of the detector had no appreciable effect on the quantities listed in 2.

CHAPTER I

INTRODUCTION

A. General Remarks

The behavior of a nuclear reactor can be characterized by the average distribution of the neutron density as a function of neutron velocity, position, and time. The statistical behavior of the neutron distribution may be characterized by its mean and variance, autocorrelation function, power spectral density function, or other appropriate quantity. An analysis of fluctuations in neutron density is of interest because of the great amount of information about a nuclear reactor which can be obtained. For example, within the limitations of the model used to analyze fluctuation data, one can determine,

1. the transfer function of the reactor
2. the prompt neutron lifetime
3. the number of prompt neutrons per fission
4. the 6 delay group parameters
5. the multiplication constant
6. the worth of control rods
7. stability criteria in a power reactor
8. operating power level of a reactor.

This partial list illustrates possible applications of fluctuation analysis which can result in useful information about a reactor system.

B. Background

A variety of approaches have been made in the past to the theoretical problem of describing fluctuations in neutron density. At

least, five different methods have been used to develop a theoretical expression for the ratio of the variance to the mean number of detected neutrons as a function of detection time. The central idea behind each of these methods can be summarized as follows:

1. physical approach employing conditional probabilities
2. detailed probability balance employing probability generating functions
3. random variates
4. application of the Rice formulation of fluctuations in electric circuits to a reactor
5. assumption of a transfer function and an input power spectral density function

The original development of the physical approach was carried out by Feynman, de Hoffman and Serber[1]. The probability balance concept was first applied to fluctuations in a reactor by Courant and Wallace[2]. More recently, Larisse and Braffort[3] used random variates to obtain the results of Courant and Wallace. Bennett[4] applied the Rice formulation to the analysis of reactor fluctuations. Moore[6,7] developed the transfer function approach. Albrecht[5] applied the transfer function approach to arrive at an expression for the ratio of the variance to mean similar to that of Bennett.

Methods 1, 4 and 5 have been restricted to an analysis of reactors operating at steady state. A notable exception is Velez[8,9], whose adaption of method 1 allowed the calculation of a time dependent autocorrelation function. Velez[9] describes, in an annotated bibliography, the works of Brownrigg and Littler[10], Frisch and Littler[11], and Feiner, Frost and Hurwitz[12], which have received little attention but are important contributions to this area of research. Pál[13,14] is the only author who

has not represented the reactor by a point model. The complexity of Pál's representation is such that an application to a practical system is unlikely. Harris[15] has made a valuable contribution to the analysis of power reactor fluctuations. Both Pál and Harris employ the technique of method 2. The treatment of Cohn[16] is novel, but inadequate for further generalization.

It is felt by the author that the method of a detailed probability balance is the most powerful for analyzing fluctuations in a nuclear reactor. The description of the fluctuations in the neutron density is in terms of a probability distribution function. By appropriate manipulation of this function, the mean value and the mean square value of the neutron density can be found. Since the mean square value is related directly to the variance and the mean value of the neutron density, one can determine both the mean value and the variance of the neutron density from the distribution function. The mean value and the mean square value of the neutron density can be described by the first and second neutron moments of the probability distribution function, respectively.

By comparing fluctuation data with the theoretical prediction of the point model, a number of reactor parameters have been deduced in the literature. The ratio of the delay fraction to the prompt neutron lifetime has been determined from spectra[17] and moment data[18]. From power spectral density data, the transfer function is determined under the assumption of a white noise input[19,20]. Cross correlation techniques[21] have been used to determine the transfer function. Recently, an autocorrelation function was measured[22] and the transfer function obtained by Fourier transformation. Knowing the prompt lifetime from an independent

measurement, the effective delay fraction[23] was determined from spectra. Using a non-linear regression analysis, two delay group parameters were estimated from moment data[5]. Additional experimental work is presently being conducted at several laboratories to refine and extend these preliminary measurements.

C. Scope of Research

In the present work, the basic methods[2,15] of a detailed probability balance are applied to a zero power reactor monitored by a pulse type BF_3 chamber. With the exception of the term in the detailed balance equation describing the detection of neutrons, the balance equation is not new[15]. However, the specialization of the resulting system of time dependent equations to the conditions under which the author performed a fluctuation experiment does give an important new relation for the ratio of the variance to mean number of detected neutrons as a function of detection time. The ratio of the variance to mean is also derived using the transfer function[5] approach. The treatment is considered more rigorous than previous work and, as such, is a new contribution. A new relation between the ratio of the variance to mean and the autocovariance function is derived.

The Ford reactor from which fluctuation data was obtained in this study, is an enriched, water moderated, graphite reflected system. The physical dimensions of the reactor are approximately 10 migration lengths for fast neutrons and, as a result, the reactor is highly coupled. It is expected that normalized fluctuation data does not exhibit a high degree of space dependence, in a highly coupled system. No experiment

has been done to verify this expectation. Also, it is expected that fluctuation data will not depend appreciably on neutron energy, but only on neutron density, since the macroscopic absorption cross section of the detector is inversely proportional to neutron speed. No experiment has been done to verify this expectation. Thus, the model chosen to study fluctuations in neutron density ignores the complicating factors of spatial and energy dependence. The validity of the model can be tested by comparing experimental results with the model's prediction.

Fluctuation data was recorded from the Ford reactor, while operating at a power level of less than 1/1000 of a watt, for k = 0.997. A pulse type BF_3 detector was used. It was convenient to obtain the data in pulse form, in order to compute the ratio of the variance to mean number of detected neutrons as a function of detection time. A BF_3 chamber was used rather than a fission chamber, because of its higher detection efficiency. It was necessary to operate at a low power level to minimize dead time losses in the BF_3 chamber. The detector was near the fuel region of the reactor to increase the detection efficiency. The efficiency is defined as the ratio of the detection rate to the fission rate in the reactor.

A reactivity oscillator was constructed and used to make perturbations of $10^{-4} \sin(\omega t)$, about the mean multiplication constant of 0.997. The purpose of the oscillator was to

1. study spatial effects due to the relative positions of the detector, perturber and region of maximum neutron density in the fuel region
2. examine any observable non-linearities

3. infer the effective input power spectral density function by treating the reactor as a linear system and separately studying the fluctuation data with and without the perturbation.

The fluctuation data consisted of the neutron induced pulses from the BF_3 chamber. The position of the chamber relative to the region of maximum neutron density in the fuel region was a parameter. The data was recorded on magnetic tape, as it was obtained. Subsequently, the data was used to compute the following three quantities:

1. The ratio of the variance to the mean number of detected neutrons as a function of detection times from 0.001 to 9.999 seconds.
2. An exponentially weighted autocovariance function for delay times from 0.0 to 0.33 seconds.
3. An exponentially weighted power spectral density function from 5 to 60 cycles per second.

The experimental contributions of this study include,

1. the first fluctuation experiment, from which moments, autocovariance and power spectral density functions are determined from the same data record
2. the first measurement of an exponentially weighted autocovariance and power spectral density function of a nuclear reactor while considerably subcritical and/or a power level less than 1/1000 of a watt
3. the observation that, for the positions of the detector used, space effects were not appreciable
4. two unexpected peaks in the moment data at approximately 0.3 and 3.0 seconds.

5. that for the magnitude of the perturbation introduced, and the frequencies considered, the effect of the perturbation was not observable in either the moment, autocovariance or power spectral density function representations of the fluctuation data.
6. that the prompt neutron lifetime of the Ford Nuclear Reactor is 130 $\pm$20 microseconds

CHAPTER II

THEORY

A. Prelude

There are three quantities, well established in statistical analysis, which can be determined from a record of the fluctuation in neutron density in a nuclear reactor. Specifically,

1. The mean value and the variance of the discrete data for a given detection time are readily computed. Since the neutrons are detected as discrete pulses in the monitoring equipment, the number of detections depends on the length of time the detection process is "observed," or the gate length.
2. The autocovariance function, i.e. the unnormalized autocorrelation function, is a measure of the correlation of the fluctuation with itself. It is a quantity which shows the effect of past reactor operating history on the present.
3. The power spectral density function is a measure of the relative importance of the frequencies making up the gross behavior of the fluctuations.

The above descriptions indicate the kind of information which can be computed from fluctuation data. Hereafter, the above quantities will be called observables.

A theory describing the observables is essential for interpretation, and to gain insight for new applications of fluctuation information to improve the operation and understanding of nuclear reactors.

This chapter is devoted to the development of mathematical descriptions of fluctuations. First, a description of the ratio of the variance to the mean number of detected neutrons as a function of gate length is developed using the method of a detailed probability balance.[2] This approach[2] is chosen because the author believes it to be fundamental. The application of this technique to include detected neutrons, as well as all the other neutrons in the reactor, was first accomplished by Harris[15]. In considering a general biological life-death process, Kendall[24] had shown that a quantity related to the net number of either living or dead units, as a function of the life span of the system comprised of all the units, could be manipulated using probability generating functions. The quantity Kendall treated is cumulative, that is, the quantity is changing with time, even when the biological system is in a steady state condition. The application of this concept to a nuclear reactor system, where the cumulative quantity is the number of detected neutrons as a function of gate length or detection time, was straightforward. Harris considered a power reactor with a fission chamber monitoring the fluctuations in neutron density. Harris' concern was with the fluctuations in the reactor power level, at high power levels.

In section B of this chapter, the method of a detailed probability balance[2,15] is applied to a zero power reactor monitored by a pulse type BF_3 chamber. With the exception of the term describing the detection of neutrons, the detailed probability balance is not new[15]. However, the specialization of the resulting system of time dependent differential equations to the conditions under which the author performed a fluctuation

experiment does give an important new relation for the ratio of the variance to the mean number of detected neutrons as a function of detection time. A complete description of the experiment is given in Chapter III.

In Section D of the present chapter, the ratio of the variance to the mean number of detected neutrons as a function of gate length is derived using the transfer function approach[5]. The treatment given in Section D is considered more rigorous than previous work and, as such, is a new contribution. The remainder of the section explicitly describes the autocovariance function, the power spectral density function and their relationship to the ratio of the variance to the mean. Another new result presented in this chapter is the derivation of a relation between the ratio of the variance to the mean number of neutrons as a function of detection time and the autocovariance function.

B. General Time Dependent Moment Equations Using a BF_3 Detector

In this section, an analysis of the fluctuation of the neutron population in a nuclear reactor is developed using a fundamental probability balance. Since the development depends on a careful definition of all the quantities required in making the detailed probability balance, and, later, the manipulation of this balance, the required definitions will be given at the outset. For reasons described above, a point reactor model with one neutron energy is employed. Let,

$$P(N, C_1, \cdots C_J, Z; t) \equiv \tag{2.1}$$

the probability that there are N neutrons, C_1 precursor atoms with decay constant $\lambda_1, \cdots$, and C_J precursor atoms with decay constant λ_J in the

reactor at time t, and that there are Z neutrons detected in the interval between t = 0 and t. Equation (2.1) describes the ensemble distribution of neutrons, precursor atoms and detected neutrons, as a function of time. For a reactor operating in steady state, ensemble and time averages are identical. Let,

$$p(n, m_1, \ldots m_J) \equiv \tag{2.2}$$

the probability that n prompt neutrons, m_1 percursor atoms with decay constant $\lambda_1, \cdots$, and m_J precursor atoms with decay constant λ_J are produced by a single fission event.

Define a probability generating function,

$$F(x, y_1, \ldots y_J, \zeta; t) \equiv \sum_{N=0}^{\infty} \sum_{C_1=0}^{\infty} \cdots \sum_{C_J=0}^{\infty} \sum_{Z=0}^{\infty} x^N y_1^{C_1} \ldots y_J^{C_J} \zeta^Z P(N, C_i, Z; t) \tag{2.3}$$

where x, y_i and ζ are continuous variables. Define another probability generating function,

$$f(x, y_1, \ldots y_J) \equiv \sum_{n=0}^{\infty} \sum_{m_1=0}^{\infty} \cdots \sum_{m_J=0}^{\infty} x^n y_1^{m_1} \cdots y_J^{m_J} p(n, m_i) \tag{2.4}$$

Define,

$$\Lambda_f N \delta t \equiv \tag{2.5}$$

the probability that a fission event occurs in the reactor containing N neutrons in the small time increment δt. Let,

$$\Lambda_c N \delta t \equiv \tag{2.6}$$

the probability that a neutron be lost from the system either by leakage or non-fission capture during δt, excluding detections. Let,

$$\Lambda_d N \delta t \equiv \tag{2.7}$$

the probability that a neutron be detected by the detector during δt.

Let,

$$S\,\delta t \equiv \tag{2.8}$$

the probability that a neutron enters the reactor as the result of some non-fission source during δt.

The following fundamental parameters may be expressed in terms of the functions previously defined. The arguments of (2.1) and (2.2), as well as the summation notation, will be contracted for convenience. Define the average number of prompt neutrons produced per fission to be,

$$\bar{\nu}_o \equiv \sum_{n,\bar{m}_i=0}^{\infty} n\ p \tag{2.9}$$

Let the average number of precursor atoms of type i produced per fission be,

$$\bar{\nu}_i \equiv \sum_{n,\bar{m}_i=0}^{\infty} m_i\ p \tag{2.10}$$

Let the difference between the average value of the square of the number of prompt neutrons produced per fission and $\bar{\nu}_o$ be,

$$\bar{\nu}_{oo} \equiv \sum_{n,\bar{m}_i=0}^{\infty} n(n-1)\ p \tag{2.11}$$

Let the average value of the product of the number of prompt neutrons and the number of percursor atoms of type i per fission be,

$$\bar{\nu}_{oi} \equiv \sum_{n,\bar{m}_i=0}^{\infty} n\ m_i\ p \tag{2.12}$$

Let the average value of the product of the number of precursor atoms of types i and j per fission be,

$$\bar{\nu}_{ij} \equiv \sum_{n,\bar{m}_i=0}^{\infty} m_i m_j\ p \tag{2.13}$$

Let the average number of neutrons in the reactor at time t be,

$$\bar{N}(t) \equiv \sum_{N,C_i,Z=0}^{\infty} N\ P \tag{2.14}$$

Let the variance in the number of neutrons in the reactor at time t, minus $\bar{N}(t)$, be,

$$\bar{\mu}_{NN}(t) \equiv \sum_{N,C_i,Z}^{\infty} (N - \bar{N})^2\ P - \bar{N} \tag{2.15}$$

Let the covariance between the number of neutrons and the number of precursor atoms of type i in the reactor at time t be,

$$\bar{\mu}_{NC_i}(t) \equiv \sum_{N,C_i,Z}^{\infty} (N - \bar{N})(C_i - \bar{C}_i)\ P \tag{2.16}$$

Let the covariance between the number of neutrons and the number of neutrons detected in the interval from t = 0 to t be,

$$\bar{\mu}_{NZ}(t) \equiv \sum_{N,C_i,Z}^{\infty} (N - \bar{N})(Z - \bar{Z})\ P \tag{2.17}$$

Let the variance in the number of neutrons detected in the time interval t, minus the average number of neutrons detected in the interval t, be,

$$\bar{\mu}_{ZZ}(t) \equiv \sum_{N,C_i,Z}^{\infty} (Z - \bar{Z})^2\ P - \bar{Z} \tag{2.18}$$

Let the covariance between the number of neutrons detected in the time interval t and the number of precursor atoms of type i at time t be,

$$\bar{\mu}_{ZC_i}(t) \equiv \sum_{N,C_i,Z}^{\infty} (Z - \bar{Z})(C_i - \bar{C}_i)\ P \tag{2.19}$$

Lastly, let the covariance between the number of precursor atoms of type i and type j in the reactor at time t be,

$$\bar{\mu}_{C_iC_j}(t) \equiv \sum_{N,C_i,Z}^{\infty} (C_i - \bar{C}_i)(C_j - \bar{C}_j)\ P \tag{2.20}$$

A detailed probability balance can be written for the probability that there are N neutrons and C_i precursor atoms in the reactor and Z neutrons have been detected in the time interval from t = 0 to t + δt. The balance is written by assuming probabilities, in terms of N, C_i and Z at t, and during δt, which combine to give the desired probability at t + δt. The balance equation describes possible changes in N, C_i and Z. The terms on the right hand side of the balance relation given below, (2.21), represent the effect of

1. an external source
2. decay of a precursor atom of the I^{th} type
3. loss by leakage or non-fission capture
4. fission
5. detection
6. nothing happening during δt

$$
\begin{aligned}
P(N,C_i,Z;\ t+\delta t) &= P(N-1,\ C_i,Z;\ t)\ S\ \delta t \\
&+ \sum_I P(N-1,C_1,\ \ldots,\ C_I+1,\ \ldots,\ C_J,Z;\ t)(C_I+1)\ \lambda_I\ \delta t \\
&+ P(N+1,\ C_i,Z;\ t)(N+1)\ \Lambda_c\ \delta t \\
&+ \sum_{n,m_i}^{\infty} P(N-n+1,\ C_i-m_i,\ Z;\ t)(N-n+1)\Lambda_f\ p(n,m_i)\delta t \qquad (2.21) \\
&+ P(N+1,\ C_i,\ Z-1;\ t)(N+1)\ \Lambda_d\ \delta t \\
&+ P(N,C_i,Z;\ t)\ [1-\{S+\sum_i \lambda_i\ C_i + N(\Lambda_c+\Lambda_f+\Lambda_d)\}\ \delta t]
\end{aligned}
$$

For later development, it is convenient to manipulate (2.21) into a more tractable form. Define a detection efficiency, $\epsilon \equiv \Lambda_d/\Lambda_f$, and substitute into (2.21). Multiply (2.21) by

$$x^N y_1^{C_1} \cdots y_J^{C_J} \zeta^Z$$

and sum over all values of N, C_i and Z. This operation converts (2.21) from an equation in P to an equation in F and f, (2.3) and (2.4). Subtract F from both sides, divide by δt and let $\delta t \longrightarrow 0$ giving,

$$\frac{\partial F}{\partial t} = (x - 1)\, SF + \sum_i (x - y_i)\, \lambda_i \frac{\partial F}{\partial y_i}$$

$$+ [\Lambda_c(1 - x) + \Lambda_f(f - x) + \epsilon\, \Lambda_f(\zeta - x)] \frac{\partial F}{\partial x} \qquad (2.22)$$

Equation (2.22) is a time dependent partial differential equation for the probability generating function, from which information about the fluctuation in neutron population can be obtained.

The procedure used to extract the information about fluctuations from (2.22), in a useful form, will be considered in detail. It is helpful to define a unit point at $x = y_1 = \cdots = y_J = \zeta = 1.0$. It is convenient to simplify the notation for partial differentiation. Let each subscript after a subscripted comma denote partial differentiation with respect to that subscript. For example,

$$F_{,xy_i\zeta} = \frac{\partial^3 F}{\partial x \partial y_i \partial \zeta} .$$

The evaluation of a function at the unit point is denoted as $F_{,x}\big|_1$. This means evaluate the partial derivative of F at $x = y_i = \zeta = 1.0$. Proceeding

with the manipulation of (2.22), take $\frac{\partial}{\partial x}$ of (2.22) and evaluate the resulting expression at the unit point. By inspection of (2.3), (2.9) and (2.10), confirm that

$$F_{,x}\Big|_1 = \bar{N};\ F_{,y_i}\Big|_1 = \bar{C}_i;\ f_{,x}\Big|_1 = \bar{\nu}_o;\ f_{,y_i}\Big|_1 = \bar{\nu}_i \qquad (2\ 23)$$

Using (2.23) in the evaluation of $\frac{\partial}{\partial x}$ of (2.22) at the unit point obtain,

$$\bar{N}_{,t} = [\Lambda_f(\bar{\nu}_o - 1 - \epsilon) - \Lambda_c]\bar{N} + \sum_i \lambda_i \bar{C}_i + S \qquad (2.24)$$

Equation (2.24) can be shown to be identical to the conventional point kinetic equation describing the rate of change of the average neutron population[25,26,27] as follows. Define the prompt lifetime, ℓ, in terms of the present model,

$$\ell \equiv \frac{1}{\Lambda_f + \Lambda_c} = \frac{1}{v[\Sigma_f + \Sigma_c]} \qquad (2.25)$$

where v is the speed of the neutrons and the Σ_f and Σ_c are conventional macroscopic cross sections. The conventional β_i, defined as the fraction of the neutrons per fission emitted by precursor atoms of type i, and $\bar{\nu}$, defined as the total number of neutrons produced per fission, are needed to make the comparison of results. The conventional point kinetic equation for neutrons can be written,

$$\bar{N}_{,t} = \frac{k(1 - \beta) - 1}{\ell}\bar{N} + \sum_i \lambda_i \bar{C}_i + S \qquad (2.26)$$

The term $k(1 - \beta)$ is the ratio of the production rate of prompt neutrons to the rate of absorption and leakage, that is,

$$k(1 - \beta) = \bar{\nu}_o\, \Lambda_f/(\Lambda_f + \Lambda_c) \qquad (2.27)$$

Substituting for $k(1 - \beta)$ and ℓ, (2.26) becomes identical with (2.24), when the detection term in (2.24) is included in Λ_c.

Proceeding with the manipulation of (2.22), take $\frac{\partial}{\partial y_i}$ of (2.22) and evaluate the result at the unit point, obtaining,

$$\bar{C}_{i,t} = \Lambda_f \bar{\nu}_i \bar{N} - \lambda_i \bar{C}_i \tag{2.28}$$

Using the above definitions for β_i, k and ℓ, (2.28) can be cast in the form of the usual point precursor equation by making the observation that

$$k = \frac{\nu_o \Lambda_f}{(1 - \beta)(\Lambda_f + \Lambda_c)} \tag{2.29}$$

and,

$$\bar{\nu}_i = \frac{\bar{\nu}_o \beta_i}{1-\beta} \tag{2.30}$$

To determine the average detection rate, take $\frac{\partial}{\partial \mathcal{Z}}$ of (2.22) and evaluate the result at the unit point, obtaining,

$$\bar{Z}_{,t} = \epsilon \Lambda_f \bar{N} \tag{2.31}$$

When the reactor is operating at steady state, i.e. $\bar{N}$ is constant, the average detection rate is constant.

By taking single partial derivatives of (2.22) and evaluating the result at the unit point, we have determined the rate of change of the average number of neutrons, precursor atoms and detected neutrons. By taking two derivatives, it is shown below that we can determine the statistical behavior of the system in terms of its second moments, or alternatively, its variances and covariances, (2.9) to (2.20). For example, $\bar{\mu}_{NN}(t)$, (2.15), can be determined by taking $\frac{\partial^2}{\partial x^2}$ of (2.22) which gives,

$$F_{,txx} = 2SF_{,x} + (x - 1)\, SF_{,xx} + \sum_i \lambda_i [2F_{,y_i x} + (x - y_i)\, F_{,yxx}] \quad (2.32)$$

$$+ \Lambda_c[-2F_{,xx} + (1 - x)F_{,xxx}] + \Lambda_f\, [f_{,xx}F_{,x} + 2(f_{,x} - 1)F_{,xx}$$

$$+ (f - x)F_{,xxx}] + \epsilon\Lambda_f[-2F_{,xx} + (\mathcal{Y} - x)\, F_{,xxx}]$$

evaluating (2.32) at the unit point, realizing that

$$F_{,y_i x}\Big|_1 = \overline{NC}_i \; ; \; F_{,xx}\Big|_1 = \overline{N^2} - \bar{N}; \; f_{,xx}\Big|_1 = \bar{\nu}_{oo} \quad (2.33)$$

gives,

$$F_{,txx}\Big|_1 = 2S\bar{N} + 2\sum_i \lambda_i\, \overline{NC}_i - 2\Lambda_f(\overline{N^2} - \bar{N}) \quad (2.34)$$

$$+ \Lambda_f[\bar{\nu}_{oo}\bar{N} + 2(\bar{\nu}_o - 1)(\overline{N^2} - \bar{N})] - 2\epsilon\Lambda_f(\overline{N^2} - \bar{N})$$

Also,

$$F_{,txx}\Big|_1 = (\overline{N^2} - \bar{N})_{,t} = \overline{N^2}_{,t} - \bar{N}_{,t} \quad (2.35)$$

But from (2.15)

$$\bar{\mu}_{NN,t} = \overline{N^2}_{,t} - 2\bar{N}\, \bar{N}_{,t} - \bar{N}_{,t} \quad (2.36)$$

Substituting for S in (2.34) from (2.24), and utilizing (2.36), (2.15) and (2.16) gives,

$$\bar{\mu}_{NN,t} = 2\bar{\mu}_{NN}\, [\Lambda_f(\bar{\nu}_o - 1 - \epsilon) - \Lambda_c]$$

$$+ \bar{N}\, \Lambda_f\bar{\nu}_{oo} + 2\sum_i \lambda_i\, \bar{\mu}_{NC_i} \quad (2.37)$$

The modified variance in the number of detected neutrons can be determined by taking $\frac{\partial^2}{\partial \mathcal{Y}^2}$ of (2.22), evaluating at the unit point and substituting from (2.18) and (2.31),

$$\bar{\mu}_{ZZ,t} = 2\epsilon\, \Lambda_f\, \bar{\mu}_{NZ} \quad (2.38)$$

It should be noted that (2.31) and (2.38) represent observables since they refer to detected neutron statistics.

Taking $\frac{\partial^2}{\partial x \partial z}$ of (2.22), evaluating at the unit point and substituting from (2.24), (2.16), and (2.17) and (2.31) gives,

$$\bar{\mu}_{NZ,t} = \bar{\mu}_{NZ}[\Lambda_f(\bar{\nu}_o - 1 - \epsilon) - \Lambda_c] + \bar{\mu}_{NN}\,\epsilon\,\Lambda_f + \bar{N}\,\epsilon\,\Lambda_f + \sum_i \lambda_i\,\bar{\mu}_{ZC_i} \tag{2.39}$$

Taking $\frac{\partial^2}{\partial z \partial y_i}$ of (2.22), evaluating at the unit point and substituting from (2.10), (2.28) and (2.31) gives,

$$\bar{\mu}_{ZC_i,t} = -\bar{\mu}_{ZC_i}\,\lambda_i + \bar{\mu}_{NZ}\Lambda_f\bar{\nu}_i + \bar{\mu}_{NC_i}\,\epsilon\,\Lambda_f + \bar{N}\,\epsilon\,\Lambda_f\bar{\nu}_i \tag{2.40}$$

Taking $\frac{\partial^2}{\partial x \partial y_i}$ of (2.22) evaluating at the unit point and substituting from (2.12), (2.15), (2.16), (2.20), (2.24) and (2.28) gives,

$$\bar{\mu}_{NC_i,t} = \bar{\mu}_{NC_i}[\Lambda_f(\bar{\nu}_o - 1 - \epsilon) - \Lambda_c - \lambda_i] + \bar{\mu}_{NN}\,\Lambda_f\bar{\nu}_i + \bar{N}\,\Lambda_f\bar{\nu}_{oi} + \sum_j \lambda_j\,\mu_{C_iC_j} \tag{2.41}$$

Lastly, taking $\frac{\partial^2}{\partial y_i \partial y_j}$ of (2.22) and reducing, obtain,

$$\bar{\mu}_{C_iC_j,t} = \bar{\mu}_{C_iC_j}[-\lambda_i - \lambda_j] + \bar{\mu}_{NC_i}\,\Lambda_f\bar{\nu}_j + \bar{\mu}_{NC_j}\,\Lambda_f\bar{\nu}_i + \bar{N}\,\bar{\nu}_{ij}\,\Lambda_f \tag{2.42}$$

For the usual six group representation of the reactor, (2.24), (2.28), (2.31), (2.37), (2.38), (2.39), (2.40), (2.41) and (2.42) are a set of 44 simultaneous first order differential equations.

In addition to describing the average behavior of the reactor system, these equations predict the variation about the averages, in terms of the variances defined by (2.15) through (2.20).

C. Steady State Moment Equations

When reactivity and the average value of the external source are constant,

$$\bar{N}_{,t} = \bar{C}_{i,t} = \bar{\mu}_{NC_i,t} = \bar{\mu}_{NN,t} = \bar{\mu}_{C_iC_j,t} = 0$$

Since

$$\bar{Z}_{,t},\ \bar{\mu}_{ZZ,t},\ \bar{\mu}_{ZC_i,t} \quad \text{and} \quad \bar{\mu}_{NZ,t}$$

describe a cumulative distribution, they are not zero, in general, unless $\bar{Z} = 0$, which is true only at $t = 0$. For example, the average number of detected neutrons increases linearly with time, since the average detection rate is constant when $\bar{N}_{,t} = 0$.

The constant values of $\bar{N}$, $\bar{C}_i$, $\bar{\mu}_{NN}$, $\bar{\mu}_{NC_i}$ and $\bar{\mu}_{C_iC_j}$ can be determined by solving the appropriate equations. For example, from (2.24), (2.25), (2.27) and (2.28),

$$\bar{N} = \frac{S\ell}{1 - k} \tag{2.43}$$

From (2.37), (2.41) and (2.42) obtain,

$$\bar{\mu}_{NN} = \frac{\bar{N}\,\Lambda_f\bar{\nu}_{oo} + 2\sum_i \lambda_i\,\bar{\mu}_{NC_i}}{2[\Lambda_c - \Lambda_f(\bar{\nu}_o - 1 - \epsilon)]} \tag{2.44}$$

$$\bar{\mu}_{NC_i} = \frac{\bar{\mu}_{NN}\Lambda_f\bar{\nu}_i + \bar{N}\Lambda_f\bar{\nu}_{oi} + \sum_i \lambda_i\,\bar{\mu}_{C_iC_j}}{\Lambda_c + \lambda_i - \Lambda_f(\bar{\nu}_o - 1 - \epsilon)} \tag{2.45}$$

and

$$\bar{\mu}_{C_iC_j} = \frac{\bar{\mu}_{NC_i}\,\Lambda_f\bar{\nu}_j + \bar{\mu}_{NC_j}\,\Lambda_f\bar{\nu}_i + \overline{N\nu}_{ij}\Lambda_f}{\lambda_i + \lambda_j} \tag{2.46}$$

The system of (2.44), (2.45) and (2.46) represents 28 equations in 28 unknowns, if a 6 delay group representation is used. The ratio of the variance to mean number of detected neutrons as a function of detection time is, by definition, $\frac{\bar{\mu}_{zz}}{\bar{z}} + 1$.

This ratio can be determined by solving the set of differential equations expressing $\bar{\mu}_{zz,t}$, $\bar{\mu}_{Nz,t}$ and $\bar{\mu}_{zc_i,t}$ for $\bar{\mu}_{zz}$, and dividing by $\bar{z}$. The solution for $\bar{\mu}_{zz}$ is simplified by using the LaPlace transform. Define the LaPlace transform, $\mathcal{L}\{f(t)\} = \bar{\bar{f}}(p)$. Take the LaPlace transform of (2.38), (2.39) and (2.40), to obtain,

$$\bar{\bar{\mu}}_{ZZ}\,p = 2\,\epsilon\,\Lambda_f\,\bar{\bar{\mu}}_{NZ} \tag{2.47}$$

$$\bar{\bar{\mu}}_{NZ}\left\{p - \Lambda_f(\bar{\nu}_o - 1 - \epsilon) + \Lambda_c\right\} = \frac{1}{p}\left\{\bar{\mu}_{NN}\,\epsilon\,\Lambda_f + \bar{N}\,\epsilon\,\Lambda_f\right\} + \sum_i \lambda_i\,\bar{\bar{\mu}}_{ZC_i} \tag{2.48}$$

$$\bar{\bar{\mu}}_{ZC_i}(p + \lambda_i) = \bar{\bar{\mu}}_{NZ}\,\Lambda_f\bar{\nu}_i + \frac{1}{p}\left\{\bar{\mu}_{NC_i}\,\epsilon\,\Lambda_f + \bar{N}\,\epsilon\,\Lambda_f\bar{\nu}_i\right\} \tag{2.49}$$

Solving for $\bar{\bar{\mu}}_{ZZ}$,

$$\bar{\bar{\mu}}_{ZZ} = \frac{g(p)}{p^2 h(p)} \tag{2.50}$$

Where,

$$g(p) = 2(\epsilon\Lambda_f)^2\left\{\bar{\mu}_{NN} + \bar{N} + \sum_i \frac{\lambda_i(\overline{N\nu}_i + \bar{\mu}_{NC_i})}{p + \lambda_i}\right\} \tag{2.51}$$

and

$$h(p) = p + \Lambda_f(\bar{\nu}_o - 1 - \epsilon) + \Lambda_c - \Lambda_f\sum_i \frac{\lambda_i\bar{\nu}_i}{p + \lambda_i} \tag{2.52}$$

The inverse form of (2.50) can be found using the convolution theorem, where $\bar{\bar{f}}_1(p) = \frac{1}{p^2}$, and $\bar{\bar{f}}_2(p) = g(p)/h(p)$. The inverse of $\bar{\bar{f}}_1(p)$ is t. The inverse of $\bar{\bar{f}}_2(p)$ is $\sum_{k=1}^{J+1} A_k e^{R_k t}$ where $A_k = \{g(p)/h(p),_p\}\big|_{R_k}$ and the R_k are the roots of (2.52), when $h(p) = 0$. Substituting (2.27), (2.29) and (2.30), into (2.52) for $h(p) = 0$,

$$p = \frac{k(1 - \beta) - 1}{\ell} - \frac{k}{\ell} \sum_i \frac{\lambda_i \beta_i}{p + \lambda_i} = 0 \tag{2.53}$$

Equation (2.53) can be put in a more recognizable form by multiplying by ℓ/k and rearranging,

$$-\frac{1 - k}{k} = \frac{\ell p}{k} + p \sum_i \frac{\beta_i}{p + \lambda_i} \tag{2.54}$$

which is the inhour equation. Thus, the R_k are the roots of the inhour equation. There are J + 1 roots.

Employing the convolution theorem,

$$\bar{\mu}_{ZZ}(t) = \int_0^t \left\{ (t - \zeta) \sum_{k=1}^{J+1} A_k e^{R_k \zeta} \right\} d\zeta \tag{2.55}$$

giving,

$$\frac{\bar{\mu}_{ZZ}}{\bar{Z}} = \frac{1}{\epsilon \Lambda_f \bar{N}} \left\{ \sum_{k=1}^{J+1} \frac{A_k}{R_k} (e^{R_k t} - 1) - \sum_{k=1}^{J+1} \frac{A_k}{R_k} \left[\frac{(R_k t - 1)e^{R_k t} + 1}{R_k t} \right] \right. \tag{2.56}$$

For purposes of comparing the result with the literature, let $R_k = -r_k$ and rearrange,

$$\frac{\bar{\mu}_{ZZ}}{\bar{Z}} = \sum_{k=1}^{J+1} \frac{A_k}{\epsilon \Lambda_f \bar{N} r_k} \left[1 - \frac{(1 - e^{-r_k t})}{r_k t} \right] \tag{2.57}$$

Substituting for A_k,

$$\frac{\bar{\mu}_{ZZ}}{\bar{Z}} = \frac{2\epsilon \Lambda_f}{\bar{N}} \sum_{k=1}^{J+1} \left\{ \frac{\mu_{NN} + \bar{N} + \sum_{j=1}^{J} \frac{\lambda_j (\bar{N}\bar{\nu}_j + \bar{\mu}_{NC_j})}{\lambda_j - r_k}}{r_k^3 [1 + \Lambda_f \sum_j \lambda_j \bar{\nu}_j / (\lambda_j - r_k)^2]} \right\} \cdot \left\{ 1 - \frac{(1 - e^{-r_k t})}{r_k t} \right\} \tag{2.58}$$

Equation (2.58) is an expression for the ratio of the variance to mean number of detected neutrons as a function of detection time, t, in terms of all the system parameters defined above.

D. Transfer Function Approach

1. Random Processes

In order to derive an expression for the ratio of the variance to mean number of detected neutrons as a function of detection time using the transfer function approach, it is necessary to introduce the concepts and formulations of correlation and power spectral density functions.

The use of these functions is common to all branches of science and technology in which random processes are studied.[28,29] This section is included for purposes of notation and unification of material presented in subsequent sections.

Consider a function, $y(t) = g(t) - \bar{g}$, generated by a stationary process. The autocorrelation function, $\psi_{yy}(\tau)$, is defined,

$$\psi_{yy}(\tau) = \frac{\overline{y(t)\, y(t+\tau)}}{\overline{y^2}} \tag{2.59}$$

The Fourier transform of y (t), Y (jω), is defined as,

$$Y(j\omega) = \int_{-\infty}^{\infty} y(t)\, e^{-j\omega t} d\omega \tag{2.61}$$

This can be used to write y(t) as a Fourier integral,

$$y(t) = \frac{1}{2\pi} \int_{-\infty}^{\infty} Y(j\omega)\, e^{j\omega t} d\omega \tag{2.60}$$

Substituting for y(t) from (2.61) into (2.59),

$$\psi_{yy}(\tau) = \frac{\int_{-\infty}^{\infty} y(t) \int_{-\infty}^{\infty} Y(j\omega)\, e^{j\omega(t+\tau)} d\omega\, dt}{\int_{-\infty}^{\infty} y(t) \int_{-\infty}^{\infty} Y(j\omega)\, e^{j\omega t} d\omega\, dt} \tag{2.62}$$

or,

$$\psi_{yy}(\tau) = \frac{\int_{-\infty}^{\infty} |Y(j\omega)|^2 e^{j\omega\tau} d\omega}{\int_{-\infty}^{\infty} |Y(j\omega)|^2 d\omega} \tag{2.63}$$

Also, Find,

$$\frac{|Y(j\omega)|^2}{\int_{-\infty}^{\infty} |Y(j\omega)|^2 d\omega} = \int_{-\infty}^{\infty} \psi_{yy}(\tau)\, e^{-j\omega\tau} d\tau \tag{2.64}$$

where the l.h.s. of (2.64) is defined to be the normalized power spectral density, denoted as $G_{yy}(w)$. Equations (2.63) and (2.64) are known as Wiener's theorem[6].

Denote the unnormalized autocorrelation (autocovariance) and power spectral density functions as ψ^o and G^o, respectively. In a linear system, the relation between y(t) and a driving function, $x(t) = d(t) - \bar{d}$, is

$$y(t) = \int_{-\infty}^{t} W(t-\tau)\, x(\tau) d\tau = \int_{0}^{\infty} W(\tau)\, x(t-\tau) d\tau \tag{2.65}$$

where W is the system's Green's function. Forming the autocovariance function using (2.65) and (2.63),

$$\psi^o_{yy}(t') = \int_{0}^{\infty} W(\tau) d\tau \int_{0}^{\infty} W(\tau_1)\, \psi^o_{xx}(t' + \tau - \tau_1) d\tau_1 \tag{2.66}$$

Multiplying (2.66) by $e^{-j\omega t'}$ and integrating, using (2.64), gives,

$$G^o_{yy}(\omega) = \int_{0}^{\infty} W(\tau)\, e^{-j\omega\tau} d\tau \int_{0}^{\infty} W(\tau_1)\, e^{j\omega\tau_1} d\tau_1\, G^o_{xx}(\omega) \tag{2.67}$$

Recalling that the Fourier transform of the system Green's function is the system transfer function[28], $T(j\omega)$, simplify (2.67) to obtain,

$$G^{o}_{yy}(\omega) = |T(j\omega)|^{2} \; G^{o}_{xx}(\omega) \tag{2.68}$$

The power spectral density can, also, be written,[30]

$$G^{o}_{yy}(\omega) = \lim_{T \to \infty} \frac{1}{2T} \left| \int_{-T}^{T} y(t) \, e^{-j\omega t} dt \right|^{2} \tag{2.69}$$

2. Application to a Reactor

Consider the special case of a reactor with an external driving signal which has a zero mean, $s(t)$, due to a reactivity oscillator, and an independent driving function, $x(t)$, due to the inherent fluctuations in the neutron density. Since the two functions are independent,

$$\psi^{o}_{input} = \psi^{o}_{ss} + \psi^{o}_{xx} + \psi^{o}_{sx} + \psi^{o}_{xs} \tag{2.70}$$

Since, the two functions are independent,

$$\psi^{o}_{sx} = \overline{s(t) \; x \; (t + \tau)} = \overline{s(t)} \; \overline{x \; (t + \tau)} \tag{2.71}$$

it is clear that the cross correlation terms are zero when either $\bar{s}$ or $\bar{x}$ is zero. If $x(t)$ is white noise[28], i.e., has a constant power spectral density function, K, for the frequency range of interest, then

$$\psi^{o}_{xx}(\tau) = K' \, \delta(\tau - o) \tag{2.72}$$

where $\delta(\tau - o)$ is the Dirac delta function.

Because white noise consists of independent random events,

$$\psi^{o}_{xx}(\tau) = \overline{x(t) \; x \; (t + \tau)} = \overline{x(t)} \; \overline{x \; (t + \tau)} \tag{2.73}$$

In order for (2.73) to satisfy (2.72), it is necessary for $\bar{x}$ to be zero, which agrees with our definition of x(t). Thus, the cross terms in (2.70) are zero, whether or not $\bar{s} = 0$. For these independent signals, (2.68) becomes,

$$G^{o}_{yy}(\omega) = |T_{ss}(j\omega)|^2 \, G^{o}_{ss} + |T_{xx}(j\omega)|^2 \, G^{o}_{xx} \tag{2.74}$$

The distinction between T_{ss} and T_{xx} is considered in Appendix B, depending whether the driving functions are expressed in terms of neutron or reactivity fluctuations.

E. No External Signal

With no external signal, using (2.63) and (2.68),

$$\psi^{o}_{yy}(\tau) = \int_{-\infty}^{\infty} |T(j\omega)|^2 \, G^{o}_{xx}(\omega) \, e^{j\omega\tau} d\omega \tag{2.75}$$

$\psi^{o}_{yy}(\tau)$ is not an observable quantity, because it is the autocovariance function of all the neutrons in the reactor, except those which are detected. $\psi^{o}_{yy}(\tau)$ can be written, alternatively,

$$\psi^{o}_{yy}(\tau) = \overline{[N(t) - \bar{N}(t)][N(t + \tau) - \bar{N}(t + \tau)]} \tag{2.76}$$

Note, $\bar{N}(t) = \bar{N}(t + \tau)$, giving

$$\psi^{o}_{yy}(\tau) = \overline{N(t) \, N(t + \tau)} - \bar{N}^2 \tag{2.77}$$

In an experiment, if $\alpha(t)$ is the continuous instantaneous detection rate, the observed autocorrelation function, ψ_{ob}, is

$$\psi_{ob}(\tau) = \frac{\overline{[\alpha(t) - \bar{\alpha}][\alpha(t + \tau) - \bar{\alpha}]}}{\overline{\alpha^2} - \bar{\alpha}^2} \tag{2.78}$$

By definition,

$$\alpha(t) = \epsilon \Lambda_f N(t) \tag{2.79}$$

Thus,

$$\psi_{ob}(\tau) = \frac{\overline{N(t)\, N(t+\tau)} - \overline{N}^2}{\overline{N^2} - \overline{N}^2}$$

Substituting from (2.77),

$$\psi_{ob}(\tau) = \frac{\psi^o_{yy}}{\overline{N^2} - \overline{N}^2} \tag{2.80}$$

and,

$$\psi^o_{ob}(\tau) = (\epsilon\Lambda_f)^2 \psi^o_{yy}(\tau) \tag{2.81}$$

Note that ψ^o_{yy} is dimensionless and ψ^o_{ob} has dimensions of time^{-2}.

In order to arrive at an expression similar to (2.58), it is convenient to write the transfer function in terms of the roots of the inhour equation, $-r_k$,

$$T(j\omega) = \sum_{k=1}^{J+1} \frac{A_k}{r_k + j\omega} \tag{2.82}$$

Introducing (2.82) into (2.75), and keeping the factor of 2π from (2.61),

$$\psi^o_{yy}(\tau) = \frac{1}{2\pi} \int_{-\infty}^{\infty} \sum_{k=1}^{J+1} \sum_{\ell=1}^{J+1} \frac{A_k A_\ell e^{j\omega\tau} G^o_{xx}}{(\omega + jr_\ell)(\omega - jr_k)}\, d\omega \tag{2.83}$$

Assume $G^o_{xx} = K$, i.e., a white noise driving function. The integral in (2.83) can be evaluated directly using contour integration in the complex plane. The poles of (2.83) in the upper half plane are at $\omega = jr_k$. The residues are $e^{-r_k t}/j(r_k + r_\ell)$. Thus

$$\psi^o_{yy}(\tau) = K \sum_{k=1}^{J+1} \sum_{\ell=1}^{J+1} \frac{A_k A_\ell e^{-r_k \tau}}{r_k + r_\ell} \tag{2.84}$$

A relationship between ψ^o_{ob} and the ratio of the variance to mean over an interval is developed in Appendix E. Because of the number of steps required to complete the derivation, the details are given in the appendix. However, the result of the derivation, (2.88), is vitally important to the present development and is one of the contributions of this study. For

$$\psi^o_{ob}(\tau) = \psi^o_{ob}(t_2 - t_1) = \overline{\alpha(t - t_1)\,\alpha(t - t_2)} - \bar{\alpha}^2 \tag{2.85}$$

where,

$$Z(t_2) = \int_0^{t_2} \alpha(t)\, dt \tag{2.86}$$

it is shown that,

$$\frac{\overline{Z^2} - \bar{Z}^2}{2} = \int_0^{\tau} \int_0^{t_2} \psi^o_{ob}\, dt_1\, dt_2 \tag{2.87}$$

Thus, the ratio of the variance to the mean for an interval τ is,

$$\frac{\sigma^2}{\bar{Z}}(\tau) = \frac{2}{\bar{Z}} \int_0^{\tau} \int_0^{t_2} \psi^o_{ob}\, dt_1\, dt_2 \tag{2.88}$$

Substituting for ψ^o_{ob} from (2.81) and (2.83),

$$\frac{\sigma^2}{\bar{Z}}(\tau) = \frac{2K(\epsilon\Lambda_f)^2}{\bar{Z}} \int_0^{\tau} \int_0^{t'} \sum_k \sum_\ell \frac{A_k\, A_\ell\, e^{-r_k t}}{r_k + r_\ell}\, dt\, dt' \tag{2.89}$$

Evaluating the integrals in (2.89), and substituting for $\bar{Z}(\tau)$ gives,

$$\frac{\sigma^2}{\bar{Z}} = 1 + \frac{2K\,\epsilon\,\Lambda_f}{\bar{N}} \sum_{k=1}^{J+1} \sum_{\ell=1}^{J+1} \frac{A_k\, A_\ell}{r_k(r_k + r_\ell)} \left\{ 1 - \frac{(1 - e^{-r_k\tau})}{r_k\tau} \right\} \tag{2.90}$$

A one has been added to the r.h.s. of (2.90) to take into account uncorrelated source neutrons, which obey a Poisson distribution.[31] The ratio of the variance to mean of a Poisson distribution is unity.

Comparing the expressions obtained for the ratio of the variance to mean number of detected neutrons as a function of detection time, using the method of a detailed probability balance, (2.58), and the transfer function approach, (2.90), it is seen that the expressions are identical in form, and that the coefficients may be identified,

$$\sum_{k=1}^{J+1} \left\{ \frac{\bar{\mu}_{NN} + \bar{N} + \sum_i \frac{\lambda_i(\overline{N\nu}_i + \bar{\mu}_{NC_i})}{(\lambda_i - r_k)}}{r_k^3\left[1 + \Lambda_f \sum_i \frac{\lambda_i \bar{\nu}_i}{(\lambda_i - r_k)^2}\right]} \right\} = K \sum_{k=1}^{J+1} \sum_{\ell=1}^{J+1} \frac{A_k A_\ell}{r_k(r_k + r_\ell)} \qquad (2.91)$$

No assumption had to be made about the driving function of the reactor using the method of a detailed probability balance. However, in the transfer function approach, one can not proceed beyond (2.83) without making an assumption on the form of G^o_{xx}. By assuming that G^o_{xx} is white noise, i.e., has a constant value for the frequency range of interest, (2.91) results. However, G^o_{xx} could have been represented by any function which is finite when evaluated at the poles of (2.83) in the upper half plane and still given the same form to the r.h.s. of (2.91). A test of the validity of the present assumption that G^o_{xx} is constant is given in Chapter VI.

CHAPTER III

THE EXPERIMENT

A. Condition of the Reactor

The experiment was performed in the Ford Nuclear Reactor at the Phoenix Memorial Laboratory of the University of Michigan. The FNR is a 90% enriched swimming pool reactor. Graphite reflector elements are placed around the fuel region. The reactor has a water reflector above and below the fuel region.

The fuel elements and partial elements around two of the shim rods and the control rod used for this experiment had been used previously for low power operation only. As a result, the fuel elements did not serve as a large gamma source. Also, three of the regulating rod partial elements were low intensity gamma sources. However, the fourth partial had been exposed to many megawatt-days integrated flux and was extremely radioactive. An additional partial element with a low power history was not available to replace this element, so it remained in the reactor during the experiment as the principal source of gamma rays and resultant photoneutrons. The graphite elements were not replaced because their contribution to the photoneutron level was negligible compared to the partial elements.

B. Core Loading

The arrangement of the BF_3 detector, reactor oscillator, reflectors, fuel elements and regulating rods is shown for each of the five different experimental conditions in Figures 3.1, 3.2, 3.3, 3.4, and 3.5. Note that the experiments are numbered consecutively in Roman numerals from I to V,

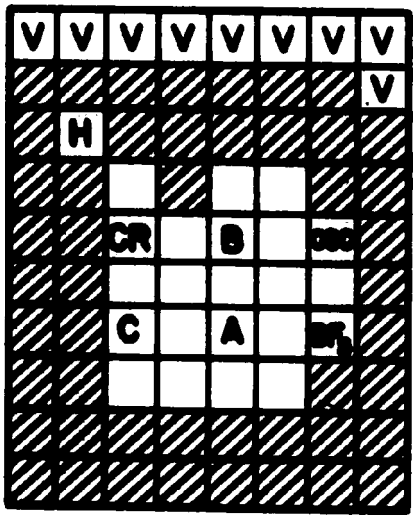


Figure 3.1. Core Loading - I.

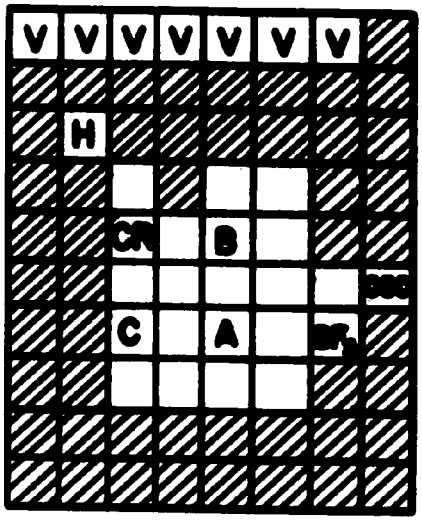


Figure 3.2. Core Loading - II.

KEY

osc	- REACTOR OSCILLATOR
BF_3	- BF_3 NEUTRON DETECTOR
	- FUEL
A	- SHIM ROD A, ETC.
	- REFLECTOR
V	- NO ELEMENT (CONTAINS H_2O)
CR	- CONTROL ROD
H	- SAMPLE HOLDER

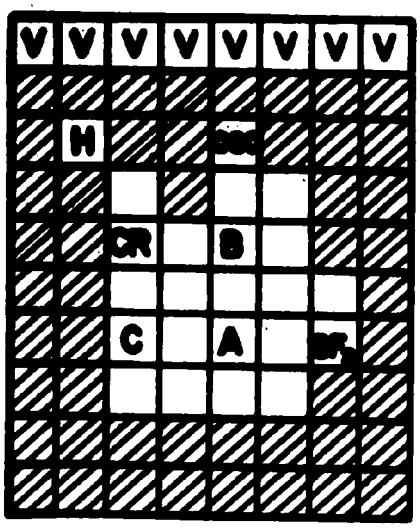


Figure 3.3. Core Loading - III.

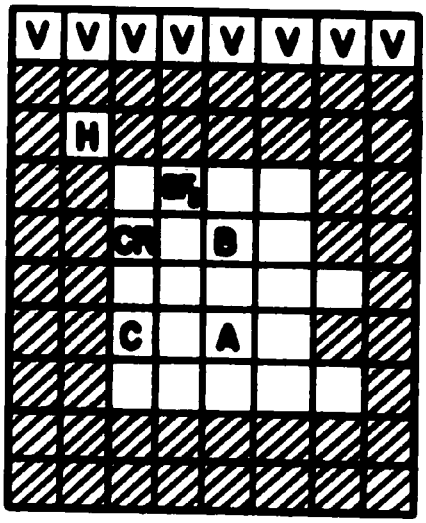


Figure 3.4. Core Loading - IV.

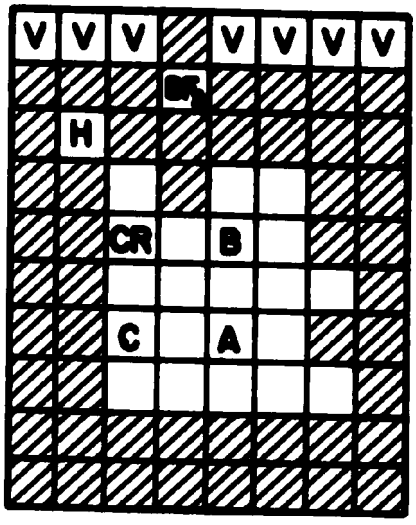


Figure 3.5. Core Loading - V.

corresponding to each core loading. Different experiments are referred to, hereafter, by the appropriate Roman numeral and a brief description of whether or not the oscillator was making a perturbation while the data was recorded. For example, I-Noise refers to data taken with core loading I, with no perturbation due to the oscillator, and I-10c/s refers to the same loading but with the oscillator making approximately 10 revolutions or cycles per second.

C. Control Rod Calibration

The control rod was calibrated using the stable positive period method for each different core loading. For loadings I, II and III, the oscillator's cadmium disk was positioned for mean worth prior to the calibration of the rod. The procedure was to go critical with the control rod fully inserted and then withdraw the rod by an amount which was estimated from experience to give a stable period between 50 and 300 second. The period was measured and the corresponding reactivity determined.[33] The rod was then reinserted to approximately the midpoint of the previous initial position and the position for which the stable period was determined. The reactor was made critical by adjusting the shim rods. When criticality was established, the control rod was again withdrawn by an amount which gave a stable period between 50 and 300 seconds. The period was determined for the rod movement over this new range. The procedure of inserting the rod to the midpoint of initial and final positions, going critical on the shims and then withdrawing the rod again was repeated until the rod was fully withdrawn. By overlapping the distance through

which the rod was moved during the calibration, it was possible to measure the total worth of the rod within ±10%. Specifically, for loading I, the results of the overlapping rod calibration are given in Table III.1, and shown as reactivity per inch, ρ/inch, vs. rod position in Figure 3.6.

The integrated worth of the rod is obtained by integrating the measured differential worth given in Figure 3.6. The result of the graphical integration is shown in Figure 3.7 as ρ vs. rod position.

Table III.2 gives the results of the control rod calibration for each core loading in terms of total rod worth. The control rod movements overlapped only for loading I.

D. Calibration of the Reactor Oscillator

The reactor was taken critical, in the range 10-100 watts, with the cadmium disk in a position of maximum worth relative to the fixed cadmium piece, see Figure 3.8. The cadmium disk was then rotated through some angle θ measured from the Z axis to the point B on the disk, as shown in the inset figure in Figure 3.8, in the direction shown. The stable positive period was determined from the linear level trace. The control rod movement required to reestablish criticality was also noted. The results for loading I are given in Table III.3. The angular worth obtained from the positive stable period is considered a better value than that determined from the control rod movement required to reestablish criticality, because of the uncertainty in rod worth between 16 and 19 inches. It should be observed that the disk worth given by the control rod calibration is equivalent to that obtained from the stable period, within the uncertainty of Figure 3.7.

TABLE III.1

CONTROL ROD CALIBRATION FOR LOADING I

Shims at Critical			Control Rod				Calculated Period	$\rho x 10^4$	$\frac{\rho x 10^4}{\text{Change}}$
A	B	C	initial	final	change	mean position			
millimeters			inches				seconds		
14.33	14.24	14.25	36	29	7	32.5	136	5.83	0.83
14.44	14.34	14.35	31 18/32	26 0.5/32	5.55	28.78	99.5	7.49	1.35
14.74	14.62	14.62	27 13/16	24 5.5/32	3.64	25.99	114	6.73	1.85
14.90	14.77	14.78	25 3/8	21 11/16	3.69	23.53	85.5	8.42	2.28
14.99	14.87	14.97	24 3/16	19 6/16	4.81	21.78	74.5	9.33	1.94
15.18	15.09	15.16	21 11/16	15 8/16	6.19	18.59	80.3	8.80	1.42
15.42	15.35	15.40	17 15/16	12	5.94	14.97	229	3.74	0.63

NOTE: 1) control rod fully inserted at 36 inches and fully withdrawn at 12 inches

2) reactivities were obtained from the calculated periods from Reference 33

3) slide rule accuracy

TABLE III.2

INTEGRATED CONTROL ROD WORTH FOR DIFFERENT CORE LOADING

Core Loading	Integrated Worth of Control Rod	Number of Steps to Withdraw Rod Fully
I	2.95×10^{-3}	7
II	3.35×10^{-3}	4
III	3.04×10^{-3}	3
IV	2.83×10^{-3}	3
V	3.04×10^{-3}	2

TABLE III.3

CALIBRATION OF CADMIUM DISK-LOADING I

θ initial degrees	θ final degrees	Stable Period seconds	$\rho x 10^4$	Control Rod initial	Control Rod final	$\rho x 10^4$ from Figure 3.7
				inches	inches	
1	90	1065	0.89	16 7/8	17 9/16	0.88 ± 0.4
0	123	555	1.67	16 7/8	18 19/64	2 ± 0.4
1	149	440	2.07	16 $\frac{57}{64}$	18 3/8	1.75 ± 0.4
0	179	387	2.33	16 7/8	18 23/32	2.6 ± 0.4
-0	211	455	2.05	16 7/8	18 27/64	2 ± 0.4
-0	273	1035	0.92	16 $\frac{15}{16}$	17 11/16	0.89 ± 0.4

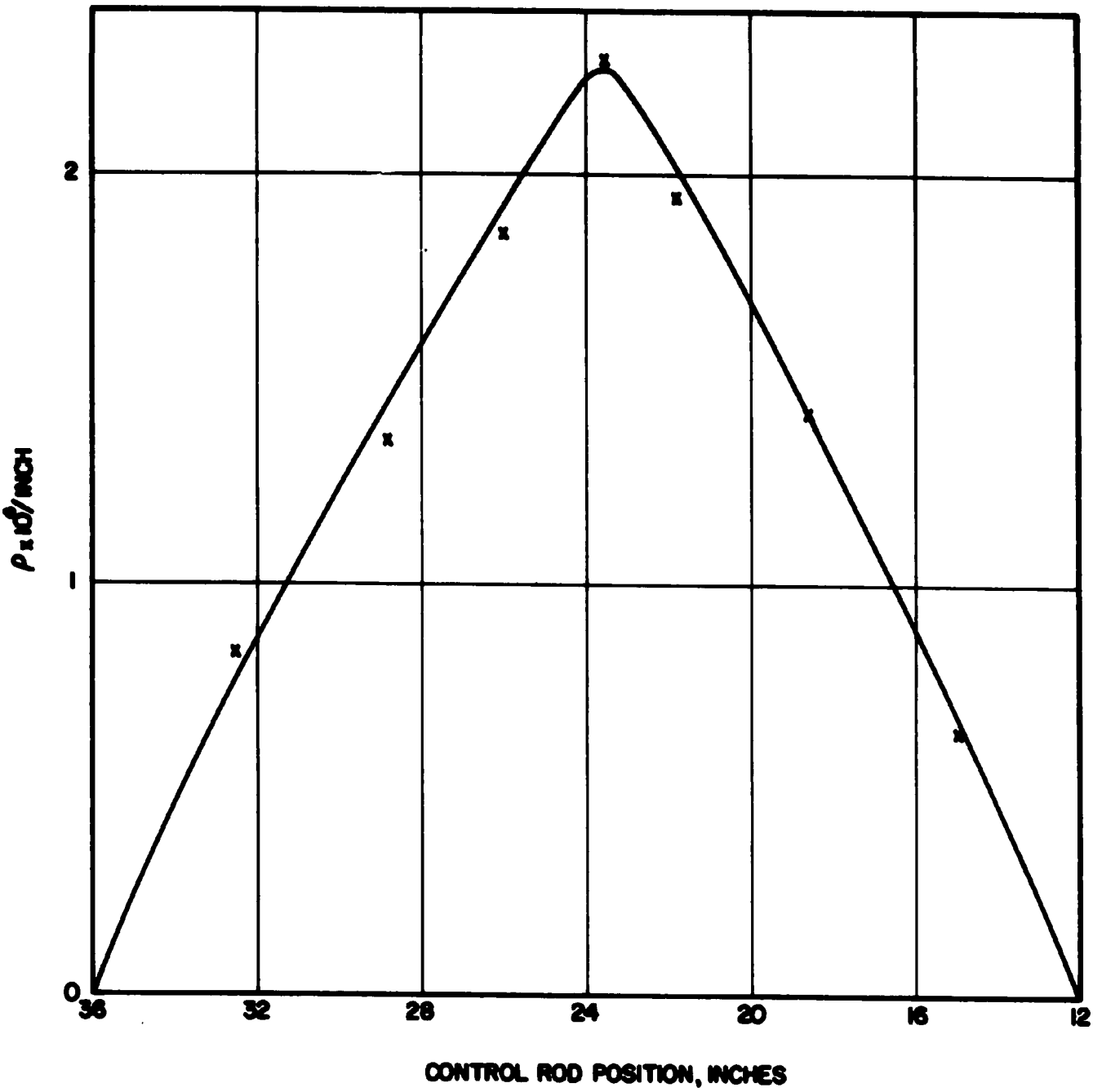


Figure 4.6. Control Rod Differential Worth, Loading I.

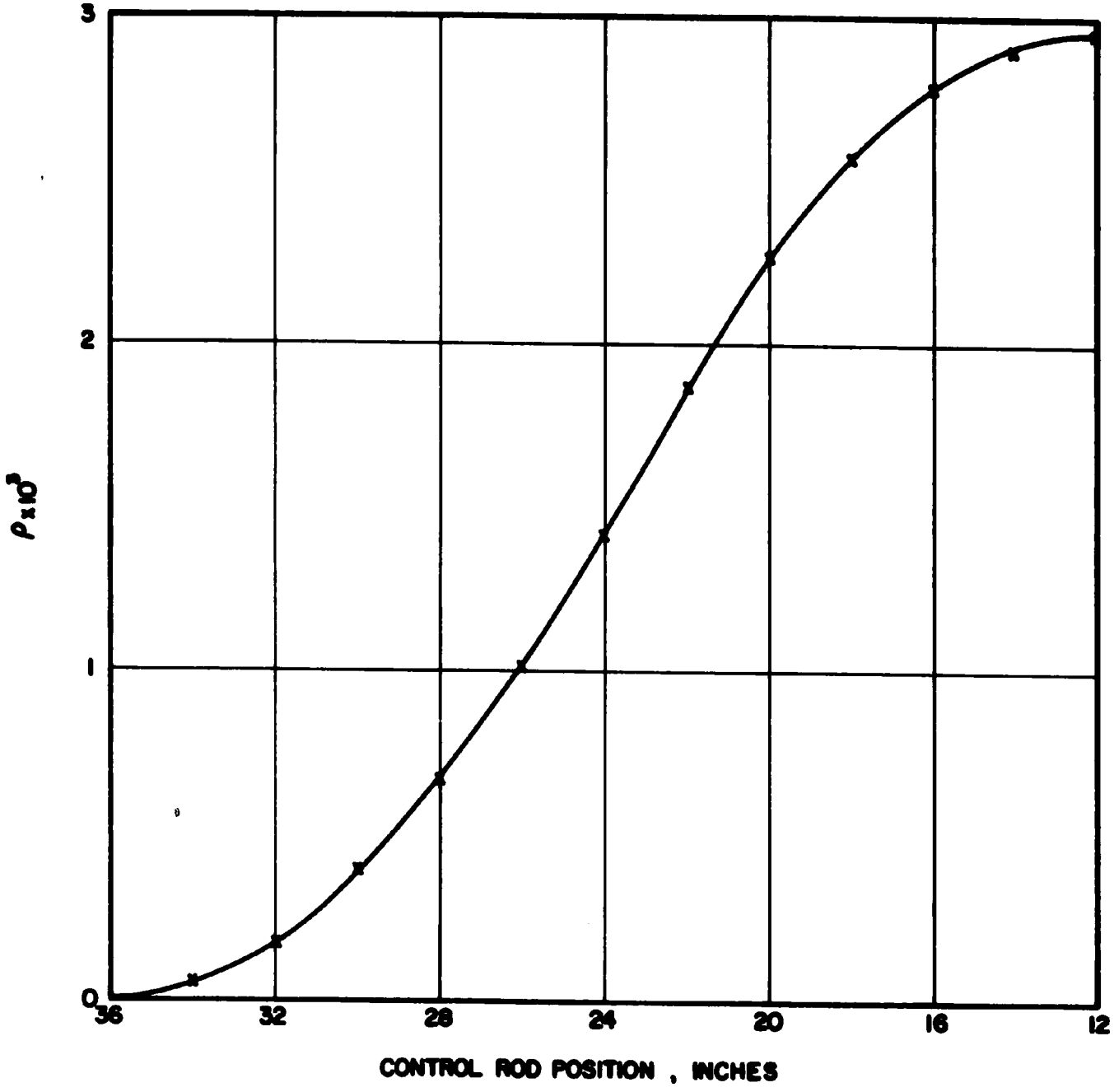


Figure 4.7. Integrated Control Rod Worth, Loading I.

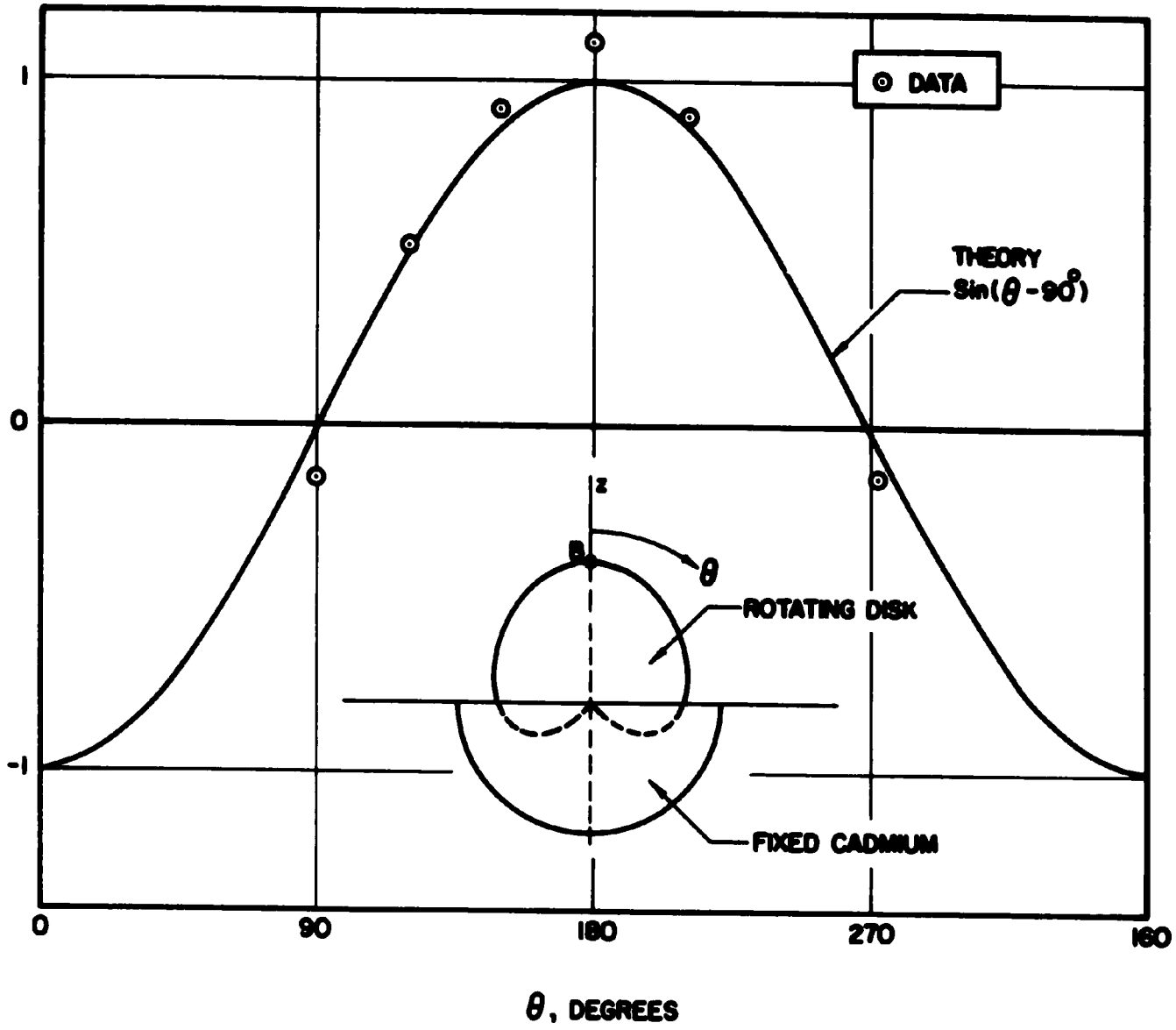


Figure 4.8. Worth of Cadmium Disk Compared to Sinusoid Normalized at $\theta = 123°$.

The results of the disk calibration are normalized to a pure sinusoid at $\theta = 123°$ and a comparison made in Figure 3.8. The disk is seen to introduce an approximately sinusoidal change in reactivity as a function of exposed surface area. The maximum worth of the disk is for $\theta = 180°$. The disk worth at $\theta = 180°$ for the three core loadings in which the oscillator was used are given in Table III.4.

TABLE III.4

Cadmium Disk Worth at $\theta = 180°$ for Different Loadings

LOADING	STABLE PERIOD SECONDS	DISK WORTH
I	387	2.33×10^{-4}
II	738	1.26×10^{-4}
III	1018	0.93×10^{-4}

E. Reactivity Associated with the Equipment

A preliminary measurement of the worth of the oscillator and the BF_3 detector relative to a graphite reflector element was made for a modified version of loading I (graphite elements replaced the oscillator and detector shown in Figure 3.1). The reactor went critical with the three shim rods 98% withdrawn and the control rod fully inserted. Then one graphite element was replaced by the oscillator, with the cadmium disk set for its mean worth. The reactor went critical with all rods 100% withdrawn. The worth of the control rod was measured to be about 3×10^{-3} and the upper 2% of all the shims was worth about 3×10^{-4}, based on a separate calibration by the Phoenix

staff. Thus, the oscillator was worth approximately -3.3×10^{-3} compared to the graphite element. For loading I, i.e. oscillator and detector inserted, criticality was reached with shims A and B at 90% and shim C 89% withdrawn. The control rod was 50% inserted. The difference between these critical rod positions and the case with graphite in both positions was worth about 1.4×10^{-3}. Thus, the oscillator has negative worth about equal to the control rod, and the BF_3 detector has positive worth about one and one-half times the control rod. The effect of the detector is positive relative to the water which it is displacing, because the water in the central part of the channel acts as a neutron sink. Relative to the displaced water the detector is essentially a void space. The experiment as a whole has a positive worth equal to about one-half that of the control rod, relative to graphite.

F Experimental Procedure

After measuring the worth of the equipment and calibrating the control rod and the cadmium disk for loading I, data was taken on the fluctuations in neutron level. The reactor was made critical, the Po-Be neutron source removed, and the reactor was then made subcritical by fully inserting the control rod. A relatively steady state in the mean neutron level was attained within one hour after insertion of the control rod. Fluctuation data was recorded on magnetic tape for 12 minutes for each set of experimental conditions. The decrease in the mean neutron level was less than 1% during the 12 minutes the data was recorded.

A discriminator traverse on the AID amplifier was made for the operating voltage of the detector to check its plateau characteristics. The discriminator was set to give a mean count rate less than 2500 neutrons/

second. Fifty one-second counts were recorded by hand. The ratio of the variance to the mean was computed by hand to determine whether proper operating conditions existed. Since this ratio was significantly different from one, conditions were considered satisfactory.

Individual neutron pulses were recorded on magnetic tape for approximately twelve minutes, after having run the recorder for more than one hour to insure its thermal equilibrium. Having obtained a record of the neutron "noise", the cadmium disk was rotated at a fixed speed. After allowing twenty minutes for the system to settle into "steady state" conditions, a new magnetic tape was used for twelve minutes to record the neutron fluctuations. This procedure was repeated for as many different rates of roration as were desired. Usually four ($\sim\frac{1}{2}$, 1, 10 and 30 cycles/second) were used for each different core loading.

The number of shaft rotations in a two minute interval were recorded using the photocell device described in the Chapter IV. At the 10 and 30 cycles/second rotation rates, a stroboscope was used as a check on the photocell device.

The above procedure, with the exception of measuring the worth of the equipment, was repeated for each new core loading. For loading IV and V, only noise data was taken, since the oscillator was not in the core.

G. Experimental Difficulties

The Aluminum box in which the oscillator mechanism was placed was not watertight with a head of 15 to 25 feet of water. The flaw in the welded seams was not found. The leak was eliminated completely by pressurizing the box to 4-5 pounds per square inch (gage).

The oscillator remained submerged in the pool at core level for 6 days. Because of the high humidity, the contact between the brushes and the rotor of the selsyn introduced considerable noise into the photocell-Schmidt trigger circuit. The noise increased as the shaft speed was increased, because the rotor was not well balanced. For rotation rates greater than 5 cycles/second, the noise made it impossible to count shaft rotations using the photocell circuit. The stroboscope was used at the higher speeds. The problem was corrected, after the experiment was concluded, by applying a lubricant to the point of contact. In future experiments, a high conductivity grease is suggested which will minimize the effect of vibrations in the rotor and humidity.

When 1600-2500 volts were applied to the BF_3 detector, noise signals about equal in magnitude to neutron induced pulses originated from its cathode follower preamplifier. The preamplifier was rebuilt several times, using better component arrangement and design, in an attempt to stop the high voltage induced phenomena, but with no success. Finally, it was discovered that this problem was caused by high humidity. During the experiment, a desiccant was placed around the preamplifier and in the tygon tube connecting the detector to the surface equipment. The desiccant eliminated the noise.

The gamma level in the reactor due to the hot partial fuel element was high for this experiment. With a 1/4 inch lead shield around the detector, the pulses caused by gamma pile-up were larger than the pulses caused by neutron interaction. An additional 1/4 inch of lead shield was added, lowering the size of the gamma induced pulses to a tolerable level. The gamma field changed the characteristics of the tube

markedly, destroying the plateau. For loading I, Figure 3.9 shows a discriminator traverse for the detector at an operating voltage of 2325 volts. Neutron level data was recorded using a discriminator setting of 46 volts. The output of the detector was observed on a cathode ray oscilloscope. The main gamma induced noise was easily separated visually from the larger neutron pulses. Changes in the tube characteristics caused by the intense gamma radiation were negligible during the 12 minutes data was recorded. For loadings II and III, a 50 volt discriminator was used. For IV and V, settings of 40 and 35, respectively, were possible because the gamma background was lower. The solution to this problem is to remove the gamma source. An additional cold partial element should be obtained for future low level experiments.

An additional problem generated by the hot partial was the high photoneutron level in the core. The experiment was performed for all loadings with the reactor subcritical by the worth of the entire control rod. One of the parameters, which was to have been varied, was the degree of subcriticality. Because of the inherent photoneutron source, and the limitation on detector counting rate due to dead time losses, the experiment could not be done for a less subcritical system with the detector used.

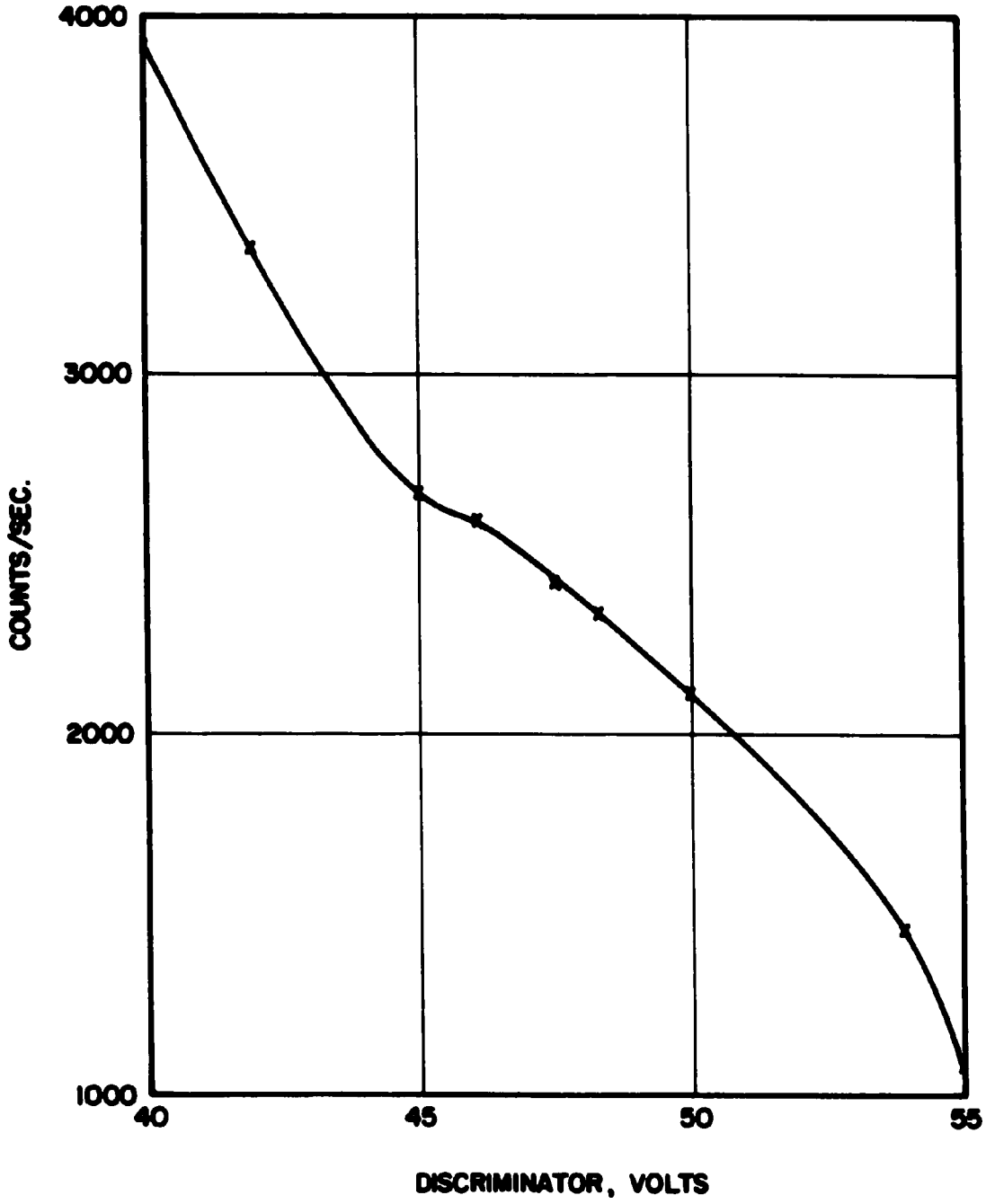


Figure 3.9. Discriminator Traverse for BF_3 Detector, Loading I.

CHAPTER IV

EQUIPMENT

The equipment used to detect and record neutron density fluctuations is independent of the equipment which introduces perturbations in reactivity. The block diagram for the neutron detection and data reduction system is given in Figure 4.1A. The block diagram of the reactivity perturbation system is given in Figure 4.1B. The remainder of this chapter describes these figures.

A. Neutron Detection System

The system used to detect, record and optionally playback fluctuations in neutron density in the reactor is basically the same as in Reference 5, with modifications as noted below. A brief description of the different components is given.

BF_3 Tube

The BF_3 tube used in this experiment was made by N. Wood Counter Laboratories, model G-10-12. The aluminum tube was 1" in outside diameter, with a sensitive length of 12". The tube was filled with 96% enriched $B^{10}F_3$ gas, and a small fraction of quenching gas, at 40 cm. of mercury. Its operating voltage was in the 2100 - 2500 volt range.

Preamplifier-A

Preamplifier-A, a transistorized, battery powered cathode follower preamplifier, is shown in Figure 4.2. It was mounted at the output of the BF_3 tube in order to match impedance. The cable from the BF_3 tube to the main amplifier was about 40 feet long, so that the millivolt pulses

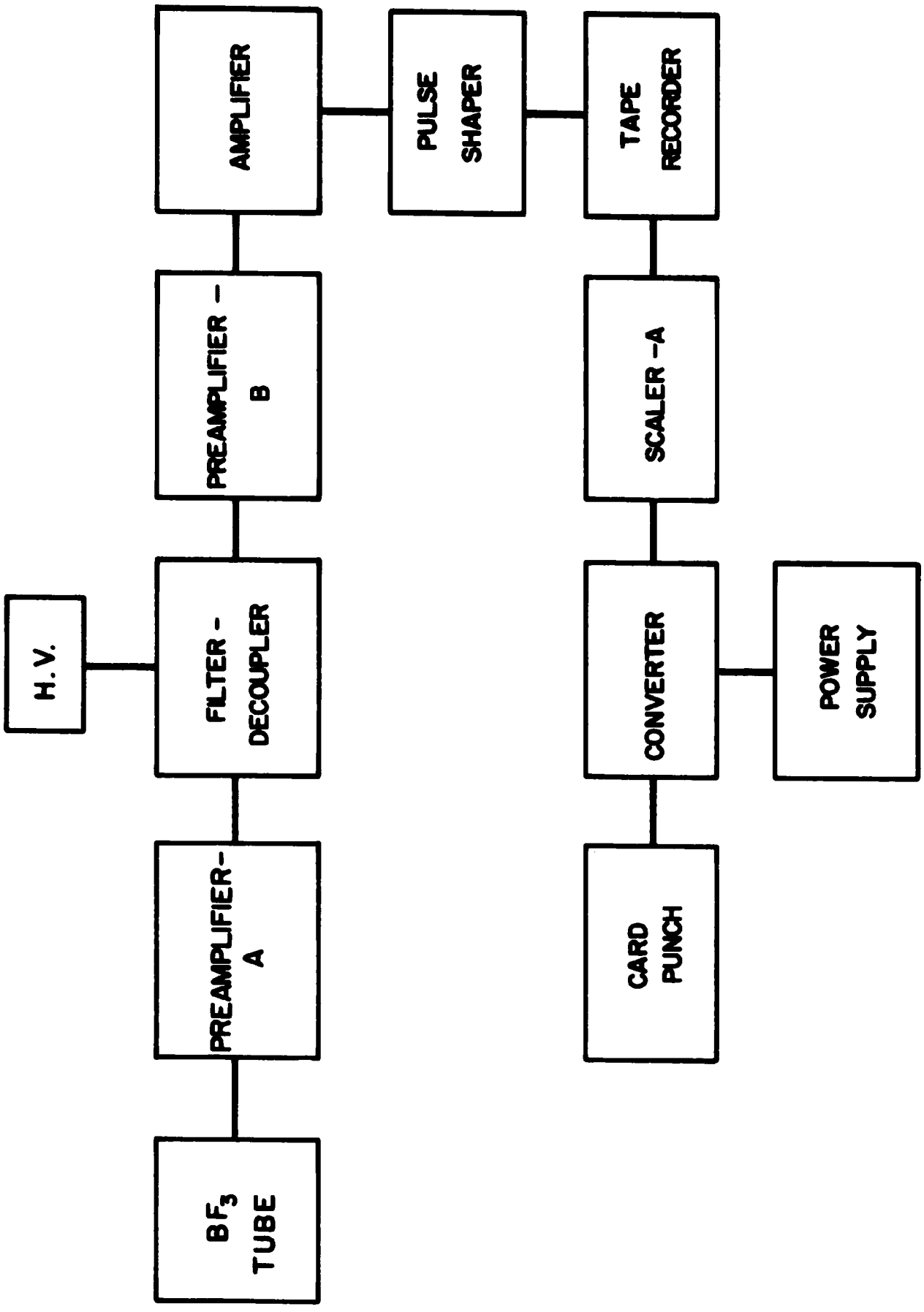


Figure 4.1A. Neutron Detection-Conversion Block Diagram.

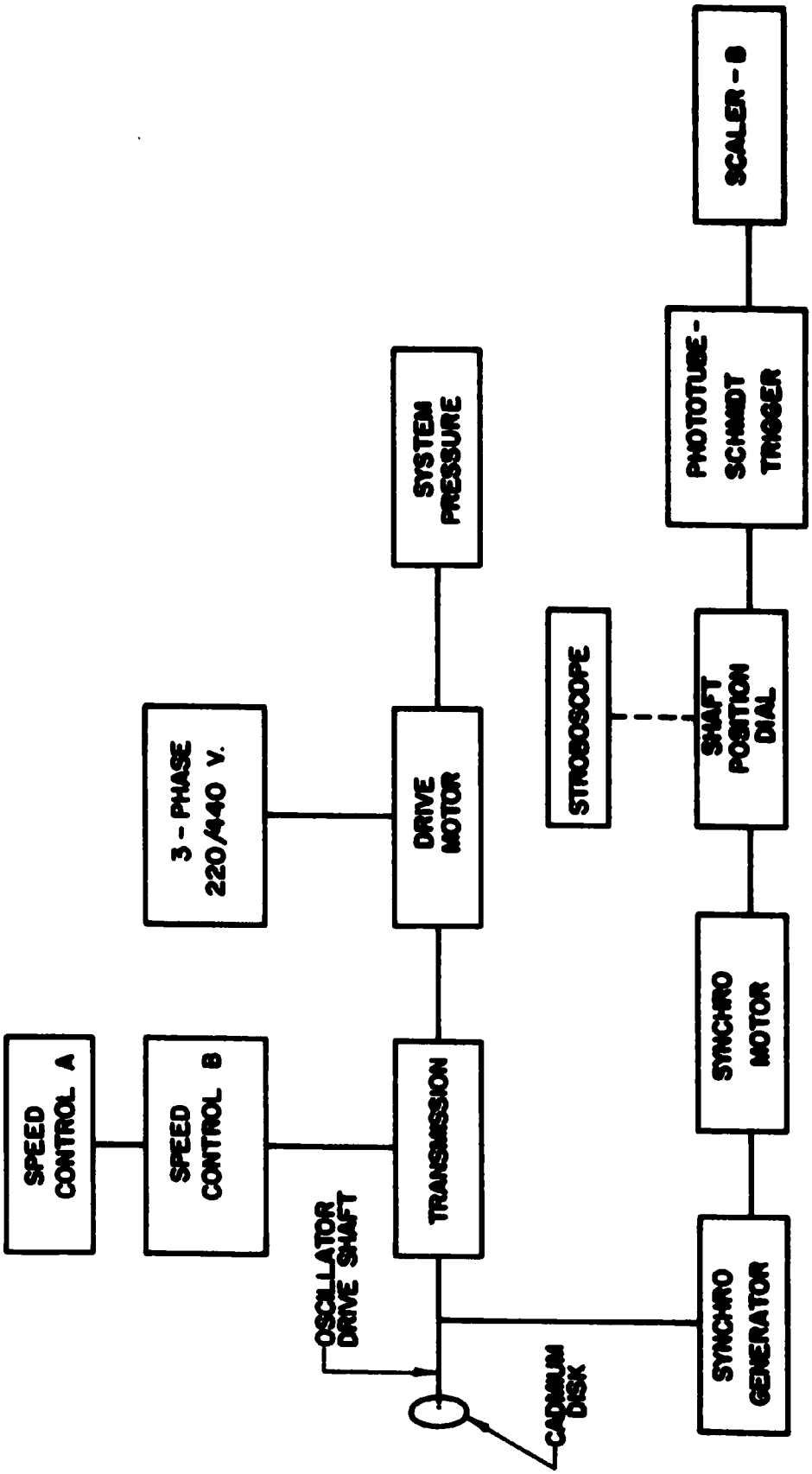


Figure 4.1B. Oscillator System Block Diagram.

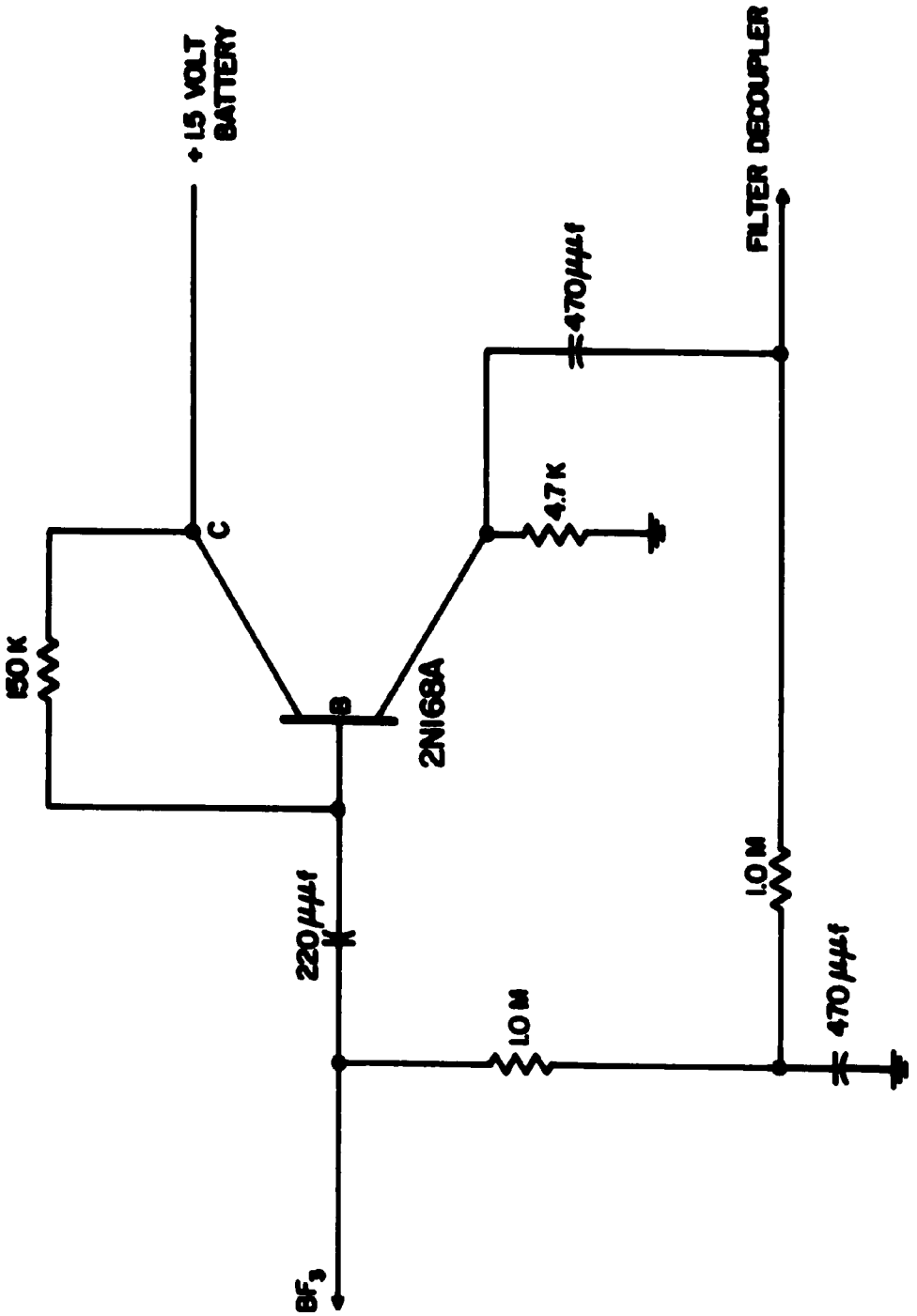


Figure 4.2. Preamplifier - A.

from the BF_3 tube would have been lost without preamplifier A. The gain of the preamplifier was about 0.3.

Filter-Decoupler

The filter-decoupler shown in Figure 4.3 served to cut down some small 60 cycle ripple in the BF_3 high voltage supply, and to isolate the high voltage from preamplifier-B.

High Voltage Supply

A Baird Atomic regulated high voltage power supply, model 318, 0-2500 volts, was used.

Preamplifier-B and Amplifier

A Radiation Counter Laboratories AID linear amplifier, and an AID-P preamplifier with a gain of 20, were used. The blocking capacitor at the preamplifier input was replaced by the decoupler shown in Figure 4.3.

Pulse Shaper and Tape Recorder

The pulse shaper converted the fast negative pulses from the AID discriminator output to positive rectangular pulses. It was found that pulses 13 volts high and about 3×10^{-6} seconds wide could be recorded on magnetic tape with no losses, if the pulses were separated by at least 10×10^{-6} seconds.

The tape recorder, an Ampex 307, had a bandwidth of 80KC at a tape speed of 60 inches per second, and measured wow and flutter less than 0.1%. The wow and flutter are caused by fluctuations in the tape speed.

Scaler-A

A Dymec model 2500 variable gate (0.001 to 9.999 in steps of 0.001 seconds) scaler was used. The display time was variable from 0.1 to

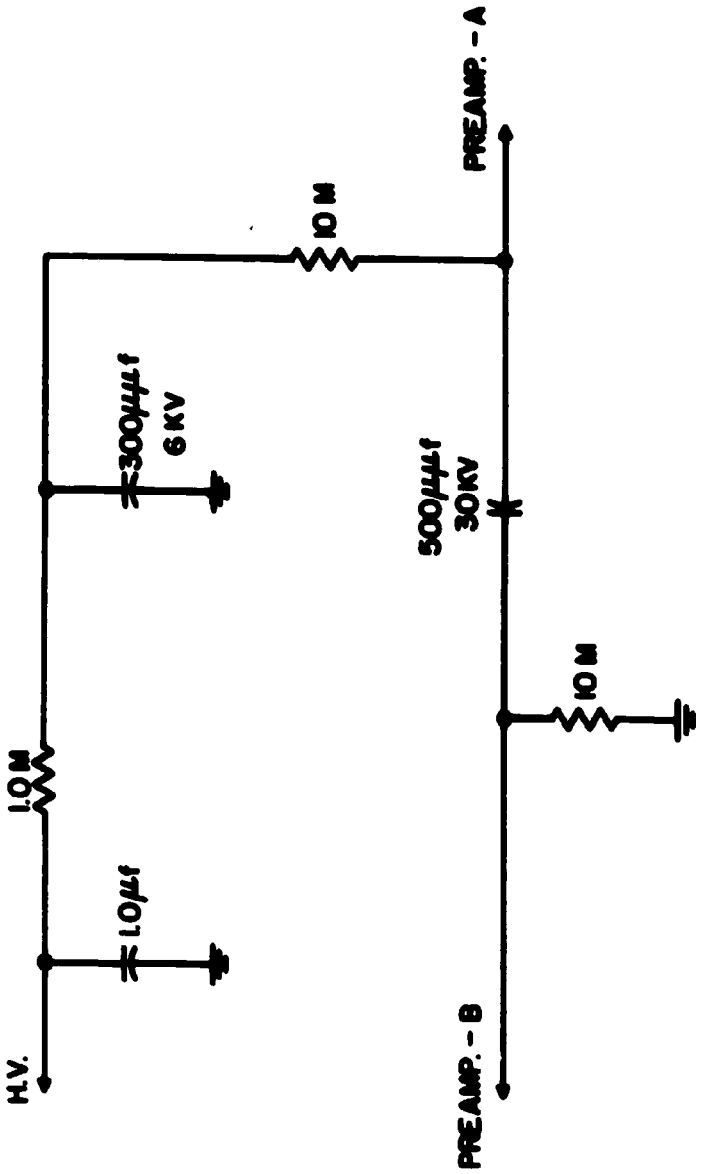


Figure 4.3. Filter - H. V. Decoupler.

10 seconds. Each of the 5 display columns gave a staircase voltage representation for the digits 0 to 9, accessible at the rear of the scaler. The conversion from pulses on the magnetic tape to numbers on an IBM card utilized the decimal output of the scaler.

Converter - Power Supply-Card Punch

The converter scans the display columns of scaler-A, one at a time from the left. Its relays open or close in a predetermined pattern for each different digit or voltage. The relay pattern is compatible with the IBM-024 card punch machine. The converter translates the digital output of the scaler to the equivalent number punched on an IBM card. Twelve different sets of numbers are punched on each card automatically. The display time of scaler-A is adjusted to allow time for punching the displayed number and resetting the converter relays.

B. Oscillator System

The oscillator and its container are shown in detail in Figures 4.4 to 4.7. The design considerations and features are briefly described in the following sections.

The oscillator container, Figure 4.6, was made from an aluminum alloy, 5056, which combined satisfactory mechanical properties with a low activation cross section. The alloy had small amounts of elements such as iron and tin which have long lived radioactive isotopes.

The container was designed to fit into the matrix plate of the Ford reactor, like a fuel or reflector element, in either of two orientations. Because of the space limitations imposed by the presence of the regulating rods and their guide tubes, the oscillator drive motor had to be located about three feet above the core upper surface.

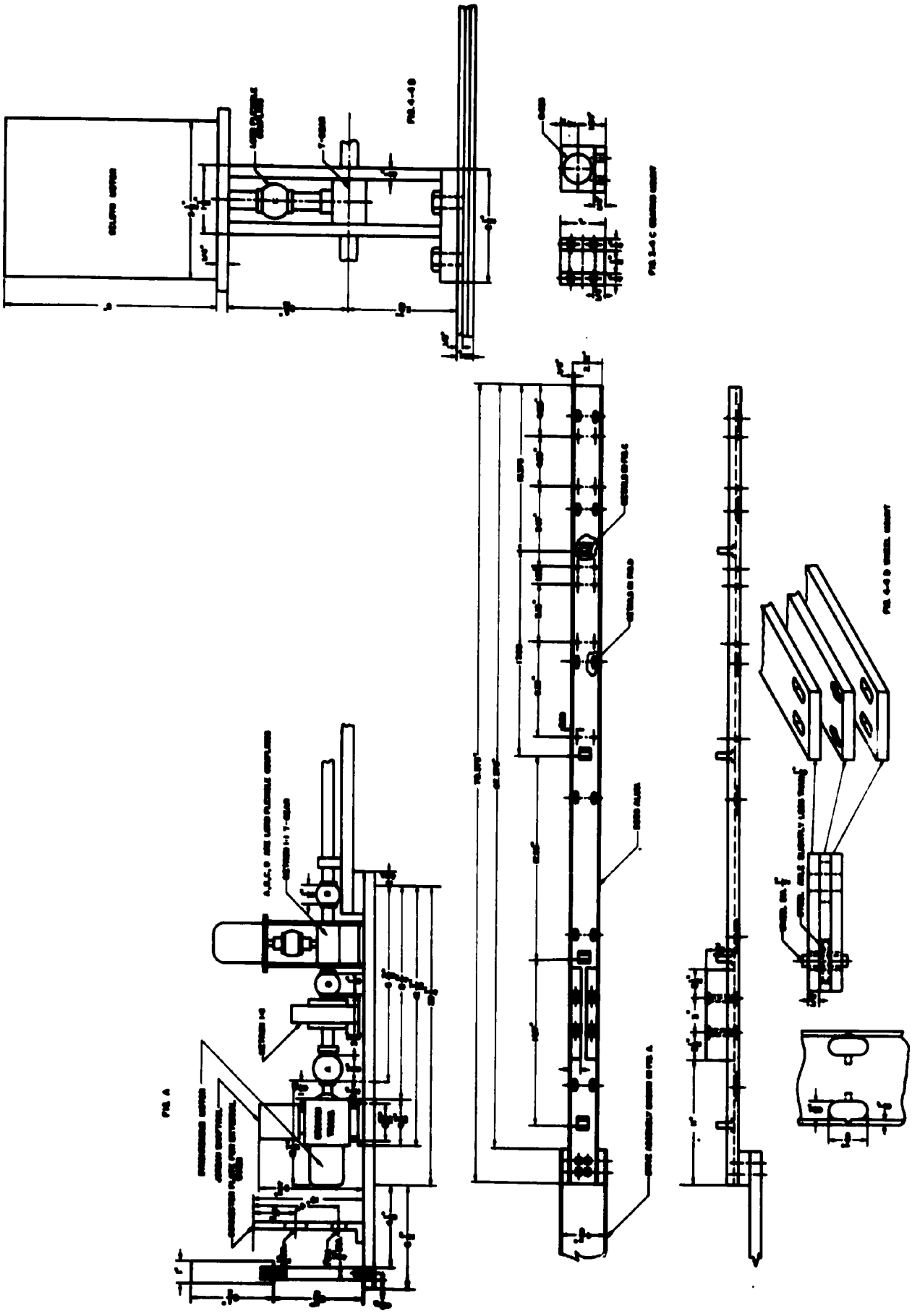


Figure 4.4. Oscillator Mount.

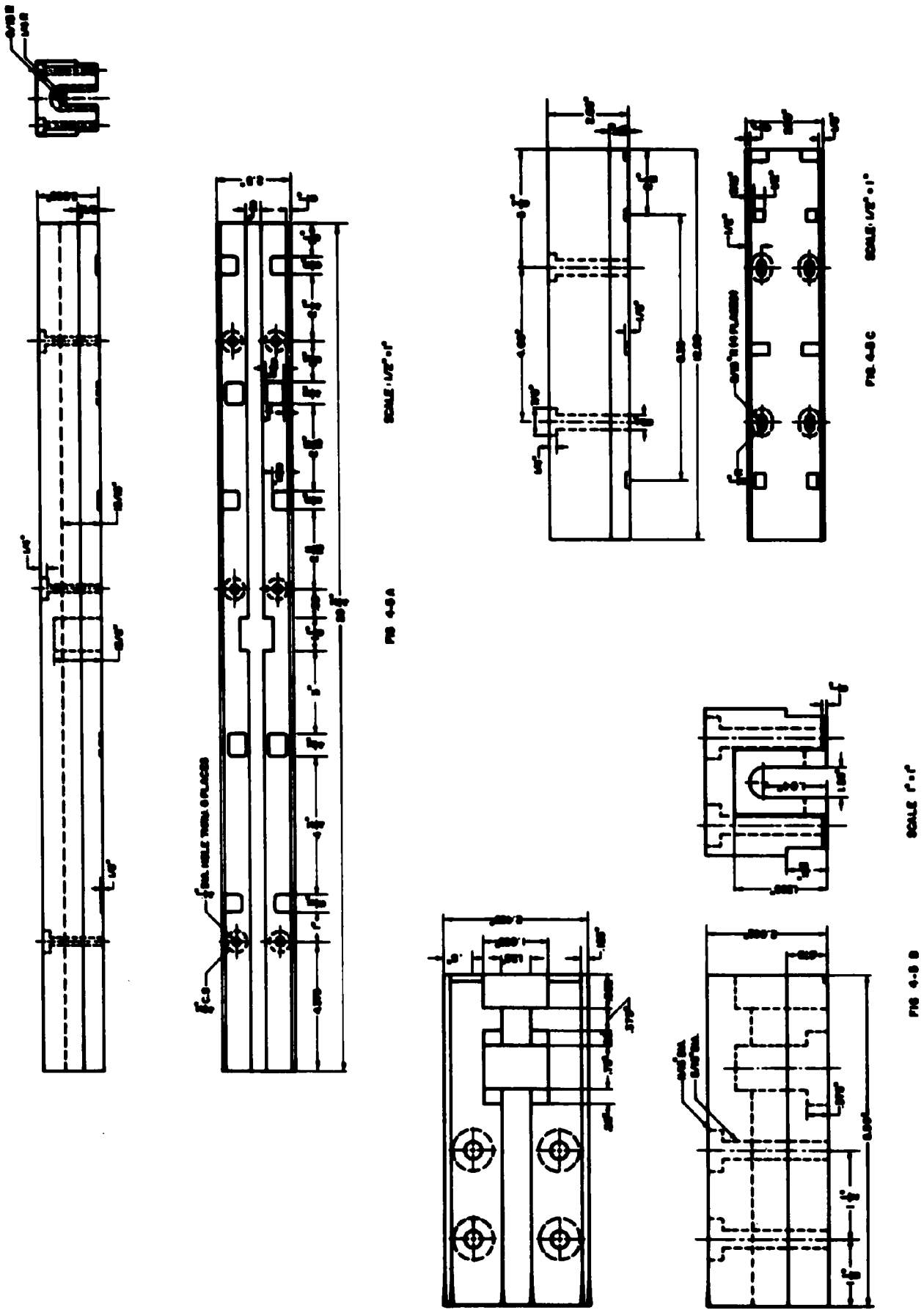


Figure 4.5. Reactor Grade Graphite Fillers.

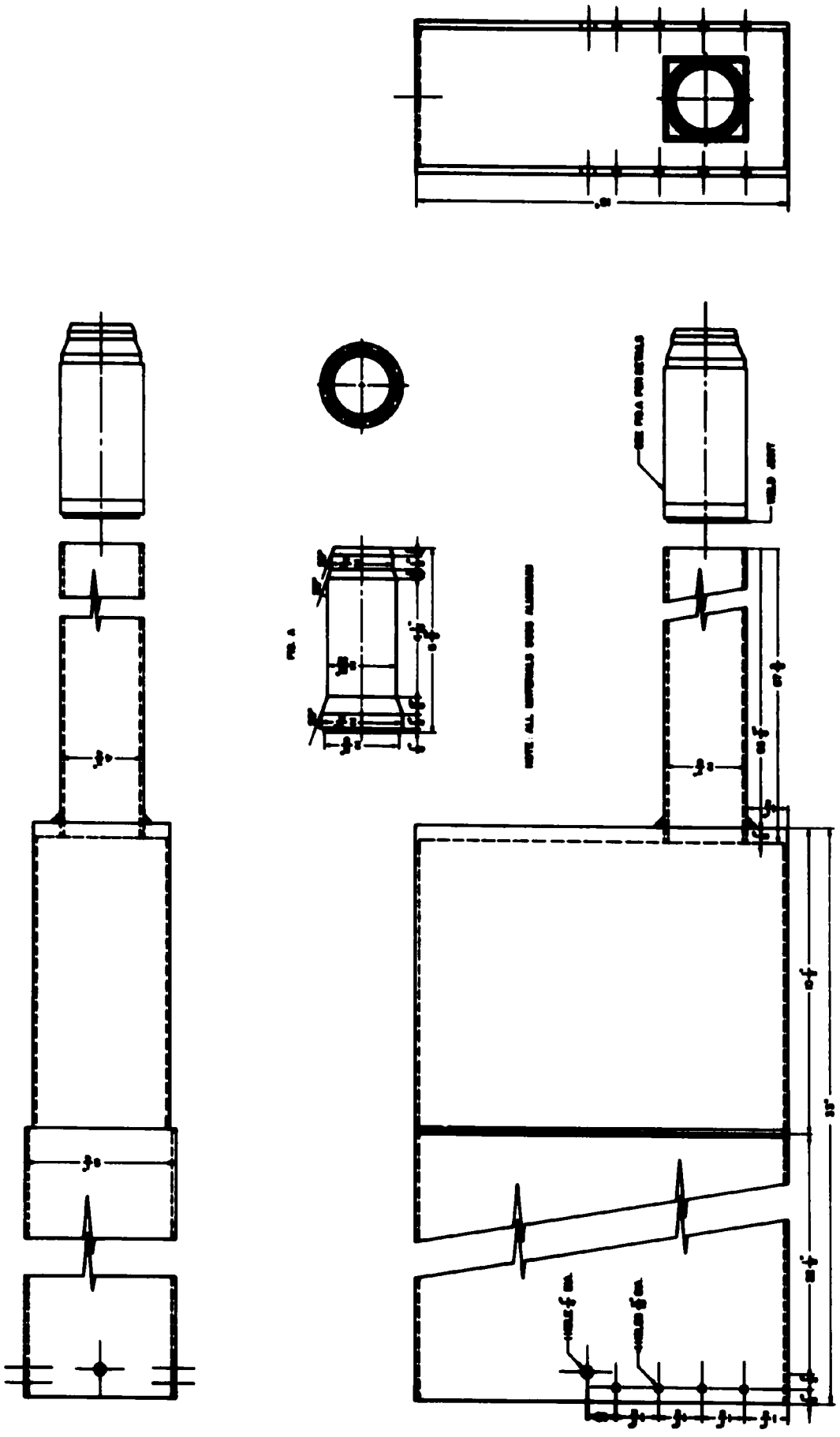


Figure 4.6. Oscillator Container.

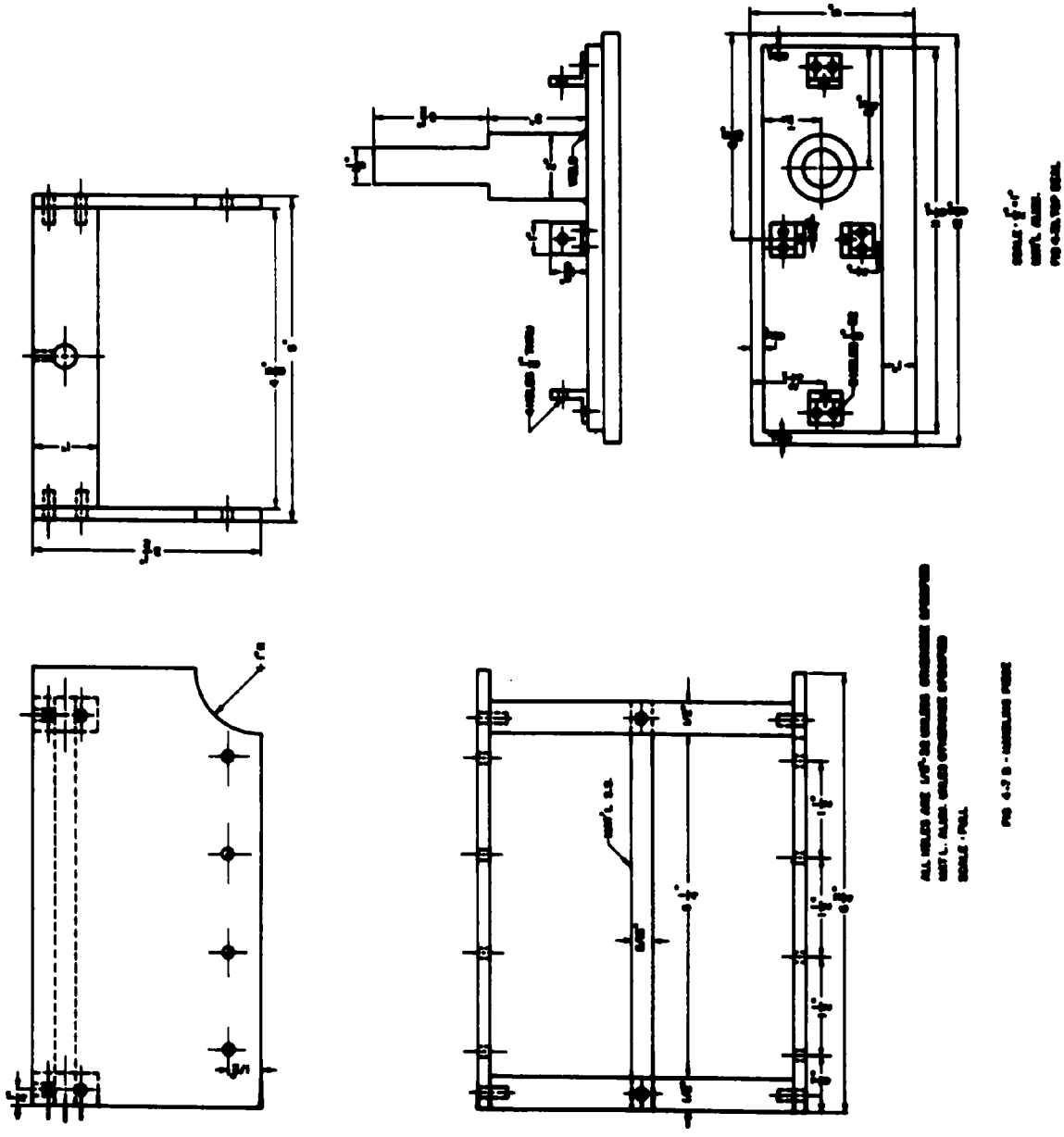


Figure 4.7. Oscillator Container Handling Piece and Seal.

Because the oscillator had to be removed from the container many times, and because of its awkward size and shape, it was imperative to make its removal as simple as possible, consistent with the problems of handling the loaded container, and keeping it watertight. The oscillator was designed to roll into the container. The container was welded together along all seams, leaving only the top open. The top seal was dependent on a heavy removable top plate, Figure 4.7A, through which all electrical connections passed. The plate fit loosely into the top opening, but could be held firmly in place by bolts to the container walls. The top was sealed by filling the space between the plate and the container walls with a heavy, pliable, caulk-like compound, Apeizon Q, usually used in vacuum systems. The compound was pressed around the sealing edges until a depth of about one inch was reached. This type of seal was very reliable. After the seal was finished, the handling piece, Figure 4.7B, was screwed on, supported by the container's walls. The time required to prepare the container for pool insertion was about 45 minutes.

Cadmium Absorbers

It was required that the change in reactivity introduced by the rotating absorber in the reactivity oscillator be as close to a sinusoid as possible. It was considered mechanically simpler to design a system in which a shaft rotated at a high frequency than one in which an absorber was pulled up and pushed down at a fast rate. Assuming a flat flux, the first approach to the problem of what shape absorber to use was to find a surface whose partially exposed area varied sinusoidally with fixed angular frequency. A derivation for the general class of functions satisfying this condition is given in Appendix A.

A piece of cadmium, which is black to thermal neutrons, is held stationary. Another black piece of cadmium is rotated so that part of its surface is behind the fixed cadmium piece and part is exposed to thermal neutrons which would not have otherwise interacted with the fixed cadmium piece. For this experiment, both cadmium pieces were 30 mils thick. The fixed cadmium piece weighed 6.787 grams and the rotating piece weighed 6.839 grams. The fixed piece was glued to the carbon inserts described in the next section. The rotating cadmium piece was glued to a lucite disk. The lucite was chosen for its thermalization properties. The spacing between the two cadmium pieces was about 1/64 inch. A 5.0 gram piece of lead was inserted into the lucite, opposite the center of gravity of the cadmium, to minimize shaft deflection at higher speeds.

When the oscillator assembly is positioned in the reactor, the cadmium is located at a point corresponding to the center of the axial fuel distribution.

Graphite Filler

In order to minimize the perturbation in the neutron flux distribution of the Ford reactor, due to the oscillator apparatus, practically all otherwise empty space inside the container was filled with reactor grade graphite. The graphite filled the container from the matrix plug to above the core surface. Three graphite pieces were machined, shown in Figures 4.5A, 4.5B, and 4.5C, in such a way as to allow easy removal of the lucite disk. The clearance between the graphite and the inside walls of the container was about 1/16 of an inch.

Oscillator Mount and Shaft

The oscillator mount is shown in Figure 4.4. The long sides of the mount were bent for strength. The mount was made by riveting three pieces of 1/8 inch aluminum together, after the axles and wheels had been positioned in the center piece, see Figure 4.4D. The distance between shaft supports was made large to minimize the amout of iron, in the form of ball bearings, in regions of high neutron flux. Most of the aluminum in the mount was the same alloy used in making the container, 5056.

The drive shaft was made by connecting two pieces of drill rod. At speeds above 50 cycles per second, the shaft vibrated, unless it was very straight. Two additional bearings would relax this requirement. Eleven pounds of lead was added to the mount to improve underwater maneuverability of the loaded container and insure good seating in the reactor matrix plate.

Shaft Drive

A 1/8 horse power Doerr standard induction motor was connected to a Graham transmission, model 20M. The motor operated on 3 phase, 60 cycle, 220/440 volts, at a constant speed of 3450 r.p.m. The Graham transmission was chosen because its speed range was continuously variable from 0 to 1100 r.p.m. The shaft speed was increased by a factor of 6 by a Metron bantam gear connected to the Graham output shaft, giving a maximum speed of 110 cycles per second at an output torque of 6 inch-pounds.

The Graham transmission was designed to operate in a vertical position with its output shaft down. There was a rapid loss of transmission fluid when the Graham was operated horizontally. The location of the Graham on the mount is shown in Figure 4.4A.

Speed Control

Remote control of the shaft speed was accomplished by a Jordan Shaftrol, model SM-10 and a Jordan Dialtrol, model d-59-S. The Shaftrol was mounted on top of the Graham transmission. A change in setting of a reference potentiometer in the Dialtrol caused the Shaftrol to change the speed position of the transmission, until the error signal between the Shaftrol and the Dialtrol was effectively zero. The Dialtrol was calibrated from 0-100% of maximum shaft speed.

Shaft Position and Speed Monitor

In order to calibrate the worth of the cadmium disk, the position of the shaft must be known. A 1 to 1 T-gear was attached to the output of the 6 to 1 speed stepup gear, and a synchro generator mounted on its leg shaft, see Figure 4.4B. The sychro was made by Bendix, MK4, model 4, type 5F, 115 volts, 60 cycles per second. It was heavy duty, weighing about 4 pounds, and transmitted considerable torque through the corresponding synchro motor located outside the pool. A disk, 10 inches in diameter, was mounted on the output shaft of this latter synchro motor. The disk was calibrated in 2 degree intervals from 0 to 360 degrees. Four holes were made in the disk at spacings of 90 degrees. The position of the oscillator shaft could be read within $\pm 1/2$ degree from the calibrated disk.

The speed of the oscillator shaft was measured by means of the phototube-Schmidt trigger circuit shown in Figure 4.8. A small light was placed behind the calibrated disk. As each of the 4 holes in the disk passed the light, the phototube, placed opposite to the light, would develop a current and consequent voltage drop on the input grid of the Schmidt

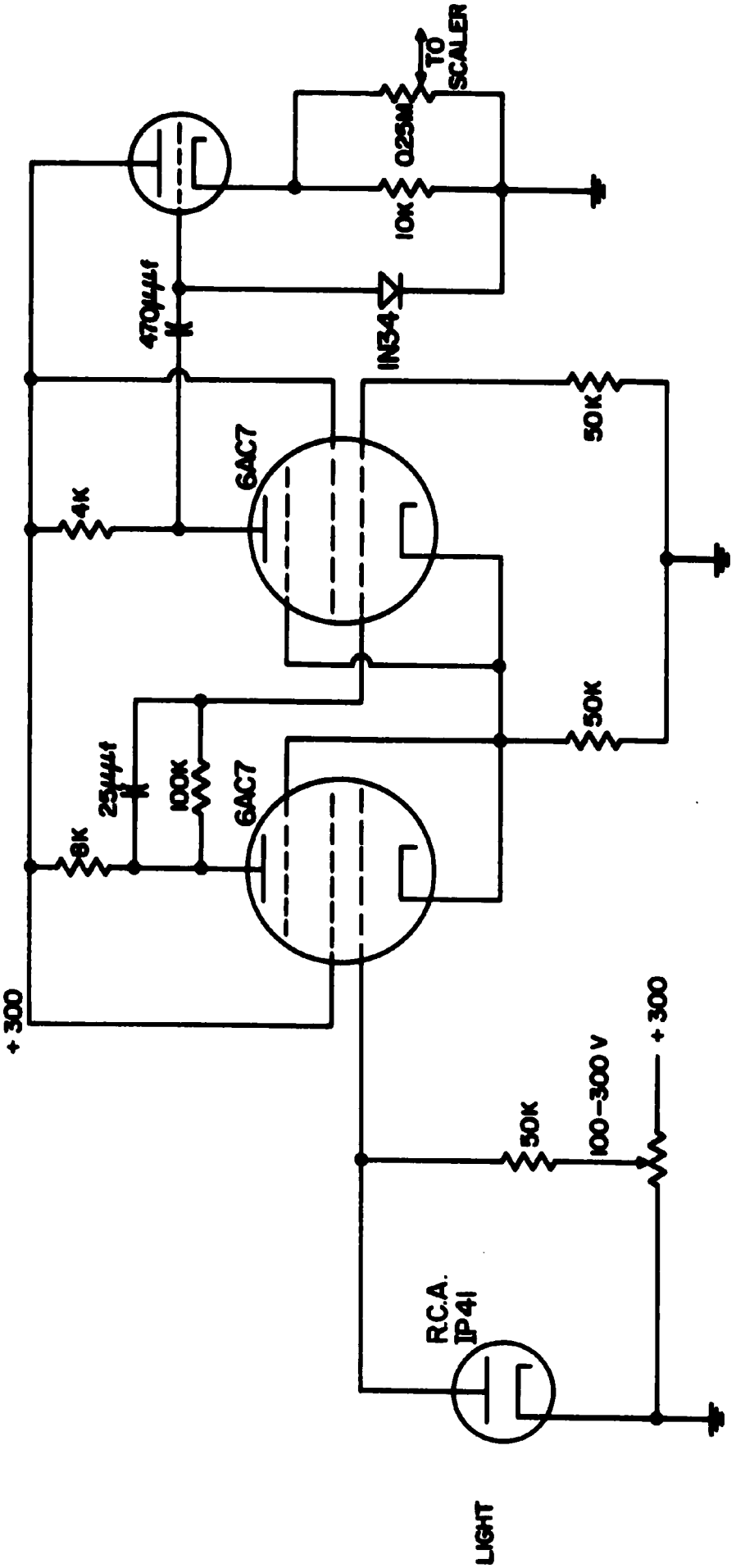


Figure 4.8. Phototube - Schmidt Trigger.

circuit. The Schmidt gave a voltage pulse when the light hit the phototube and when the light stopped. The diode on the input grid of the output cathode follower suppressed one of these pulses. The output pulses, about -5 volts with a fast rise time, were fed to a Tracerlab utility scaler and counted for a preset time. The number of recorded counts (divided by 4 times the counting time) gave the shaft speed within 1/4 of a revolution per counting time. The synchro motor speed was checked with a stoboscope. The oscillator shaft speed and the synchro speed were identical from 0 to 50 cycles per second. Higher speeds were not checked, since they were not used in this experiment.

System Pressure

A 3/8 inch tygon tube was passed, along with all electrical connections, through the 1 inch tygon tube from the surface to the oscillator container. The small tygon tube was connected to a compressed air supply available in the reactor building. The large tygon tube was clamped partially shut on the surface end and a balance between air flow rate and clamp pressure was reached which put about 4 to 5 pounds per square inch (gage) on the container. The air flow at a positive gage pressure served two purposes. First, was to insure that the container would not leak due to the 25 foot head of water and second, to prevent the Doerr motor and Graham transmission from overheating. As an additional safety feature, cotton resistance wire was connected to the oscillator mount and its resistance measured on the surface. If the measured resistance had dropped from "infinity" to about 10,000 ohms. it would have shown that the container was leaking. A thermocouple located on the base of the Jordan Shaftrol

monitored the motor temperature throughout the experiment. Because of the forced air flow, the temperature of the motor never exceeded the normal operating level of 130 to 150 degrees Farenheit.

CHAPTER V

EXPERIMENTAL RESULTS

A description of the methods used to compute the following results is given in Chapter VI, Section A.

A. Moments

The ratio of the variance to mean number of detected neutrons as a function of detection time was computed from the magnetic tape records of the fluctuation in neutron density. The results are presented in Figures 5.1, 5.2, 5.3, 5.4 and 5.5 for lattice loadings designated in Chapter III as I - Noise, I - 1/2 c.p.s., I - 10 c.p.s., IV - Noise, and V - Noise, respectively. The number of data points or gates for each gate length, and the calculated mean and ratio of the variance to the mean, from which these figures were constructed, are listed in Appendix F.

B. Autocovariance Function

The exponentially weighted autocovariance functions, presented in Figures 5.6, 5.7, 5.8 and 5.9, were obtained from data taken while using lattice loadings I - Noise, I - 10 c.p.s., V - Noise, and the tape record of Albrecht's data[5] referred to as BF_3-1, respectively.

C. Power Spectral Density Function

Exponentially weighted power spectral density functions are presented in Figures 5.10, 5.11, 5.12, 5.13, 5.14, and 5.15. These functions were obtained from data taken while using lattice loadings I - Noise, I - 1/2 c.p.s., I - 10 c.p.s., V - Noise, and BF_3-1.

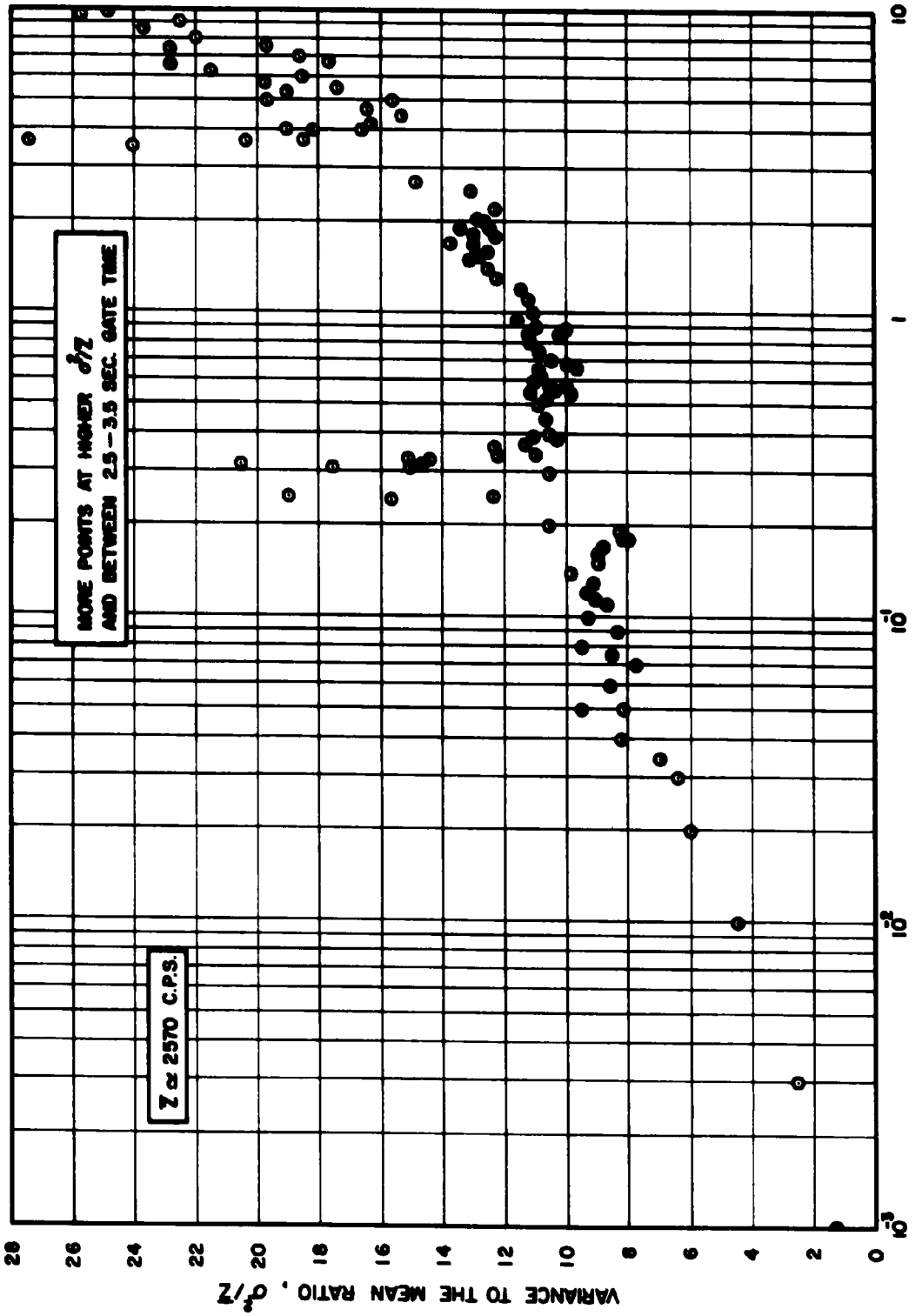


Figure 5.1. Ratio of the Variance to the Mean vs. Gate Time, Loading I - Noise.

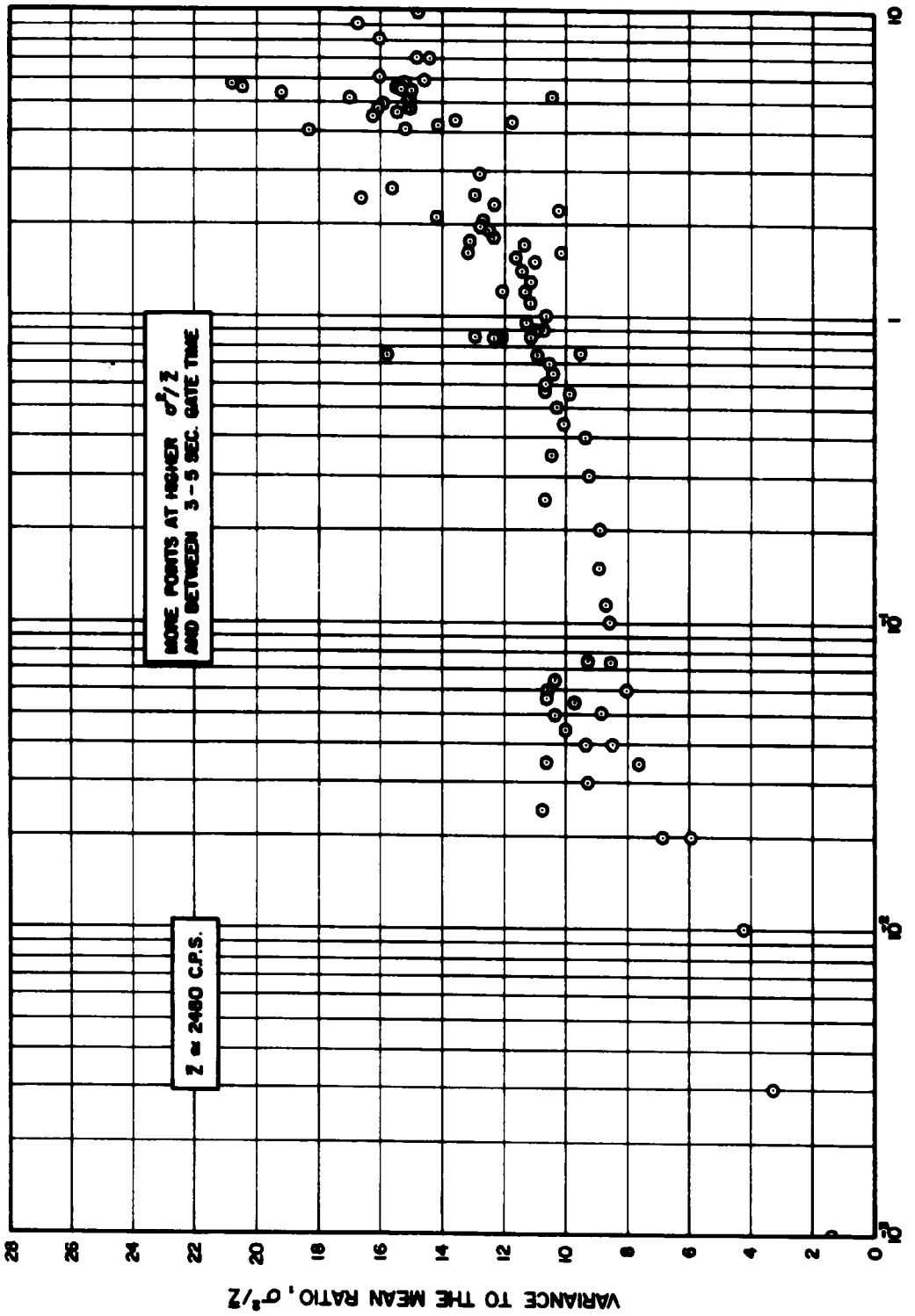


Figure 5.2. Ratio of the Variance to the Mean vs. Gate Time, Loading I - $\frac{1}{2}$ c/s.

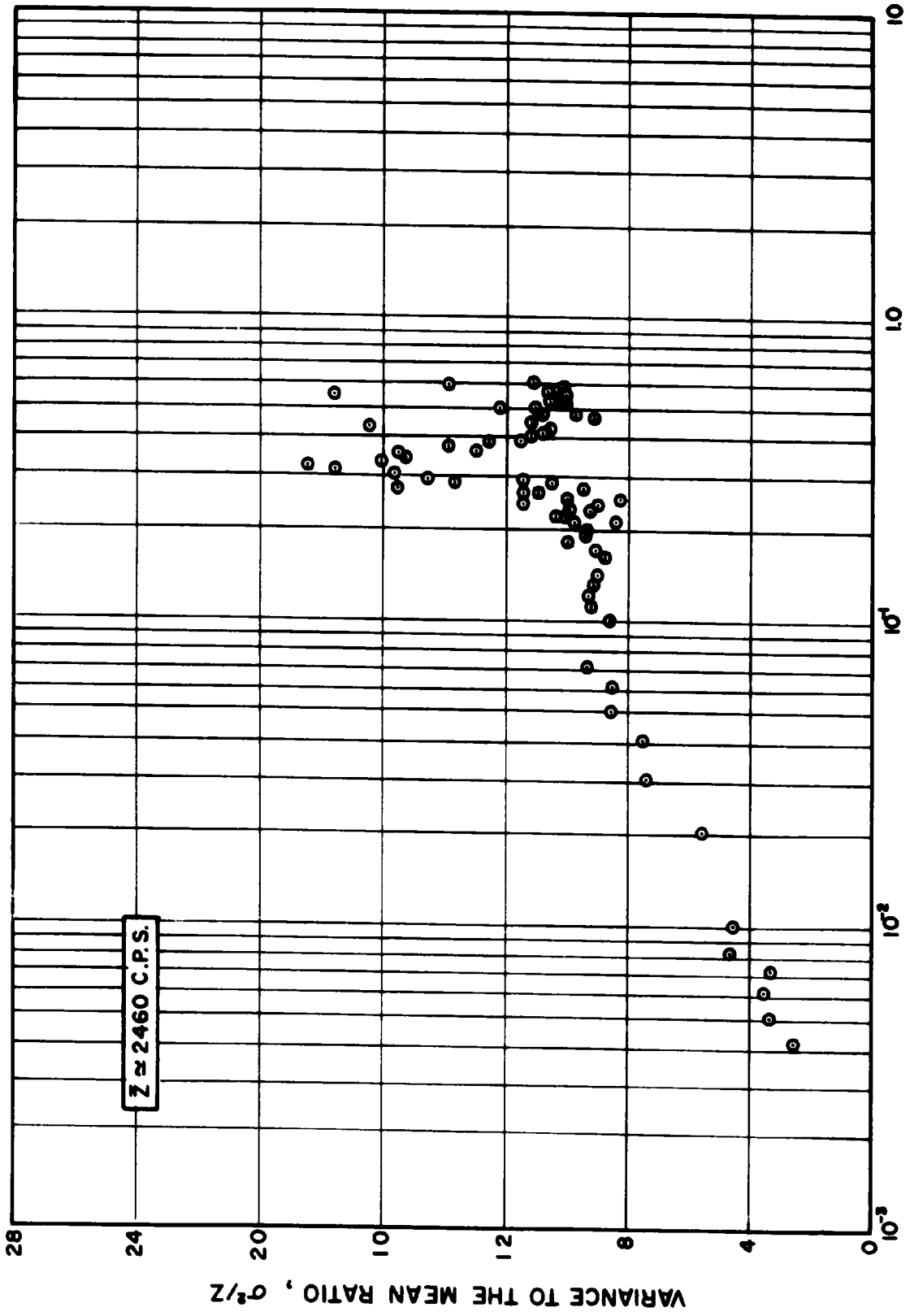


Figure 5.3. Ratio of the Variance to the Mean vs. Gate Time, Loading I - 10 c/s.

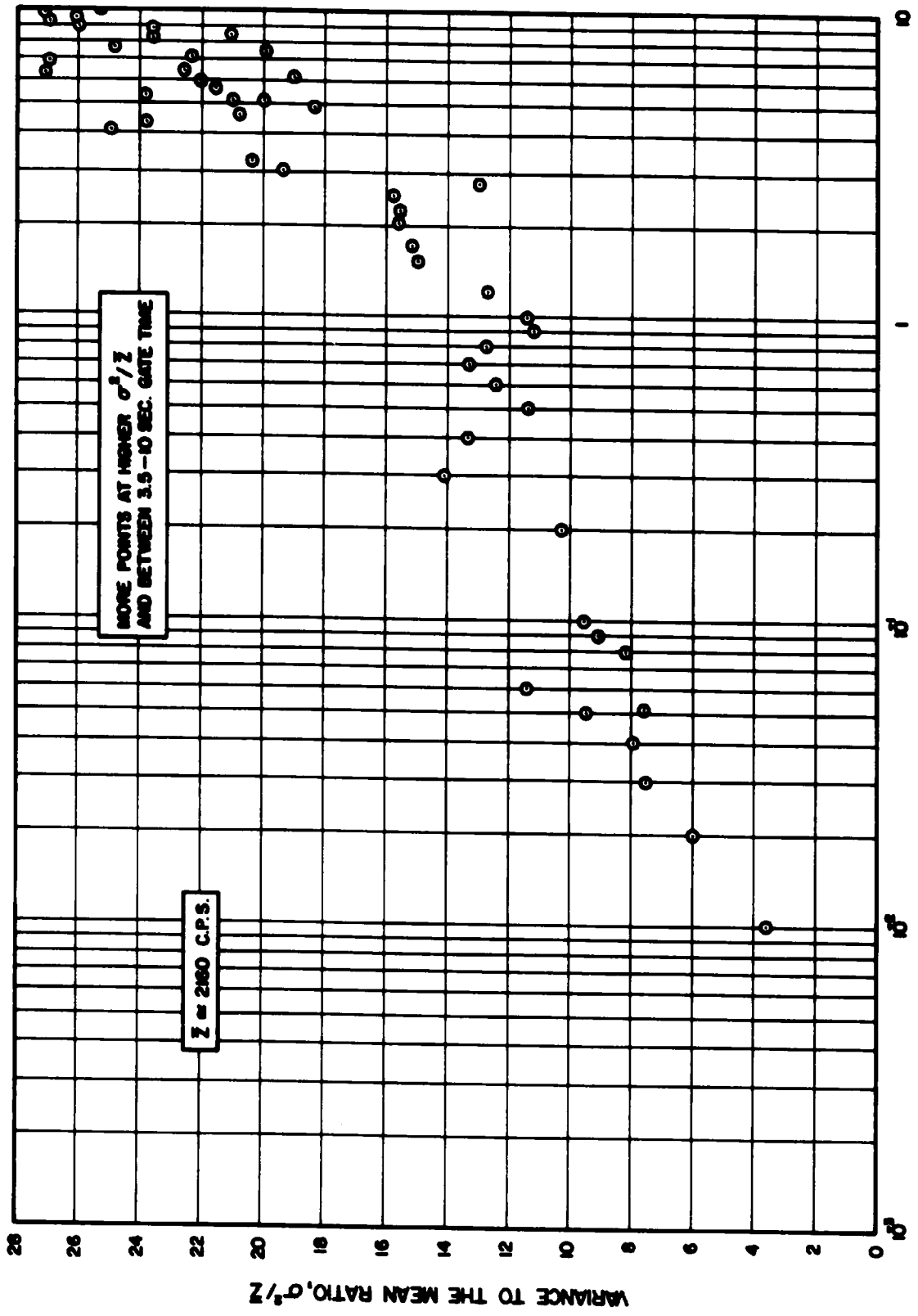


Figure 5.4. Ratio of the Variance to the Mean vs. Gate Time, Loading IV - Noise.

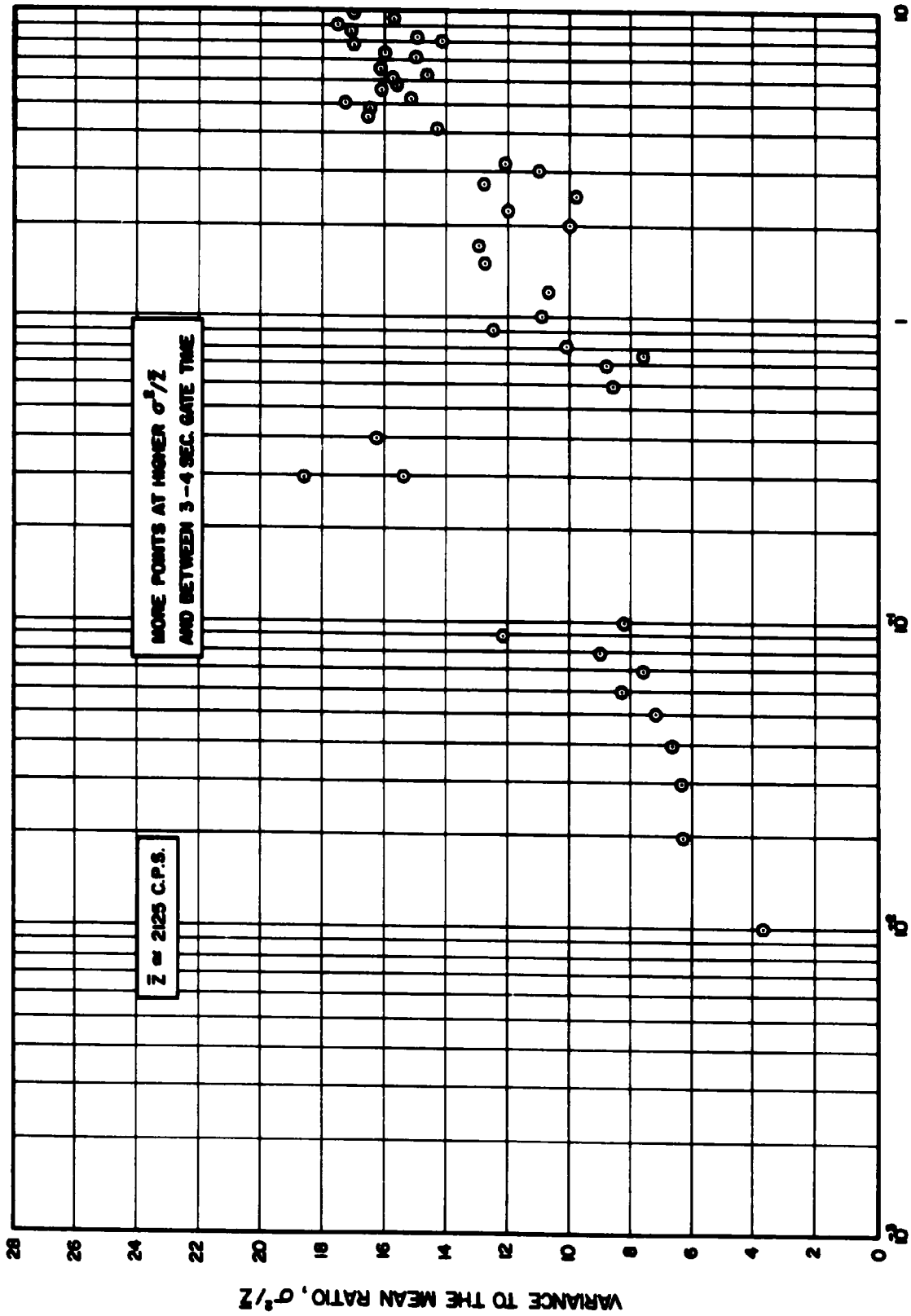


Figure 5.5. Ratio of the Variance to the Mean vs. Gate Time, Loading V - Noise.

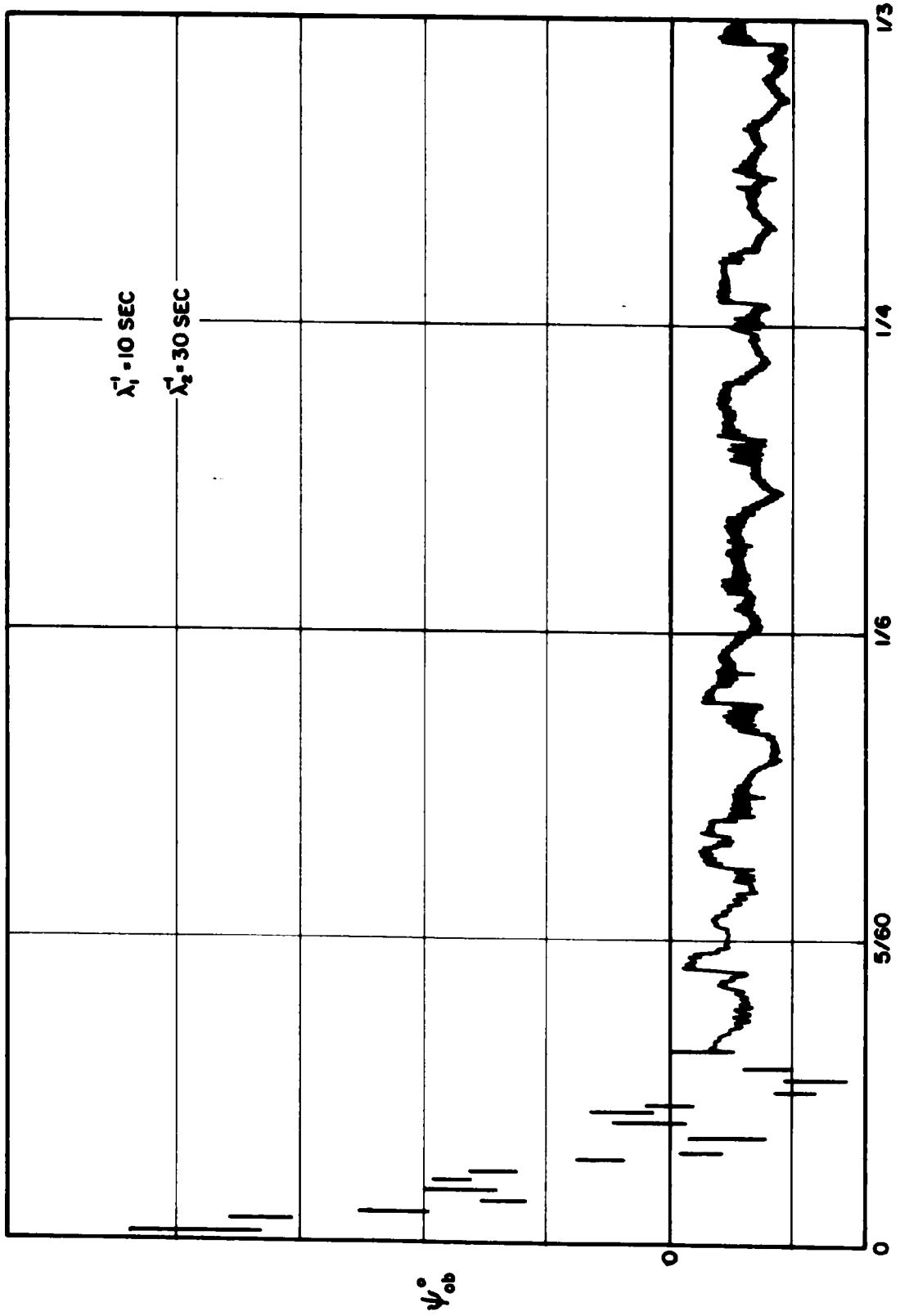


Figure 5.6. Autocovariance Function, Loading I - Noise.

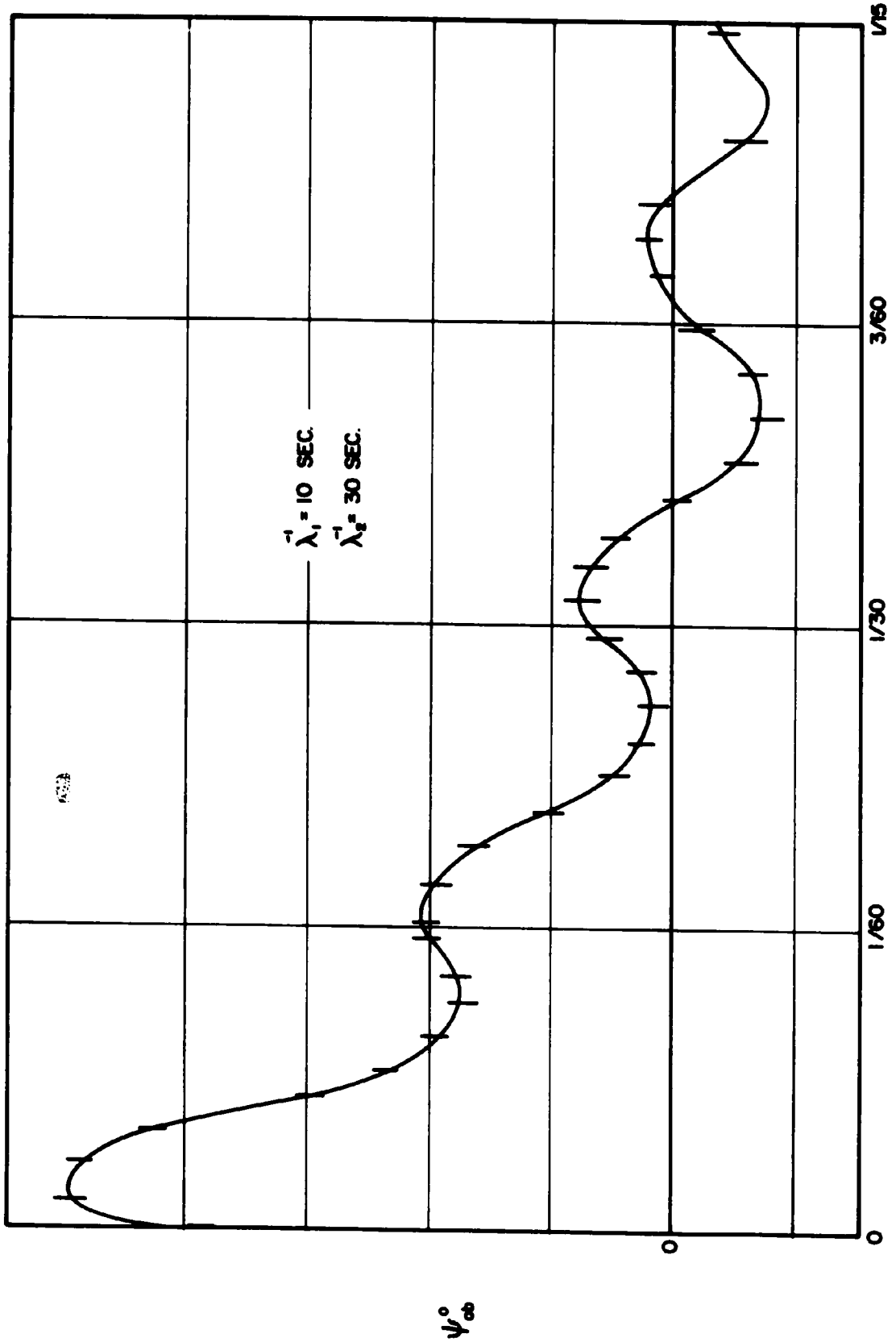


Figure 5.7. Autocovariance Function, Loading I - 10 c/s.

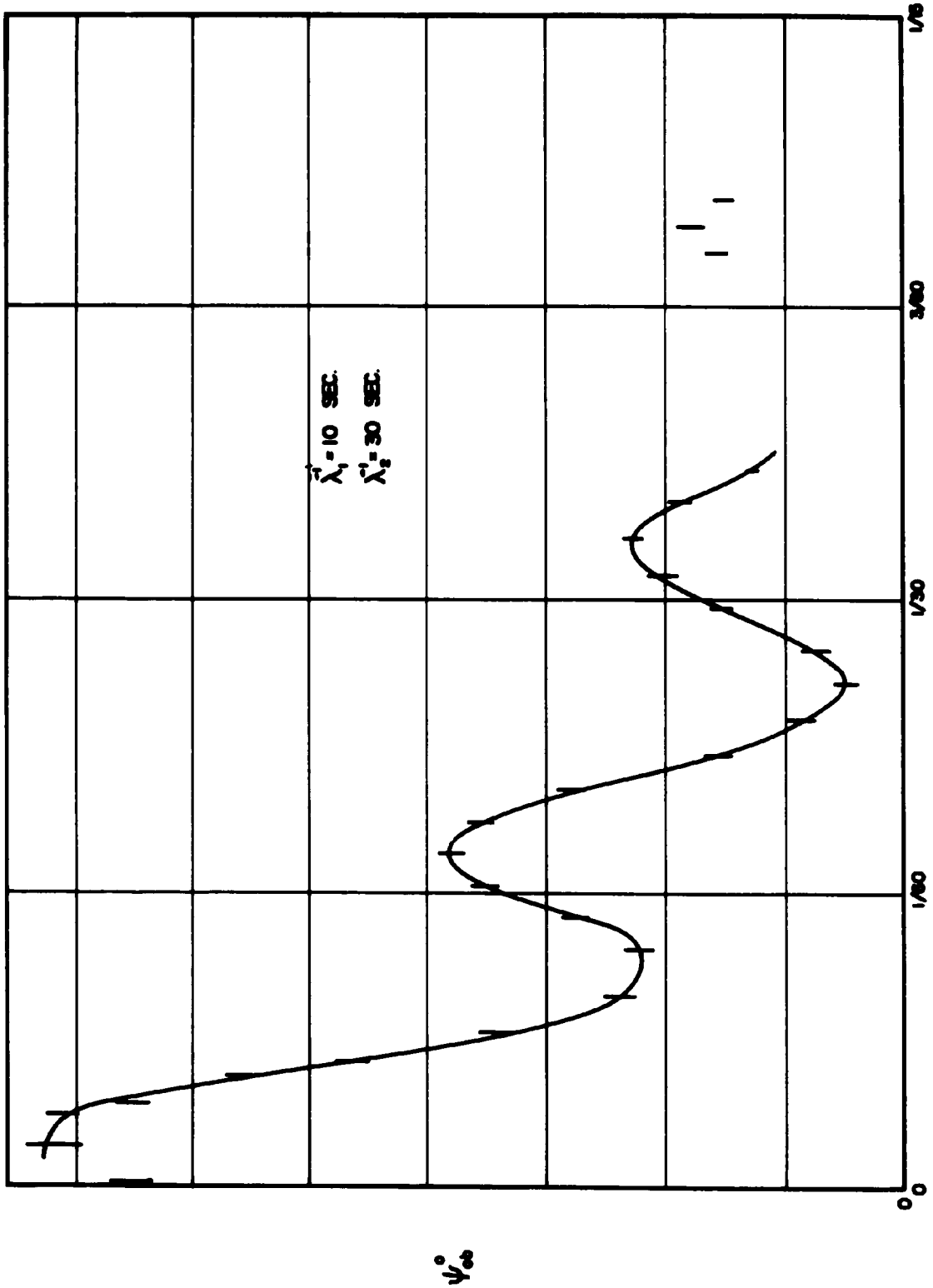


Figure 5.8. Autocovariance Function, Leading V - Noise.

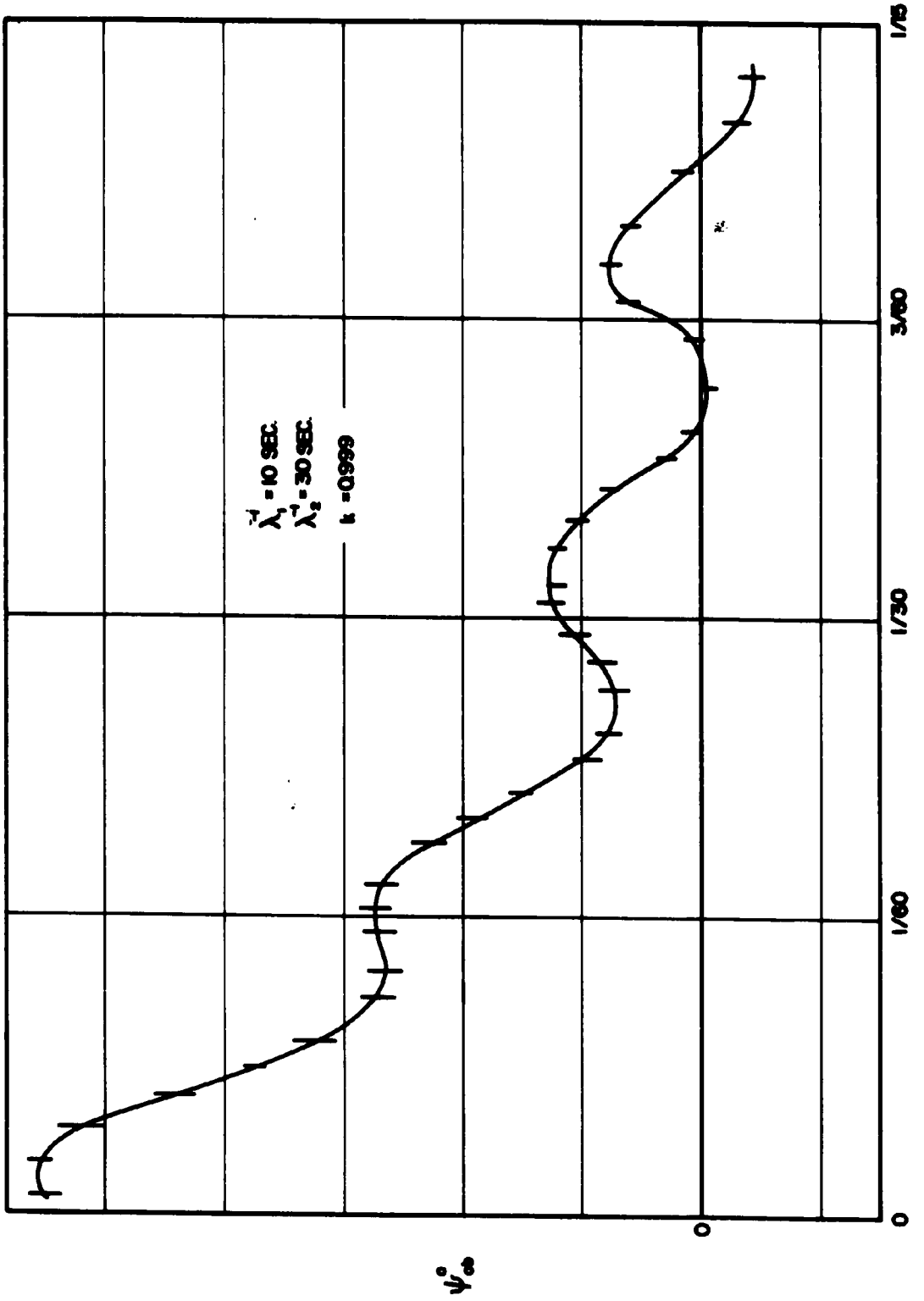


Figure 5.9. Autocovariance Function, Loading W_3 - 1.

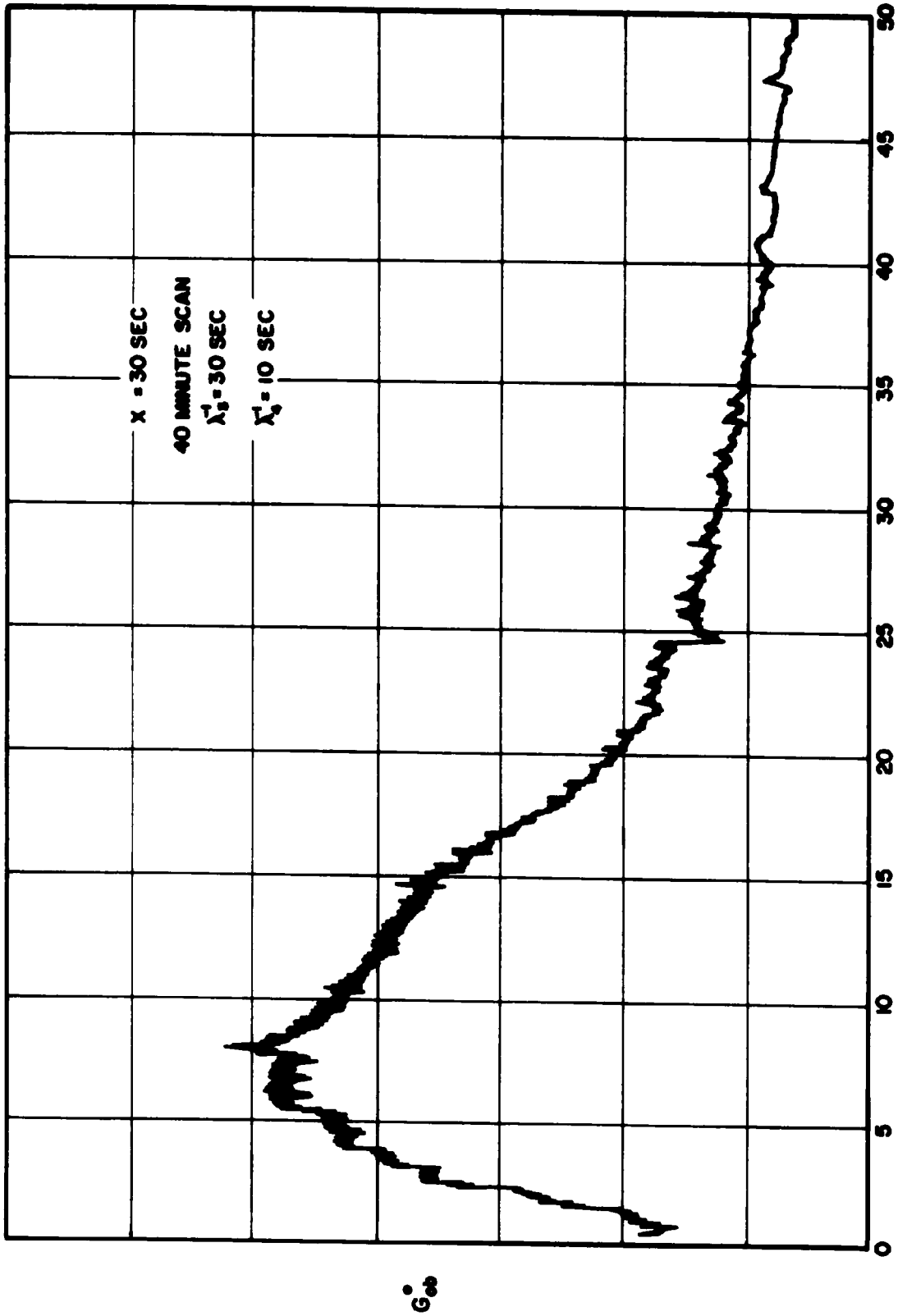


Figure 5.10. Power Spectral Density Function, Loading I - Noise.

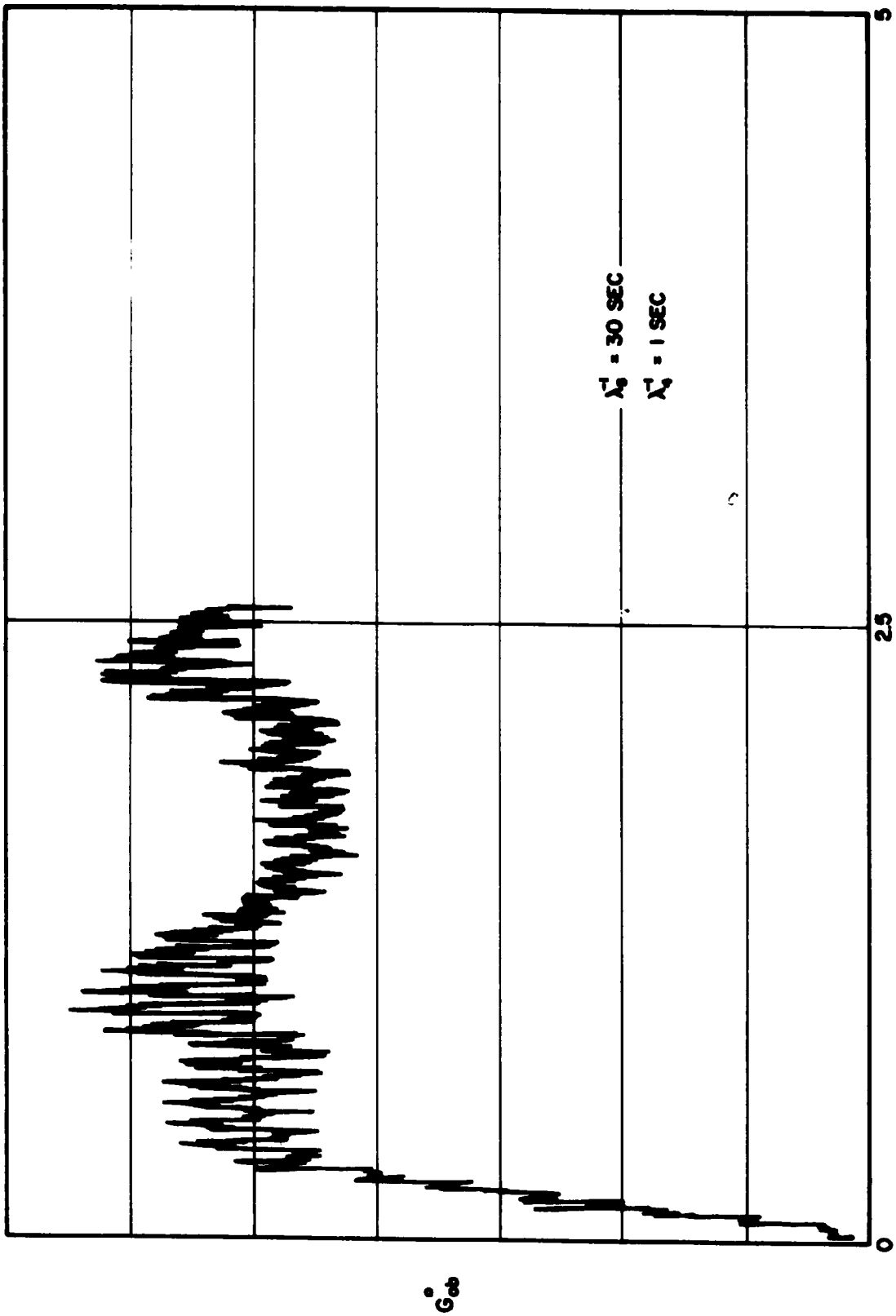


Figure 5.11. Power Spectral Density Function, Loading I - $\frac{1}{2}$ c/s.

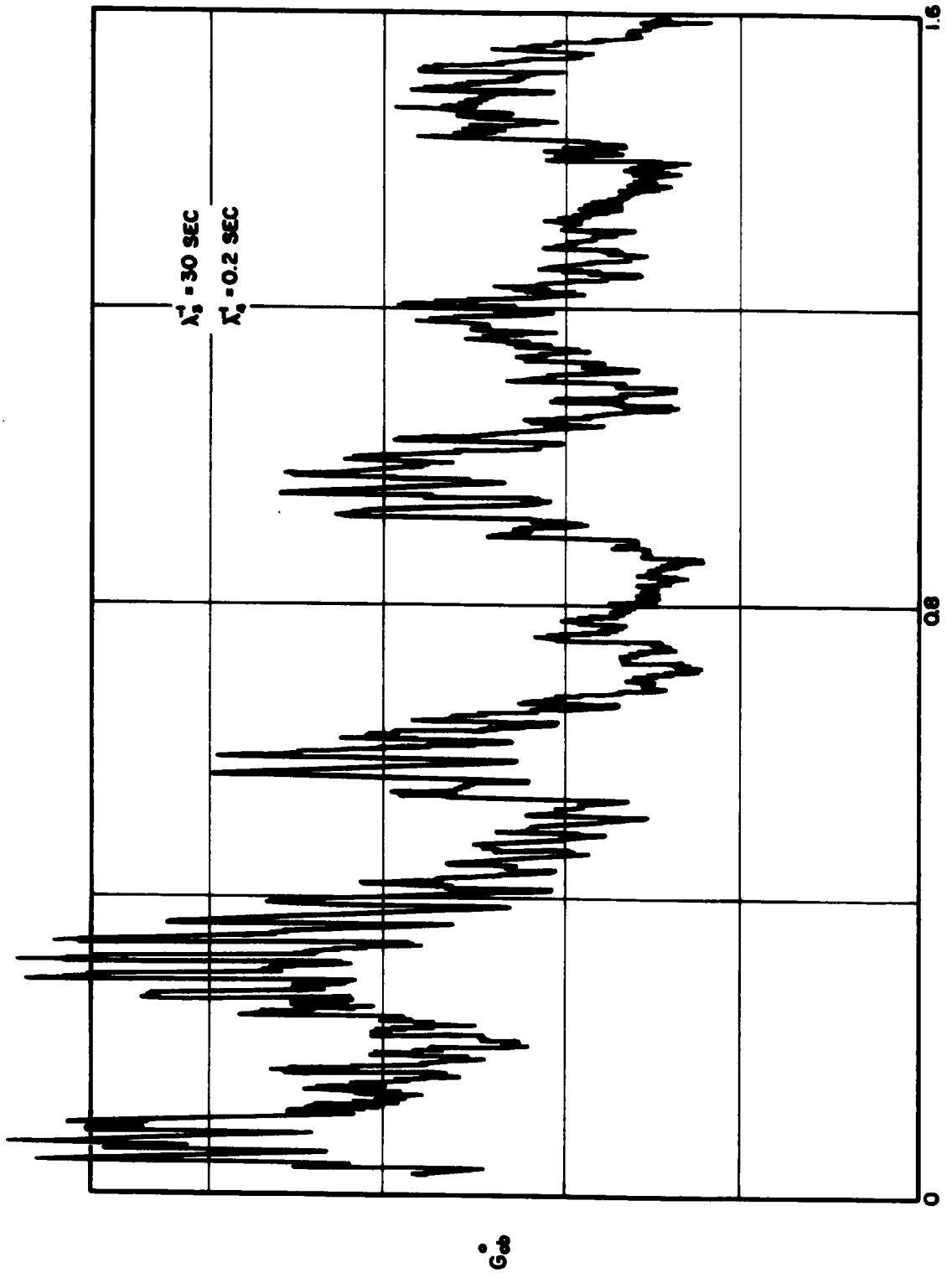


Figure 5.12. Power Spectral Density Function, Loading I - $\frac{1}{2}$ c/s

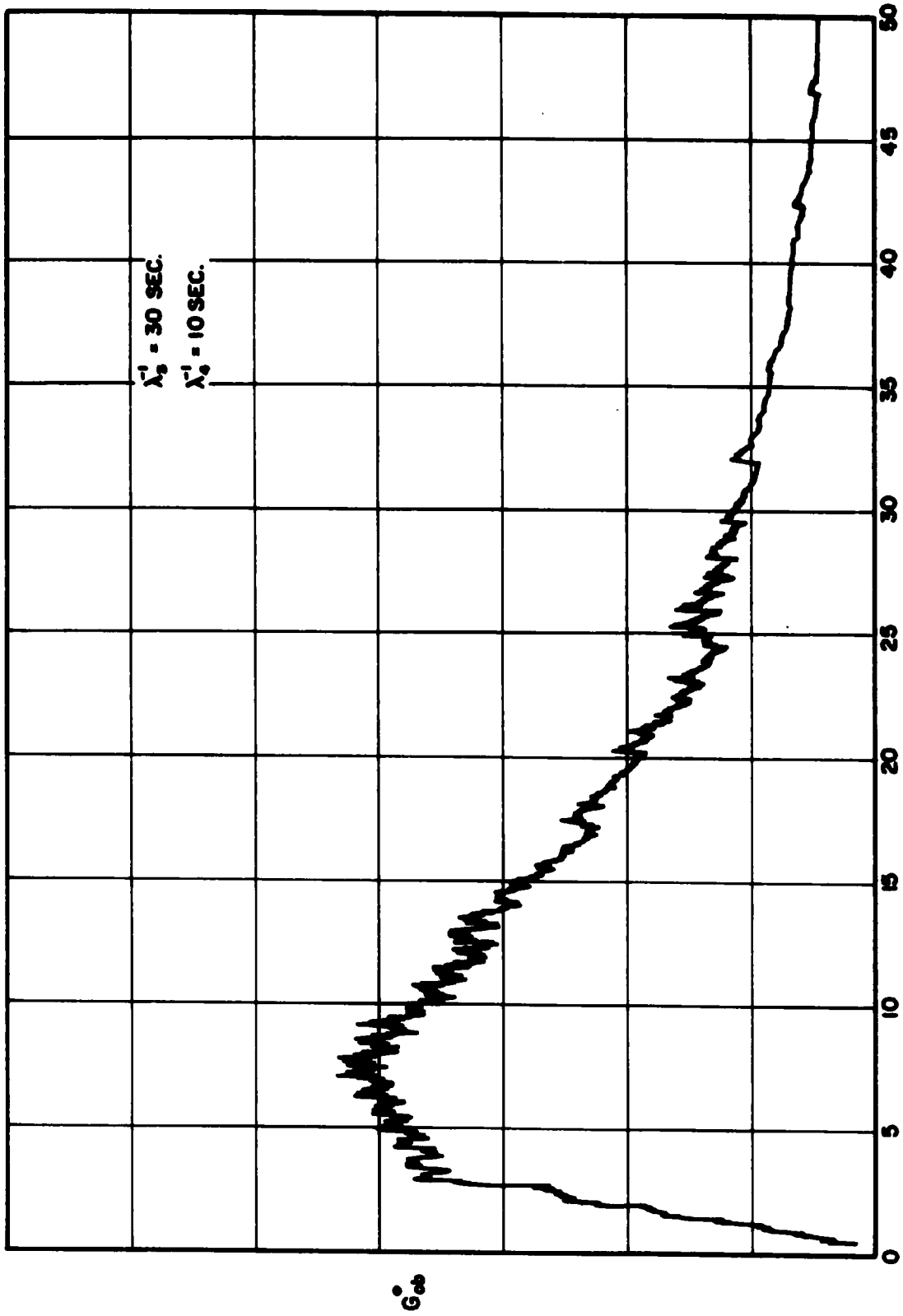


Figure 5.13. Power Spectral Density Function, Landing I - 10 c/s

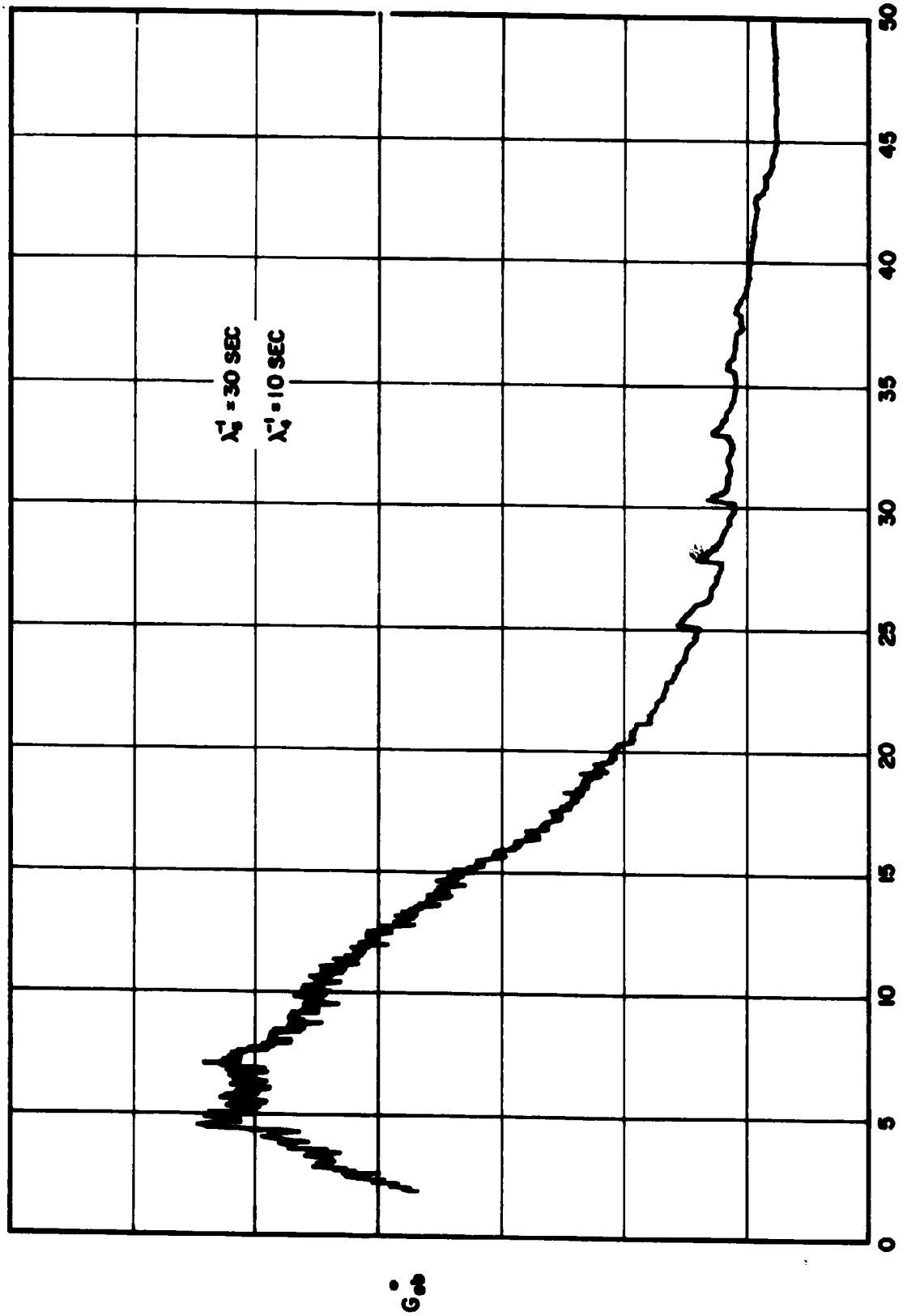


Figure 5.14. Power Spectral Density Function, Loading V - Roll

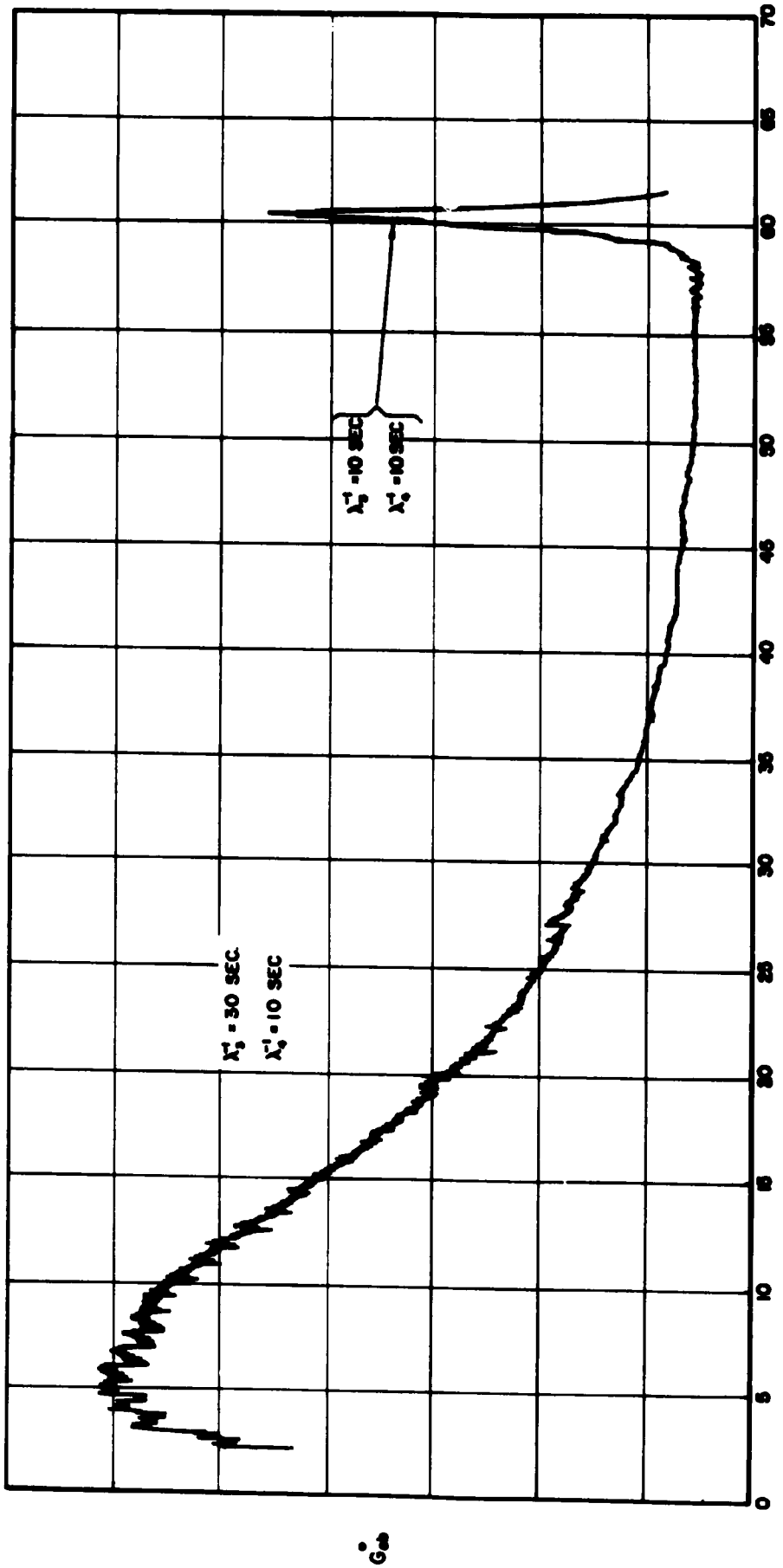


Figure 5.15. Power Spectral Density Function, Loading BF_3 - 1.

CHAPTER VI

DATA ANALYSIS

The only fluctuation data taken was in the form of discrete pulses, from a BF_3 chamber, recorded on magnetic tape. The analysis of this data has two distince phases,

A. Manipulate the original pulse data to obtain an experimental estimate of the moments, autocovariance function and power spectral density function

B. compare these estimates with the prediction of a model describing these quantities

A. Manipulation of Pulse Data

1. Moments

The first and second moments of the detected neutron population can be obtained from the magnetic tape records of the fluctuation experiment. Using the equipment described in Chapter IV, the number of pulses occuring on the tape for a fixed counting time or gate length was determined repeatedly, until sufficient data had been obtained for a statistically significant calculation of the ratio of the variance to the mean for that gate length. An exhaustive theoretical study of the statistical properties of this ratio is given in the literature.[34] As the gate length is increased, fewer gates are required to obtain a significant estimate of the ratio. This is convenient, because the time required to collect the data increases with increasing gate length.

The number of gates used in this work varied from approximately 100 for gate lengths near 10 seconds to greater than 1000 for gate lengths less than 1 second. Gate lengths from 0.001 to 9.999 seconds were considered.

Appendix F lists the number of gates, the gate length, mean number of detections and ratio of the variance to mean for the different lattice loadings used in this experiment. The digital computer program used to compute the mean and the ratio of the variance to mean from the gate data is given in Appendix G under the name VAROMEAN-WESTERVELT.

2. Autocovariance Function

An autocovariance function is defined in terms of a continuous function, rather than a series of discrete pulses. In order to compute an autocovariance function, it was necessary to convert the pulse data to an equivalent continuous function. The block diagram describing this operation is given in Figure 6.1. The general procedure was to measure the inverse time between successive pulses, i.e. an effective instantaneous detection rate, and use the resulting continuous function to frequency modulate the output of a voltage controlled oscillator. It is not necessary to record the detection rate information as FM. However, by using FM rather than AM, a more accurate estimate of the autocovariance function may be obtained, see Figure 6.1. The process of converting the pulse data to a continuous function and recording as an FM signal is described in more detail below. The electric tachometer measures the inverse time between pulses and supplies a continuous voltage between 0 and 1 volt, proportional to the inverse time, to the Kintel amplifier. The amplifier serves as an impedance match

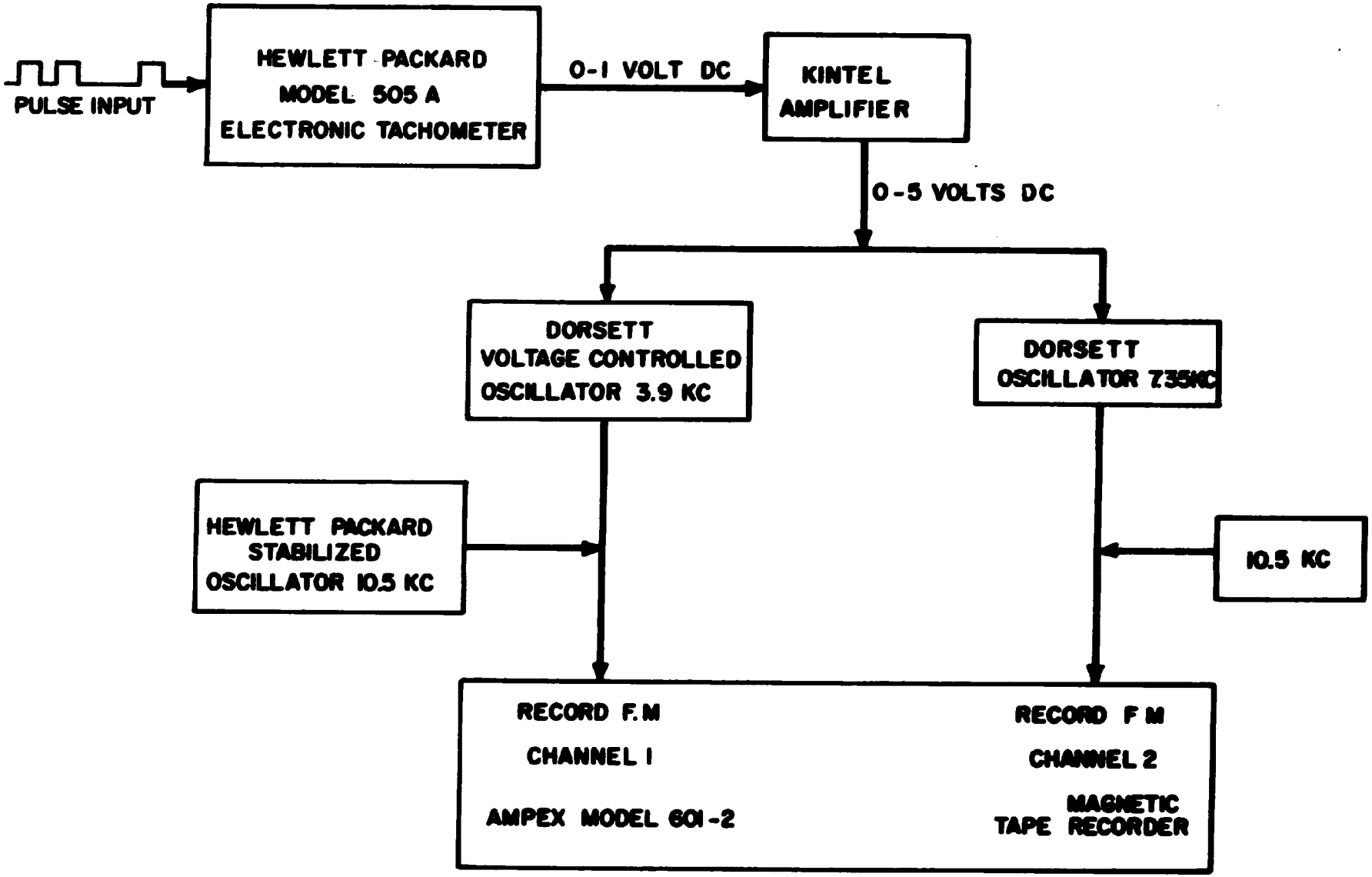


Figure 6.1. Block Diagram for Conversion of Pulse Data to a Frequency Modulated Recorded Signal.

between the tachometer and the Dorsett voltage controlled oscillators. The Dorsett oscillators have a 3.9KC and a 7.5KC center frequency. Their frequency modulated output may vary as much as ± 7.5% around the center frequency, depending on the amplitude of the voltage from the Kintel amplifier. Subsequent error in the computation of the autocovariance function due to changes in tape speed are effectively eliminated by recording a 10.5KC signal, concurrently.

The actual computation of the autocovariance function is performed by an analog computer. The FM signal is demodulated prior to the computation as shown in Figure 6.2. Note the time compensation feature to correct for small variations in tape speed during the computation.

As described in Figure 6.2, the demodulation system has 2 tape heads which monitor different channels of the tape. The position of one head is fixed. The other head can be positioned arbitrarily by means of a mechanical drive. The position of the movable head relative to the fixed head is known. To compute the autocovariance function, the average value of the product of the demodulated signal at both tape heads must be determined as a function of the time lag between heads. Two channels of information are required, because only one demodulation device was available for each of the recorded center frequencies (7.5KC and 3.5KC). Physically, it was impossible to have both heads reading from the same location on the tape. This difficulty was avoided by rerecording part of the FM tape in a special way. The movable head was positioned at an arbitrary location relative to the fixed head. Channels 1 and 2 of the original FM tape were then rerecorded through the movable and fixed heads onto another tape. A

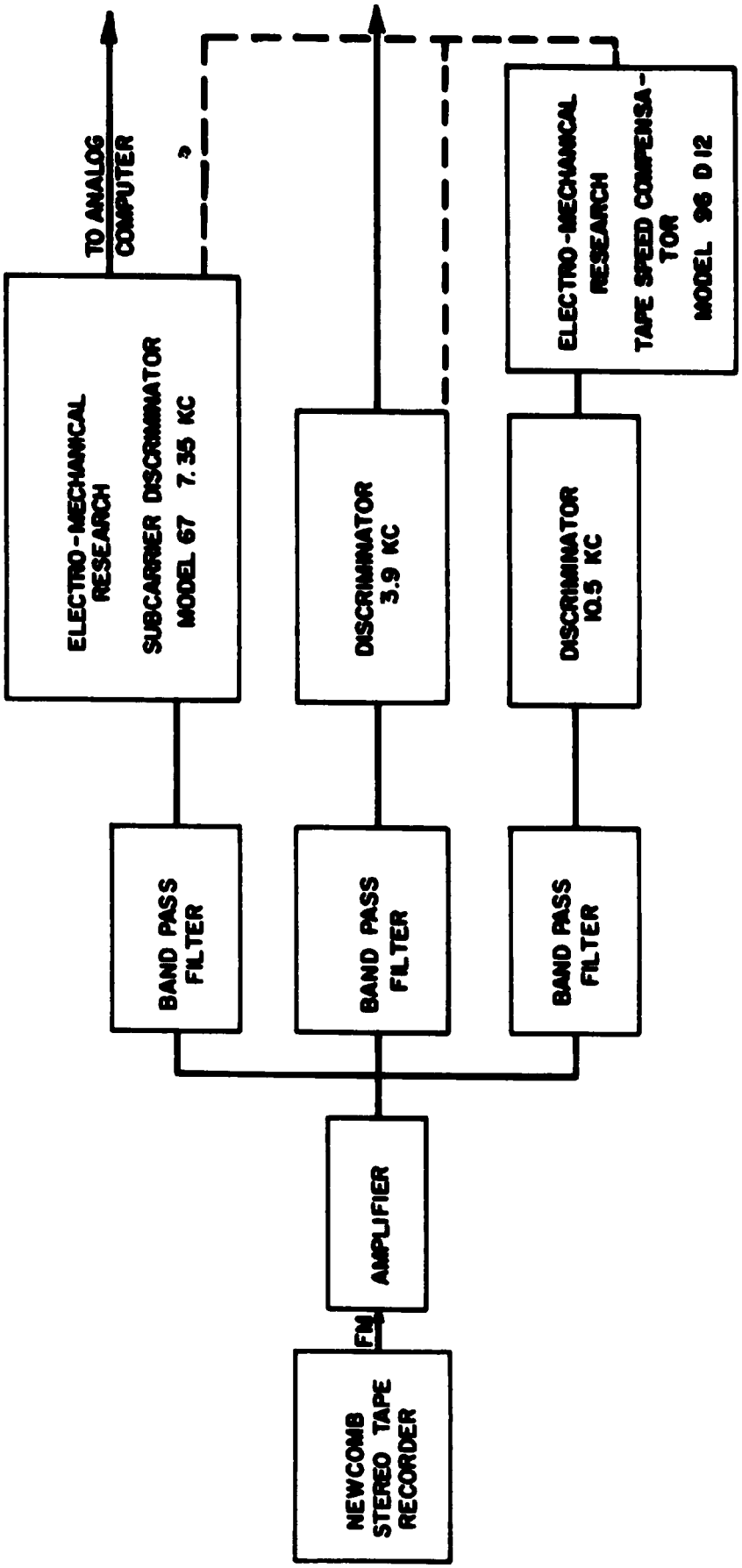


Figure 6.2. Signal Demodulation.

30 second tape loop was made from a representative portion of the new tape. Although the information in channel 1 and channel 2 is separated by the distance between the heads as the tape recording was made, there is zero time lag between the information seen by the heads in the reference position.

Since we have neither an infinite amount of data or time, it is necessary to estimate the autocovariance function. A well established technique,[35,36] for estimating the autocovariance function is to form an exponentially weighted autocovariance function from a tape loop. The basic definitions which are required to describe this estimated function are briefly outlined for completeness. For a continuous function, $y(t)$, define the exponentially weighted average, $y_{\lambda_1}(T)$,

$$y_{\lambda_1}(T) = \lambda_1 \int_0^T y(t)\, e^{\lambda_1(t-T)}dt \qquad (6.1)$$

This average is a function of the averaging time constant, λ_1^{-1}, and the averaging time, T. Due to the exponential decay of the weighting function, the weighting of values three time constants prior to t is 5% of the present weighting. The choice of λ_1^{-1} determines how much weight is given to past events. Since the tape loops used are 30 seconds in duration, λ_1^{-1} of 10 seconds was chosen. For this value of λ_1^{-1}, the weight of past events has dropped to 5% after 30 seconds. Define the difference between the function and its average value to be

$$Y_{\lambda_1}(t) = y(t) - \overline{y_{\lambda_1}(T)} \qquad (6.2)$$

The exponentially weighted autocovariance function is defined by the expression,

$$\overset{\circ}{\psi}(\tau, T, \lambda_1, \lambda_2) = \lambda_2 \int_0^T Y_{\lambda_1}(t)\, Y_{\lambda_1}(t - \tau)\, e^{\lambda_2(t - T)} dt \quad (6.3)$$

The product averaging time constant, λ_2^{-1}, used in this work was 30 seconds. For each delay time, τ, the integration described by (6.3) was done for $T > 2$ minutes. The combination of a 30 second decay constant and greater than 2 minutes integration gives an average in which past events contribute less than 2%. The operations described by (6.2) and (6.3) were performed on an analog computer, the Berkley EASE, model 1032. All multiplications were performed using electronic multipliers. These multipliers were able to follow frequencies greater than 60 cycles per second with no observable loss. The analog circuits used to carry out these computations are given in the literature.[35]

Figures 5.6 to 5.9 were obtained by fixing the position of the movable tape head, corresponding to a known delay time, τ, and then integrating (6.3) for several minutes. After several minutes, the analog solution for $\overset{\circ}{\psi}(\tau, T, \lambda_1, \lambda_2)$ was plotted, using a Mosely Autograf x-y recorder. For each τ, the plotted result is a vertical straight line. The result appears as a line, rather than a point, because of the finite sample of data and the finite integration time. The pen of the x-y recorder plotted $\overset{\circ}{\psi}(\tau, T, \lambda_1, \lambda_2)$ for about 30 seconds, the length of the tape loop, after an equilibrium was reached. In Figure 5.6, for values of $\tau > 1/20$ of a second, the movable recorder head was driven at a slow speed to give a continuous representation of $\overset{\circ}{\psi}$. The head was moving too fast, however, to give anything but a qualitative estimate of $\overset{\circ}{\psi}(\tau, T, \lambda_1, \lambda_2)$.

3. Power Spectral Density Function

An exponentially weighted power spectral density function was computed from the same tape loop used to determine the weighted autocovariance function. The normalized Fourier transform of $Y_{\lambda_1}(t)$ is defined,

$$\mathcal{F}\{Y_{\lambda_1}(t)\} = \lim_{T\to\infty} \frac{1}{2T} \int_{-T}^{T} Y_{\lambda_1}(t)\, e^{-j\omega t}\, dt \qquad (6.4)$$

Letting $\lambda_1 \to 0$, the square of the modulus of (6.4) becomes the classical definition of a power spectral density function. The exponentially weighted Fourier transform is defined,

$$\mathcal{F}(\omega, \lambda_4, \lambda_1, T) = \lambda_4 \int_{0}^{T} Y_{\lambda_1}(t)\, e^{-j\omega t}\, e^{\lambda_4(t - T)}\, dt \qquad (6.5)$$

Thus, the exponentially weighted power spectral density function is given by,

$$\overset{o}{G}(\omega, \lambda_4, \lambda_1, T) = \lambda_4^2 \left| \int_{0}^{T} Y_{\lambda_1}(t)\, e^{-j\omega t} e^{\lambda_4(t - T)}\, dt \right|^2 \qquad (6.6)$$

The frequency bandwidth of the analog filter used in the computation of $\overset{o}{G}(\omega, \lambda_4, \lambda_1, T)$, or the filter width at half maximum, is given by $2\lambda_4$, expressed in radians per second. The r.h.s. of (6.6) is the product of an exponentially weighted Fourier transform with its complex conjugate. These functions are approximately sinusoidal for small λ_4, 90 degrees out of phase, and of equal magnitude. Thus, the sum of the squares of the real and imaginary parts is equal to the square of the amplitude of either function. Recalling the trigonometric definition that $\sin \omega t = \frac{1}{2}(1 - \cos 2\omega t)$, and that the average value of $\cos 2\omega t$ is zero, the amplitude of the function may be written alternatively as

twice the average of the square of either function. The simplified calculation required to form the exponentially weighted power spectral density function is,

$$\overset{\circ}{G}(\omega, \lambda_4, \lambda_3, \lambda_1, T) = 2\lambda_4^2\lambda_3 \int_0^T e^{\lambda_3(x-T)} \left[\int_0^x Y_{\lambda_1} e^{\lambda_4(t-x)} \sin(\omega t + \phi)dt \right]^2 dx \tag{6.7}$$

The effect of ϕ on the calculated value of $\overset{\circ}{G}(\omega, \lambda_4, \lambda_3, \lambda_1, T)$ is not observable for large time constant averaging, $\lambda_3 \ll \omega$. In Figures 5.10 to 5.15, λ_1^{-1} was 10 seconds, the same as during the calculation of the weighted autocovariance function, and λ_3^{-1} was 30 seconds. The analog circuit for computing (6.7) is in the literature.[35]

The effect of the chosen bandwidth on the computation of the exponentially weighted power spectral density function for low frequencies and the stability of the result is demonstrated in Figures 5.10, 5.11, and 5.12. In Figure 5.10, the fluctuations in the exponentially weighted spectra are relatively small for all frequencies. For Figure 5.10, λ_4^{-1} is 10 seconds, which corresponds to a bandwidth of about 3.2 cycles per second. The power spectral density is an increasing function from zero to approximately 5 cycles per second. In Figure 5.11, the bandwidth time constant has been reduced by a factor of 10 to $\lambda_4^{-1} = 1$ second, giving a bandwidth of about 0.32 c.p.s. The spectra has more fluctuation than in Figure 5.10 and builds up to a "level" value in about 0.25 c.p.s. In Figure 5.12, λ_4^{-1} has been reduced by another factor of 5, giving a bandwidth of about 0.066 c.p.s. Since the tape loop is only 30 seconds long, it is meaningless to investigate frequencies smaller than about 1/20 cycles per second. Thus, for

practical estimates of the power spectral density function, we chose a bandwidth of 3.2 c.p.s., realizing that corrections had to be made to the low frequency spectra.

A more complete discussion of the error introduced by using exponentially weighted functions and tape loops to estimate autocovariance and power spectral density functions is given in References 35 and 36. A more detailed mathematical treatment of autocovariance and spectra is given in Reference 37.

B. Comparison of Experiment and Theory

Albrecht[5] investigated the relationship between moment data and the point model theory in his doctoral research done at Michigan. By using a non-linear regression fitting technique on the moment data, Albrecht concluded that the prompt lifetime of the Ford reactor was $80 \pm 10 \times 10^{-6}$ seconds. With the exception of the peaks in the moment data at approximately 0.3 and 3.0 seconds, the moment data presented in Figures 5.1 to 5.5 is similar to Albrecht's. Since the theoretical expression for the ratio of the variance to mean as a function of gate length depends on the detection efficiency, which is not known for this experiment, no attempt will be made to repeat Albrecht's analysis.

The semi-empirical procedure required to obtain a comparison between theoretical and experimental values of the variance to mean ratio is outlined below for completeness.

a. For a gate length less than 0.01 seconds, where one of the exponential terms in (2.58) or (2.90) is dominant, estimate the true value of the ratio from the data.

b. Choose values for the parameters required to determine the roots of the inhour equation, and calculate these roots.

c. Equate the value obtained in a to an undetermined constant times the time dependent part of (2.58) or (2.90). Using the roots obtained in b, calculate the above constant.

d. Calculate the ratio of the remaining J coefficients from (2.58) or (2.90).

e. Using the constant obtained in c, calculate the magnitudes of the J coefficients from the ratios found in d.

f. Using a non-linear regression analysis, feasible only on a high speed digital computer, obtain estimates of the coefficients and exponential arguments of (2.58) or (2.90) by fitting the data.

g. Using an iterative technique, choose new values in b, until the agreement between the "theoretical" and fitted values is maximized.

During the course of the pulse data reduction to obtain moments, care was taken that the scaler used to sum the pulses on the magnetic tape was in proper operating condition. The scaler had a 100 KC internal oscillator for the express purpose of checking the performance of the scaling circuits. While the data for gate lengths of approximately 0.3 and 3.0 seconds was being taken, the scaler was checked repeatedly, using the 100 KC oscillator, and was found to be operating properly. The moment data was obtained over a three month period. All the moment data is listed in Appendix F.

It should be noticed that there are not two peaks in each of the Figures 5.1 to 5.4. This is because the data which caused the peaks, e.g. an abnormally high number of pulses for a given gate length, was discarded

in the early stages of the data reduction, before the author was convinced that the equipment was working properly. An explanation for these peaks, if they are not caused by equipment malfunction, is not available. Because the peaks are present for the different detector positions used, they can not be ascribed to the influence of the reflector region.

A sinusoidal reactivity perturbation introduces a sinusoidal change in the local neutron density. Higher harmonics in the flux are introduced, also, as explained in Appendix C. For the conditions of this experiment, a computer computation based on the results of Appendix C, showed that the ratio of the first harmonic to the fundamental was less than 1% at 1 c.p.s. For higher frequencies, this percentage decreased. Thus, the main effect of the reactivity oscillator on the observables will be due to the fundamental mode.

Appendix D is a derivation of the effect a sinusoidal change in the neutron population, superimposed on the natural fluctuation, would have on the observed moments, if an unlimited amount of data were available. The data was represented as a continuous variable, to allow the replacement of summations by integrations. Appendix D shows that the effect of the oscillator on the measured moments is negligible for frequencies above about 0.5 c.p.s. For lower frequencies, the effect of the oscillator on the moment data is theoretically observable. However, the finite amount of data associated with the actual data reduction introduced a spread in the moment data[34], which masked the effect of the oscillator.

Qualitatively, we observe the expected behavior, (2.58), in the moment data comparing Figures 5.1 and 5.5. By removing the detector

from the region of high thermal flux, the detection efficiency decreased and the ratio of the variance to mean decreased. Because of the high (γ, n) source present during the experiment, it was not feasible to make measurements for $k > 0.997$. To minimize dead time losses in the BF_3 chamber, the average count rate was kept below 3000 counts per second. If k had been increased, the count rate would have increased due to additional subcritical multiplication. The experiment was performed as close to critical as dead time losses would allow, so that the computed ratio of the variance to mean would be significantly greater than unity.

Autocovariance Functions

The equation used to evaluate the autocorrelation function can be deduced from (2.84) and (2.80), and is independent of the detection efficiency,

$$\psi^{o}_{ob}(\tau) = \frac{\sum_{k=1}^{J+1} \sum_{\ell=1}^{J+1} \frac{A_k A_\ell}{(r_k + r_\ell)} e^{-r_k \tau}}{\sum_{k=1}^{J+1} \sum_{\ell=1}^{J+1} \frac{A_k A_\ell}{r_k + r_\ell}} \qquad (6.8)$$

Based on the success of the 2 delay group model in predicting the behavior of moment data,[5] all theoretical calculations using (6.8) were made for 2 and 6 delay groups. The 6 delay group parameters of Keepin et al[38] and an "effective" group[33] are used in this work, see Table VI.1. The effective delay fraction takes account of the fact that delayed neutrons are born with a lower energy spectrum than prompt neutrons. Employing the method of Skinner and Cohen[39], 2 group parameters are computed from the 6 group data of Table VI.1. The program used to compute the 2 group parameters is given in Appendix F, and is called TWO GROUP. The calculated 2 group

TABLE VI.1

6 DELAY GROUP PARAMETERS

λ_i^{-1} seconds	β_i x 100 Keepin	β_i x 100 effective
0.01244	0.021	0.025
0.0305	0.140	0.165
0.1114	0.125	0.148
0.3014	0.253	0.298
1.136	0.074	0.087
3.014	0.027	0.032
	β = 0.640	β = 0.755

TABLE VI.2

2 DELAY GROUP PARAMETERS

λ_i^{-1} SECONDS	A_i KEEPIN	β_i x 100 KEEPIN	A_i EFFECTIVE	β_i x 100 EFFECTIVE
0.02526157	.2969	0.189987	.2963	0.223692
0.5674351	.7031	0.450013	.7037	0.531308
		β = 0.640		β = 0.755

parameters are listed in Table VI.2. The A_i in Table 6.2 refer to the relative abundance of the i'th delay group. The roots of the inhour equation, $R_k = -r_k$, are required to evaluate (6.8). The programs to compute the roots of the 6 and 2 delay group inhour equations are listed in Appendix F as ROOT 6 and ROOT 2, respectively.

The J+1 values of A_k appearing in (6.8) were determined by solving (2.82) for J+1 different frequencies. The programs to compute the A_k for 6 and 2 delay groups are given in Appendix F as CORR 6 and TWO GROUP COEFFICIENTS, respectively. The form of the transfer function used in (2.82) is given in Appendix B, (B.6).

Since the prompt neutron lifetime in the Ford reactor has been estimated as $80 \pm 10 \times 10^{-6}$ seconds[5], the values used in evaluating the theoretical expression for the autocorrelation function were 70, 80, and 90 microseconds. In order to see the effect of the delay fraction on the calculated results, both Keepin and effective delay fractions were used. The multiplication constants used in the calculations were 1.0, 0.998, 0.997 and 0.99. Although the experiment was performed at 0.997, the other values chosen show trends and the sensitivity of the result to k. Table VI.3 lists the roots of the 6 group inhour equation and the A_k from (2.82), for both sets of delay fractions, with the multiplication constant and the prompt lifetime as parameters. Table VI.4 is a similar listing for the 2 group parameters of Table VI.2.

The theoretical autocorrelation functions are computed by CORR 6 and CORRELATION 7 for 6 and 2 delay groups, respectively. The roots of the inhour equation and the A_k listed in Tables VI.3 and VI.4 were used to

TABLE VI.3

ROOTS OF THE 6 GROUP INHOUR EQUATION AND SOLUTIONS OF (2.82), A_k, FOR KEEPIN (UPPER) AND EFFECTIVE (LOWER) DELAY PARAMETERS

$\ell \times 10^6$ seconds	$-R_1$ seconds^{-1}	$-R_2$	$-R_3$	$-R_4$	$-R_5$	$-R_6$	$-R_7$	A_1 seconds^{-1}	A_2	A_3	A_4	A_5	A_6	A_7
k = 1.0														
90	71.52346	2.89735	1.01864	0.19470	0.06834	0.01436	0.0	109.9577	0.0217	0.1354	0.1117	0.0761	0.0127	0.0
	84.30038	2.89743	1.01920	0.19494	0.06830	0.01438	0.0	109.8989	0.0157	0.1151	0.0943	0.0645	0.0108	0.0
80	80.41168	2.89783	1.01880	0.19472	0.06834	0.01436	0.0	123.7584	0.0193	0.1360	0.115	0.0761	0.0127	0.0
	94.78593	2.89784	1.01934	0.19496	0.06830	0.01438	0.0	123.6833	0.0140	0.1155	0.0942	0.0645	0.0108	0.0
70	91.83959	2.89830	1.01896	0.19475	0.06835	0.01436	0.0	141.5019	0.0169	0.1365	0.0111	0.0762	0.0127	0.0
	108.2675	2.89824	1.01947	0.19498	0.06830	0.01438	0.0	141.4061	0.0123	0.1159	0.0094	0.0646	0.0108	0.0
k = 0.998														
90	93.30413	2.92118	1.04177	0.21277	0.08081	0.01813	0.01007	110.1438	0.0098	0.0958	0.0827	0.0467	0.0167	0.0174
	106.2680	2.92004	1.04111	0.21205	0.08018	0.01788	0.00987	110.0383	0.0078	0.0794	0.0740	0.0433	0.0129	0.0205
80	105.1529	2.92354	1.04391	0.21454	0.08188	0.01864	0.01038	123.9431	0.0087	0.0883	0.0835	0.0468	0.0158	0.0185
	119.5105	2.92031	1.04121	0.21206	0.08018	0.01788	0.00987	123.8225	0.0069	0.0796	0.0740	0.0433	0.0129	0.0205
70	120.1296	2.92383	1.04401	0.21456	0.08189	0.01864	0.01038	141.6863	0.0076	0.0886	0.0834	0.0468	0.0159	0.0185
	135.7081	2.91873	1.03948	0.21054	0.07921	0.01743	0.00951	141.5449	0.0420	0.0985	0.0705	0.0443	0.0136	0.0195
k = 0.997														
90	104.5107	2.93235	1.05282	0.22251	0.08642	0.02087	0.01123	110.1945	0.0070	0.0730	0.0715	0.0355	0.0140	0.0086
	117.2641	2.92838	1.04932	0.21920	0.08445	0.01995	0.01095	110.0804	0.0058	0.0673	0.0649	0.0341	0.0129	0.0101
80	117.5393	2.93259	1.05290	0.22252	0.08642	0.02087	0.01123	123.9947	0.0062	0.0731	0.0714	0.0355	0.0140	0.0086
	131.8851	2.92860	1.04940	0.21922	0.08446	0.01995	0.01095	123.8646	0.0052	0.0675	0.0648	0.0341	0.0129	0.0101
70	134.2904	2.93283	1.05299	0.22254	0.08643	0.02087	0.01123	141.7378	0.0054	0.0733	0.0713	0.0355	0.0140	0.0086
	150.6837	2.92882	1.04948	0.21923	0.08446	0.01995	0.01926	141.5871	0.0045	0.0677	0.0644	0.0351	0.0111	0.0101
k = 0.99														
90	181.6700	2.96625	1.08694	0.25490	0.10004	0.02670	0.01215	110.3324	0.0013	0.0272	0.0274	0.0086	0.0031	0.0007
	194.3362	2.96140	1.08236	0.25034	0.09843	0.02611	0.01209	110.2027	0.0013	0.0275	0.0278	0.0094	0.0035	0.0008
80	204.3587	2.96633	1.08698	0.25491	0.10004	0.02670	0.01215	124.1325	0.0012	0.0272	0.0274	0.0086	0.0031	0.0007
	218.6062	2.96149	1.08239	0.25035	0.09843	0.02611	0.01209	123.9868	0.0011	0.0276	0.0278	0.0094	0.0035	0.0008
70	233.5300	2.96641	1.08701	0.25492	0.10004	0.02670	0.01215	141.8754	0.0010	0.0272	0.0274	0.0086	0.0031	0.0007
	249.8105	2.96157	1.08242	0.25036	0.09843	0.02611	0.01209	141.7092	0.0010	0.0276	0.0278	0.0094	0.0035	0.0008

TABLE VI.4

ROOTS OF THE 2 GROUP INHOUR EQUATION AND SOLUTIONS OF (2.82), FOR KEEPIN (UPPER) AND EFFECTIVE (LOWER) DELAY PARAMETERS

$\ell \times 10^6$ seconds	$-R_1$ seconds^{-1}	$-R_2$	$-R_3$	A_1 seconds^{-1}	A_2	A_3
	k = 1.0					
90	71.52069	0.18535	0.0	109.76533	0.51433	0.0
	84.29664	0.18517	0.0	109.73451	0.43585	0.0
80	80.40725	0.18544	0.0	123.56526	0.51441	0.0
	94.78244	0.18523	0.0	123.51843	0.43592	0.0
70	91.83572	0.18554	0.0	141.3080	0.51450	0.0
	108.2645	0.18533	0.0	141.2407	0.43599	0.0
	k = 0.998					
90	93.50376	0.26968	0.01263	110.02916	0.33838	0.03249
	106.2658	0.25893	0.01158	109.93418	0.30583	0.03219
80	105.1503	0.26980	0.01263	123.8292	0.33829	0.03249
	119.5084	0.25901	0.01158	123.71826	0.30578	0.03219
70	120.1274	0.26986	0.01263	141.57218	0.33821	0.03249
	136.5349	0.25909	0.01158	151.44063	0.30573	0.03219
	k = 0.997					
90	104.5106	0.30023	0.01523	110.10334	0.27594	0.02074
	117.2624	0.28696	0.01420	109.99473	0.26515	0.02131
80	117.5372	0.30031	0.01523	123.90343	0.27584	0.02075
	131.8834	0.28703	0.01420	123.77882	0.25610	0.02131
70	134.2886	0.30039	0.01523	141.64637	0.27575	0.02074
	150.6822	0.28710	0.01420	141.50120	0.25604	0.02131
	k = 0.99					
90	181.6714	0.41349	0.02120	110.30168	0.09302	0.00356
	194.3357	0.39775	0.02060	110.17141	0.09691	0.00390
80	204.3580	0.41352	0.02120	124.10213	0.09438	0.00349
	218.6056	0.39778	0.02060	123.95547	0.09687	0.00390
70	235.5294	0.41356	0.02120	141.84502	0.09434	0.00349
	249.8101	0.39782	0.02060	141.67782	0.09684	0.00390

compute the autocorrelation function. The calculated autocorrelation functions are listed in Tables VI.5 and VI.6, for 6 and 2 delay groups, respectively. Except for delay times greater than 0.10 seconds, Tables VI.5 and VI.6 show that the 6 and 2 group autocorrelation functions are for all practical purposes, indistinguishable. As k decreases, the autocorrelation function decreases for a given delay time. A change in β of approximately 20% is comparable to a 10% change in prompt neutron lifetime, for delay times on the order of milliseconds.

The autocorrelation function drops to less than 2% of its original value in 0.10 seconds. This is in sharp contrast to a power reactor which may have appreciable correlation for several seconds.

The measured autocovariance functions are shown in Figures 5.6 to 5.9. The measured or analog computed functions have a characteristic cyclic behavior, which has a frequency of 60 cycles per second. Upon checking the equipment used to convert from pulse data on magnetic tape to an FM signal, it was found that the Hewlett Packard electronic tachometer, introduced the 60 cycle noise. Since the autocorrelation function of a sinusoidal function is cosinusoidal, with amplitude independent of delay time, it was straightforward to correct for the presence of the 60 cycle noise. The amplitude of the cosine function was estimated for delay times at which the autocovariance function was approximately zero. It was necessary to adjust the "zero" delay time by 1/600 of a second to account for a systematic error in the referenced "zero" position, caused by a low precision microswitch.

TABLE VI.5

THEORETICAL AUTOCORRELATION FUNCTION FOR DIFFERENT DELAY TIMES, τ, USING KEEPIN (UPPER) AND EFFECTIVE (LOWER) 6 GROUP CONSTANTS WITH ℓ AND k AS PARAMETERS

$\ell \times 10^6$	k = 1.0												
	0	0.001	0.002	0.003	0.004	0.006	0.008	0.01	0.02	0.03	0.04	0.10	1.0 seconds
90	1.0	0.932	0.868	0.809	0.753	0.654	0.568	0.494	0.246	0.125	0.066	0.0095	0.0063
	1.0	0.920	0.846	0.778	0.716	0.606	0.513	0.435	0.191	0.087	0.042	0.0076	0.0054
80	1.0	0.923	0.853	0.787	0.727	0.620	0.529	0.452	0.207	0.097	0.048	0.0081	0.0056
	1.0	0.910	0.828	0.754	0.687	0.569	0.472	0.392	0.156	0.065	0.029	0.0066	0.0048
70	1.0	0.913	0.833	0.761	0.695	0.579	0.483	0.403	0.165	0.070	0.032	0.0069	0.0049
	1.0	0.898	0.806	0.724	0.651	0.525	0.424	0.343	0.120	0.045	0.019	0.0057	0.0042
	k = 0.998												
90	1.0	0.912	0.831	0.758	0.691	0.574	0.478	0.398	0.161	0.068	0.031	0.0072	0.0056
	1.0	0.900	0.810	0.729	0.656	0.532	0.431	0.350	0.126	0.048	0.021	0.0070	0.0055
80	1.0	0.901	0.812	0.731	0.659	0.535	0.435	0.354	0.128	0.049	0.021	0.0065	0.0050
	1.0	0.888	0.789	0.701	0.622	0.491	0.388	0.307	0.097	0.034	0.015	0.0062	0.0049
70	1.0	0.887	0.788	0.699	0.621	0.489	0.386	0.305	0.096	0.033	0.014	0.0095	0.0043
	1.0	0.874	0.764	0.667	0.583	0.446	0.341	0.261	0.071	0.022	0.0095	0.0051	0.0043
	k = 0.997												
90	1.0	0.901	0.812	0.732	0.660	0.536	0.436	0.355	0.128	0.049	0.021	0.0052	0.0039
	1.0	0.890	0.793	0.705	0.628	0.497	0.395	0.313	0.101	0.035	0.014	0.0051	0.0039
80	1.0	0.890	0.792	0.704	0.627	0.496	0.393	0.312	0.099	0.034	0.014	0.0046	0.0035
	1.0	0.877	0.769	0.675	0.592	0.456	0.351	0.271	0.076	0.024	0.0097	0.0045	0.0034
70	1.0	0.875	0.765	0.670	0.586	0.449	0.344	0.264	0.072	0.022	0.0088	0.0040	0.0030
	1.0	0.861	0.741	0.638	0.549	0.407	0.302	0.225	0.053	0.015	0.0064	0.0039	0.0029
	k = 0.99												
90	1.0	0.834	0.696	0.580	0.484	0.337	0.235	0.164	0.028	0.0057	0.0021	0.0014	0.0009
	1.0	0.824	0.678	0.559	0.460	0.313	0.212	0.145	0.022	0.0044	0.0019	0.0014	0.0010
80	1.0	0.815	0.665	0.542	0.442	0.294	0.196	0.131	0.018	0.0034	0.0015	0.0012	0.0008
	1.0	0.804	0.646	0.520	0.418	0.270	0.175	0.114	0.014	0.0027	0.0015	0.0013	0.0009
70	1.0	0.792	0.627	0.497	0.394	0.247	0.155	0.098	0.010	0.0020	0.0012	0.0011	0.0007
	1.0	0.779	0.607	0.473	0.369	0.224	0.137	0.083	0.0079	0.0017	0.0012	0.0011	0.0008

TABLE VI.6

THEORETICAL AUTOCORRELATION FUNCTION FOR DIFFERENT DELAY TIMES, τ USING KEEPIN (UPPER) AND EFFECTIVE (LOWER) 2 GROUP CONSTANTS WITH ℓ AND k AS PARAMETERS

k = 1.0

$\ell \times 10^6$	0	0.001	0.002	0.003	0.004	0.005	0.006	0.01	0.02	0.03	0.04	0.10	1.0sec.
90	1.0	0.932	0.869	0.810	0.756	0.657	0.572	0.498	0.252	0.132	0.073	0.018	0.014
	1.0	0.920	0.847	0.780	0.718	0.609	0.517	0.439	0.197	0.093	0.048	0.015	0.012
80	1.0	0.924	0.854	0.789	0.729	0.623	0.533	0.456	0.213	0.104	0.055	0.015	0.013
	1.0	0.911	0.830	0.756	0.689	0.572	0.475	0.396	0.161	0.071	0.035	0.013	0.011
70	1.0	0.913	0.834	0.762	0.697	0.582	0.487	0.407	0.171	0.076	0.038	0.013	0.011
	1.0	0.899	0.808	0.726	0.653	0.528	0.427	0.346	0.125	0.050	0.024	0.011	0.0096

k = 0.998

90	1.0	0.912	0.831	0.758	0.692	0.576	0.479	0.340	0.164	0.071	0.035	0.011	0.0083
	1.0	0.900	0.811	0.730	0.658	0.534	0.434	0.353	0.129	0.052	0.025	0.011	0.0091
80	1.0	0.901	0.812	0.732	0.660	0.537	0.437	0.356	0.131	0.052	0.025	0.010	0.0083
	1.0	0.888	0.790	0.702	0.624	0.493	0.391	0.310	0.101	0.037	0.018	0.0097	0.0081
70	1.0	0.888	0.788	0.700	0.622	0.491	0.388	0.307	0.099	0.036	0.017	0.0089	0.0072
	1.0	0.873	0.763	0.667	0.583	0.446	0.341	0.262	0.073	0.025	0.013	0.0085	0.0071

k = 0.997

90	1.0	0.902	0.813	0.733	0.661	0.538	0.438	0.357	0.131	0.051	0.023	0.0081	0.0064
	1.0	0.890	0.793	0.706	0.629	0.499	0.396	0.315	0.103	0.038	0.017	0.0080	0.0064
80	1.0	0.890	0.792	0.705	0.628	0.498	0.395	0.314	0.102	0.037	0.016	0.0072	0.0057
	1.0	0.877	0.770	0.656	0.593	0.457	0.353	0.273	0.078	0.026	0.012	0.0071	0.0057
70	1.0	0.875	0.768	0.671	0.597	0.450	0.348	0.268	0.074	0.024	0.011	0.0063	0.0050
	1.0	0.861	0.741	0.639	0.550	0.409	0.304	0.227	0.055	0.017	0.0067	0.0062	0.0050

k = 0.99

90	1.0	0.835	0.670	0.582	0.486	0.339	0.236	0.165	0.029	0.0064	0.0028	0.0020	0.0014
	1.0	0.824	0.679	0.559	0.461	0.313	0.213	0.145	0.023	0.0052	0.0027	0.0022	0.0016
80	1.0	0.816	0.665	0.543	0.443	0.295	0.197	0.131	0.019	0.0040	0.0022	0.0018	0.0013
	1.0	0.804	0.647	0.520	0.418	0.271	0.176	0.114	0.015	0.0033	0.0021	0.0019	0.0013
70	1.0	0.792	0.627	0.497	0.394	0.248	0.156	0.098	0.011	0.0025	0.0017	0.0016	0.0011
	1.0	0.779	0.607	0.474	0.369	0.225	0.137	0.084	0.0085	0.0023	0.0018	0.0017	0.0012

The corrected, normalized autocovariance functions data, obtained from Figure 5.7 and 5.9, is presented in Figure 6.3. The values used to construct Figure 6.3 are listed in Table VI.7. Theoretical autocorrelation functions are presented in Figure 6.3, based on values in Table VI.5, for the following parameters: $k = 0.997$, Keepin delay constants, and $\ell = 70$ and 90 microseconds. Qualitatively observe that there is more correlation in the data entitled BF_3-1 than in I-10c/s. This behavior is predicted by Table VI.5, since the data was taken for $k = 0.999$ and 0.997, respectively. However, the disagreement between the data and the theoretical prediction for $\ell = 70$ and 90 microseconds is not within the error assignable to the measured function. On the basis of Figure 6.3, it can be concluded that the prompt lifetime of the Ford reactor is greater than 90 microseconds. Theoretical autocorrelation functions are presented in Figure 6.3 for Keepin delay data and prompt lifetimes of 110, 130 and 150 microseconds. A comparison of theory and experiment, Figure 6.3, predicts a prompt neutron lifetime of 130 ± 20 microseconds.

Power Spectral Density Functions

The experimental power spectral density functions are presented in Figures 5.10 to 5.15. As explained in Section A.3, the observed spectra below 10 cycles per second must be corrected to account for the finite bandwidth determined by λ_4. Low frequency corrections for Figures 5.10 and 5.13 to 5.15 were estimated from the results of Figures 5.11 and 5.12. The corrected and normalized values of spectra are listed in Table VI.8.

The theoretical power spectral density functions are computed from (2.68) by TRANSFER 6, listed in Appendix F, for 6 delay groups. A

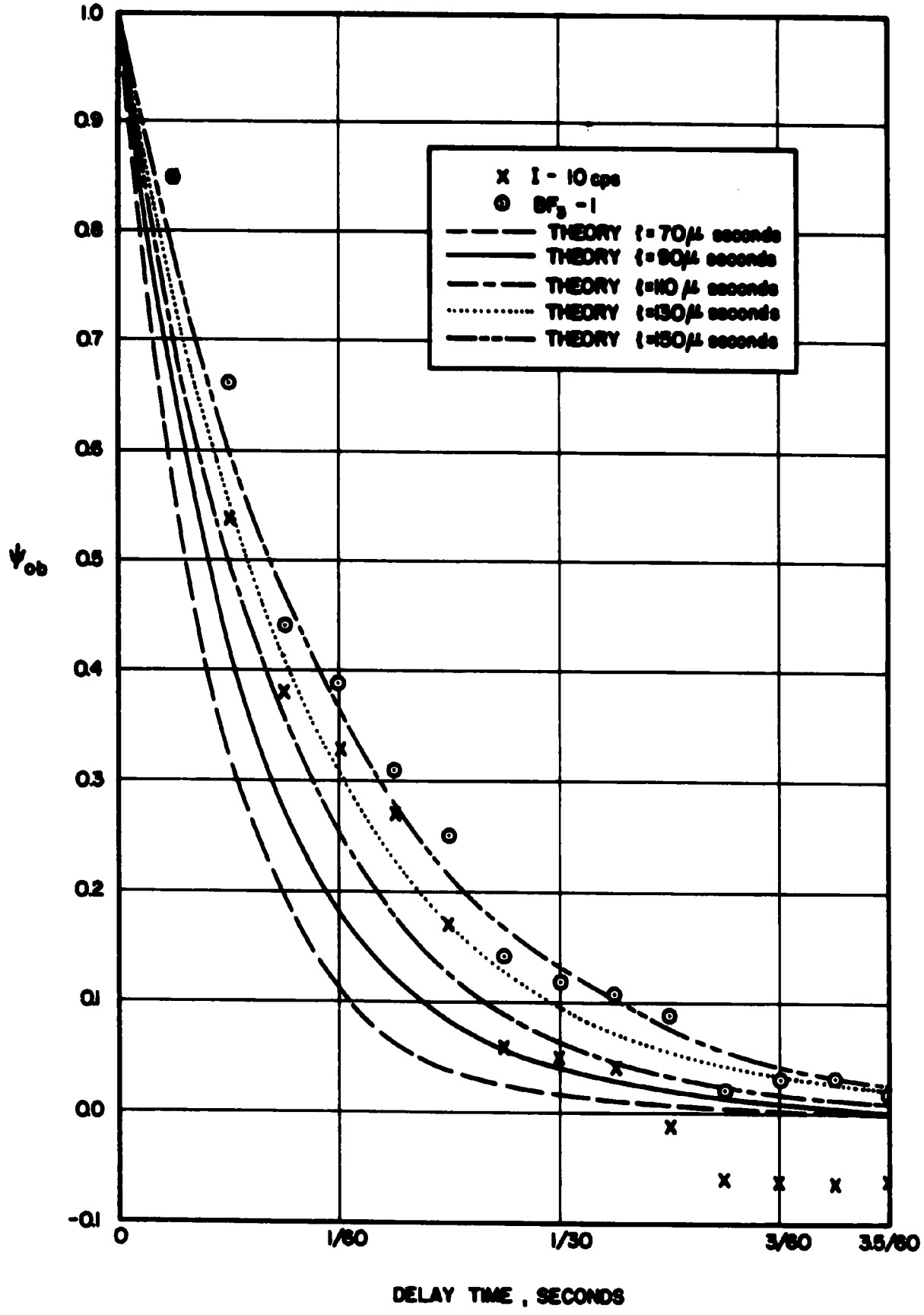


Figure 6.3. Measured and Theoretical Autocorrelation Functions.

TABLE VI.7

CORRECTED NORMALIZED AUTOCOVARIANCE FUNCTION AS A FUNCTION OF DELAY TIME, τ

T seconds	I - 10 c/s	BF_3 - 1
0	1.0	1.0
1/240	0.85	0.85
2/240	0.54	0.66
3/240	0.38	0.44
1/60	0.33	0.39
5/240	0.27	0.31
6/240	0.17	0.25
7/240	0.06	0.14
1/30	0.05	0.12
9/240	0.04	0.11
10/240	-0.01	0.09
11/240	-0.06	0.02
3/60	-0.06	0.03
13/240	-0.06	0.03
14/240	-0.06	0.02

TABLE VI.8

MEASURED POWER SPECTRAL DENSITY FUNCTIONS
NORMALIZED TO 15 c.p.s.

c.p.s.	I - Noise	I - 10 c/s	V - Noise	BF_3-1
5 est.	1.39	1.50	1.57	1.50
10	1.22	1.29	1.36	1.35
15	1.0	1.0	1.0	1.0
20	0.60	0.69	0.63	0.71
25	0.44	0.49	0.44	0.49
30	0.36	0.40	0.37	0.38
35	0.30	0.30	0.33	0.27
40	0.25	0.23	0.29	0.21
45	0.22	0.18	0.23	0.17
50	0.17	0.15	0.23	0.15

similar program was written for 2 delay groups. The two calculations were in agreement to $\pm$ 5% over the frequency range from 5 to 60 cycles per second. The calculated 6 group spectra is given in Table VI.9, normalized to 15 cycles per second for ℓ = 70, 80 and 90 microseconds. The parameters chosen in Table VI.9 illustrate the effect on power spectra due to changes in k, β and ℓ.

The experimental and theoretical power spectral density functions are plotted in Figure 6.4, using values from Tables VI.8 and VI.9. Table VI.9 was constructed using (2.68). For a prompt neutron lifetime of 90 microseconds, theory and experiment agree for frequencies above 35 c.p.s. However, for frequencies from 15 to 35 c.p.s., the theory and experiment differ by as much as 20%. Figure 6.4 supports the conclusion drawn from Figure 6.3 that the prompt lifetime of the Ford reactor is greater than 90 microseconds. Theoretical power spectral density functions for ℓ = 110, 130 and 150 microseconds are, also, presented in Figure 6.4. A comparison of theory and experiment, Figure 6.4, predicts a prompt neutron lifetime of 130 $\pm$ 20 microseconds. The data in the time (autocorrelation) and frequency (power spectral density) domain predicts the same prompt lifetime.

The low frequency data in Figure 6.4, which was "corrected" on the basis of Figures 5.11 and 5.12, illustrates that the corrections were not sufficient. In other words, to determine low frequency spectra accurately requires a modification in the analog computation procedure. For example, a different combination of analog circuit time constants might be more appropriate for low frequency spectra. Unfortunately, since the analog facility was in heavy use by Chrysler personnel, the author did not have an opportunity to make a more detailed investigation.

TABLE VI.9

THEORETICAL POWER SPECTRAL DENSITY FUNCTIONS NORMALIZED TO 15 c.p.s. USING KEEPIN (UPPER) AND EFFECTIVE (LOWER) 6 OR 2 GROUP CONSTANTS, WITH ℓ AND k AS PARAMETERS

$\ell \times 10^6$ seconds	k = 1.0 5	10	20	25	30	35	40	45	50 cycles/second
90	2.29	1.54	0.67	0.47	0.34	0.26	0.20	0.16	0.13
	1.97	1.45	0.70	0.50	0.37	0.29	0.23	0.18	0.15
80	2.06	1.47	0.69	0.49	0.37	0.28	0.22	0.18	0.15
	1.79	1.38	0.72	0.53	0.40	0.31	0.25	0.20	0.17
70	1.84	1.40	0.71	0.52	0.39	0.30	0.24	0.20	0.16
	1.62	1.31	0.75	0.57	0.44	0.34	0.28	0.22	0.19
	k = 0.998								
90	1.81	1.39	0.72	0.53	0.40	0.31	0.25	0.20	0.16
	1.64	1.32	0.74	0.56	0.43	0.34	0.27	0.22	0.18
80	1.66	1.33	0.74	0.56	0.43	0.34	0.27	0.22	0.18
	1.52	1.27	0.77	0.59	0.47	0.37	0.30	0.25	0.21
70	1.51	1.27	0.77	0.60	0.47	0.37	0.30	0.25	0.21
	1.40	1.22	0.80	0.64	0.51	0.41	0.34	0.28	0.23
	k = 0.997								
90	1.66	1.33	0.74	0.56	0.43	0.33	0.27	0.22	0.18
	1.54	1.28	0.77	0.59	0.46	0.36	0.29	0.24	0.20
80	1.53	1.28	0.77	0.59	0.46	0.37	0.29	0.24	0.20
	1.43	1.23	0.79	0.62	0.50	0.40	0.33	0.27	0.23
70	1.42	1.22	0.80	0.63	0.50	0.41	0.33	0.27	0.23
	1.33	1.19	0.82	0.67	0.54	0.44	0.37	0.31	0.26
	k = 0.99								
90	1.23	1.13	0.86	0.73	0.61	0.51	0.44	0.37	0.32
	1.20	1.12	0.87	0.75	0.64	0.54	0.46	0.40	0.34
80	1.18	1.11	0.88	0.76	0.66	0.56	0.48	0.42	0.36
	1.16	1.10	0.89	0.78	0.68	0.59	0.51	0.44	0.39
70	1.14	1.08	0.90	0.80	0.70	0.62	0.54	0.47	0.41
	1.12	1.07	0.91	0.82	0.73	0.64	0.57	0.50	0.44

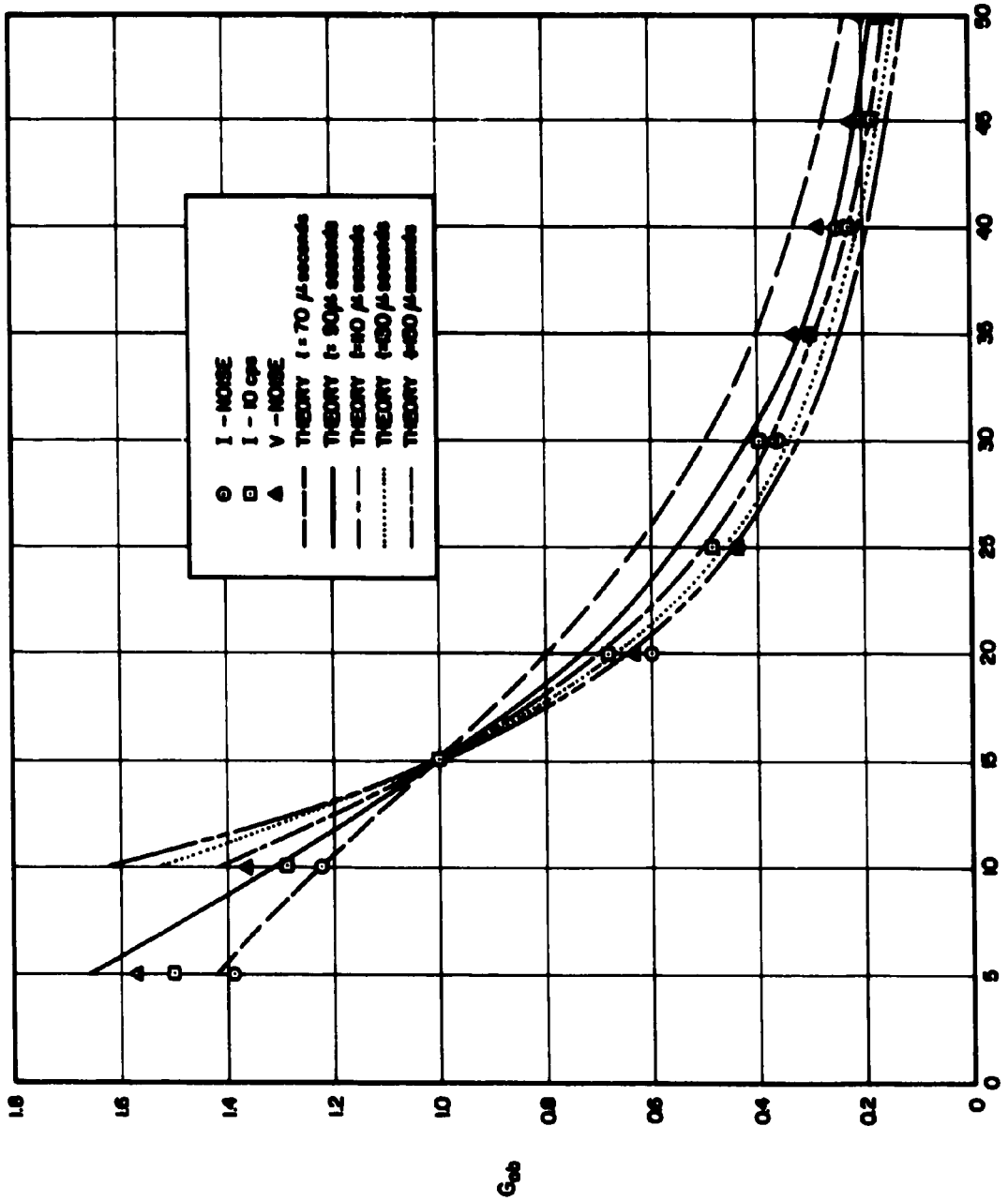


Figure 6.4. Measured and Theoretical Power Spectral Density Functions.

The 60 cycle noise introduced by the electronic tachometer is clearly seen in Figure 5.15. The presence of this signal in the spectra at 60 c.p.s. does not require that any corrections be made to the amplitude of lower frequency spectra, because of the computational method used.

CHAPTER VII

CONCLUSIONS

A. Theory

In Chapter II, two different methods are used to obtain an expression for the ratio of the variance to mean number of detected neutrons as a function of detection time. The first method makes use of a detailed probability balance on the number of neutrons, precursor atoms, and detections in the reactor between the ensemble states represented by time t and $t + \delta t$. By introducing probability generating functions and using a limiting process, the detailed balance equation is converted into a time dependent equation. By manipulating the time dependent equation, a set of 44 first order differential equations is obtained for a reactor model which assumes 6 groups of delayed neutrons. This set of equations is necessary and sufficient to describe the average values and the variances of the system parameters. This is in contrast to the 8 equations needed to describe the average behavior of the neutrons, precursor atoms and detected neutrons.

When the set of 44 equations is specialized to describe a reactor operating at steady state, an expression is obtained for the ratio of the variance to mean number of detected neutrons as a function of detection time. The ratio is in terms of the 42 parameters described by the above set of differential equations and quantities such as the number of prompt neutrons per fission, the covariance between the number of precursor atoms of group i and group j formed per fission, and the detection efficiency. The value of the ratio for any given detection time depends on all these

quantities, and can not be made independent of detection efficiency. The coefficients of the time dependent factors in the expression for the ratio are uniquely determined.

The second method used to obtain an expression for the ratio of the variance to mean number of detections as a function of detection time requires assumptions for the form of the reactor transfer function and for the driving function of the reactor. Having chosen a form for these two functions, it is a straightforward procedure to arrive at a relation for the ratio, for a reactor operating at steady state. This method is limited to steady state applications, because the form of the appropriate time dependent driving function, G^{o}_{xx} in (2.68), is unknown. This limitation is inherent in the transfer function approach. The expression for the ratio is in terms of the quantities associated with the transfer and driving functions, and with the detection efficiency. However, the driving function is not known uniquely, and therefore the coefficients of the time dependent factors are not known uniquely.

The form of the expression for the ratio of the variance to the mean is identical in the steady state for both methods, (2.58) and (2.90). The detailed probability balance method has the following advantages:

1. It allows a unique description of the coefficients in the relation describing the ratio of the variance to mean number of detections.

2. No assumption of the form of the transfer function of the reactor is required.

3. No assumption of the form of the driving function of the reactor is required.

Also, the results of the detailed probability balance are not limited to monoenergetic neutrons. Using a 1/v neutron detector, for example, the detection term depends only on the neutron density. In order to evaluate the theoretical expression for the ratio of the variance to mean, (2.58), it is necessary to know values for Λ_c and Λ_f. By averaging these quantities over the neutron energy distribution in the reactor, appropriate weighted values can be obtained.

Theoretical calculations of the autocorrelation functions show that a 2 delay group representation of the 6 delay group model agrees with 6 group results within 5% for delay times from 0.0 to 0.02 seconds. Also, the power spectral density functions are within 5% for frequencies from 5.0 to 60.0 cycles per second.

B. Experiment

This research shows the basic information available from an analysis of reactor fluctuations in terms of its moments, autocorrelation and power spectral density functions. For the data obtained in this work, the following can be concluded:

1. Moments

With the exception of the peaks at approximately 0.3 and 3.0 seconds, Figures 5.1 to 5.5, the ratio of the variance to mean number of detected neutrons as a function of detection time agrees qualitatively with moment data taken by Albrecht,[5] and with theory, for detection times from 0.001 to 9.999 seconds. The peaks remain unexplained and warrant further investigation. Using a non-linear regression analysis of moment data, for a two delay group model, Albrecht estimated that the prompt neutron lifetime of the Ford Nuclear Reactor was 80 $\pm$ 10 microseconds. The values obtained in 2 and 3 below do not agree with Albrecht's result.

2. Autocorrelation Function

Using Keepin delay constants, a comparison of theory and experiment, Figure 6.3, predicts a prompt neutron lifetime of 130 ± 20 microseconds for the Ford Nuclear Reactor.

3. Power Spectral Density Function

Using Keepin delay constants, a comparison of theory and experiment, Figure 6.4, predicts a prompt neutron lifetime of 130 ± 20 microseconds for the Ford Nuclear Reactor.

4. Effect of Reactivity Perturbation

For the frequency range from 0.5 to 30 cycles per second, the presence of a sinusoidal reactivity perturbation of approximately 10^{-4} sin (ωt) did not change the observed values of the ratio of the variance to mean, of the autocorrelation or of the power spectral density functions. In Appendix D, it is shown that this could be expected, based on the limited quantity of data obtained in this work.

5. Effect of Detector Position

The observed moments, autocorrelation and power spectral density functions were not appreciably affected by the relative position of the detector to the core. The positions used in this work are shown in Figures 3.1 to 3.5. No previous measurements of this kind are reported in the literature. The observed lack of dependence on the position of the detector substantiates the assumption in the development of the detailed balance equation that space effects are of second order importance in a highly coupled system.

C. Future Research

1. Theory

The theoretical description of fluctuations should be extended to include the effects of neutron position, energy and direction, giving the transport equation as a first moment. These effects might be included in the argument of the ensemble probability distribution function, (2.1), and an appropriate detailed probability balance equation could be developed from this assumption. In attempting to make this extension, the author has been unsuccessful to date in the formulation of the term in the detailed balance describing the scattering of neutrons from an arbitrary direction into the direction on which the balance is made. The solution of this problem requires extremely careful consideration of the implication of the terms in the detailed balance equation.

Methods for determining the power level of a reactor using stochastic processes should be developed. A direct approach would be to theoretically study the behavior of the ratio of the variance to mean number of detected neutrons as a function of power level. An extension of the initial study by Harris[15] would be an effective starting point.

Criteria for power reactor stability should be developed using the methods of stochastic processes. Having obtained the necessary moment equations describing the reactor, and the coupled feedback system equations due to the external load, the most general method for studying overall stability is the application of Lyapunov's second method. Since it is difficult to obtain a Lyapunov function for this complex situation, a parameter study of this set of equations could be obtained directly using computers.

By studying the theoretical description of fluctuations it may be possible to deduce the subcriticality of a reactor. Preliminary work by the author shows that certain ratios of the power spectral density function are sensitive to k. For example, it was noticed during the course of a computer study of spectra values that the ratio of two ratios of spectra values was strongly dependent on k. The ratio of the value of the ratio of the spectra at say 40 cycles per second to 1.0 c.p.s. at critical to the value of the same ratio for k = 0.997 changed 100% when k was changed to 0.99.

Cross correlation techniques[21] should be investigated for possible improvements and new applications in the extraction of information from a reactor, such as determining rod worths.

2. Experiment

Non-linear regression analysis was unfeasible before the advent of modern computing machines. As faster digital computers and new non-linear regression techniques are developed, it should be feasible to determine the majority of system parameters making up the moment equations, including such parameters as β_i, λ_i, and $\bar{\nu}_o$, from fluctuation data. Equipment and techniques should be developed to exploit the information available from both transient and steady state fluctuation data, in order to gain more understanding of nuclear reactors.

BIBLIOGRAPHY

1. Feynman, R. P., De Hoffman, F., and Serber, R., "Statistical Aspects of Pile Theory," Science and Engineering of Nuclear Power, 103, Addison-Wesley, Cambridge, (Mass.) (1949).

2. Courant, E. D., Wallace, P. R., "Fluctuations in the Number of Neutrons in a Pile," Physical Review, 72, No. 11, 1038 (1947).

3. Larisse, J., Braffort, P., "Equations Differentialles Stochastiques Rigissant L'Evolution de La Densite Neutronique Dans un Milieu Multiplicateur," J. Nuclear Energy Part A, 13, 133 (1961).

4. Bennett, E. F., "The Rice Formulation of Pile Noise," Nuclear Science and Eng., 8, 53 (1960).

5. Albrecht, R. W.,"The Measurement of Dynamic Nuclear Reactor Parameters by Methods of Stochastic Processes, Univ. of Michigan, Ph. D Thesis, (1961)

6. Moore, M. N., "On the Determination of Reactor Transfer Functions from Measurements at Steady Operation," Nuclear Science and Eng., 4, 134 (1958).

7. Moore, M. N., " The Power Noise Transfer Function of a Reactor", Nuclear Science and Eng., 6, 448 (1959).

8. Velez, C., "Autocorrelation Functions of Counting Rate in Nuclear Reactors", Nuclear Science and Eng., 6, 414 (1959).

9. Velez, C.,"Autocorrelation Functions of Counting Rate in Nuclear Reactors and their Application to the Design of Reactor Control Instrumentation," Thesis, Univ. of Michigan (1959).

10. Brownrigg, W. G. and Littler, D. J., "Pile Modulation and Statistical Fluctuation in Piles," AERE N/R 476, Harwell (1950).

11. Frisch, O. R., Littler, D. J., "Pile modulation and Statistical Fluctuations in Piles," Phil-Mag, 45, 126 (1954).

12. Feiner, F., Frost, R. T., Hurwitz, H., Jr., "Pile Oscillator Measurements," KAPL - 1703 (1956).

13. Pál, L., "On the Theory of Stochastic Processes in Nuclear Reactors, Nuovo Cimento, 7, Series 10, Suppl. 1, 25 (1958).

14. Pal, L., "Statistical Fluctuations of Neutron Multiplication," Proc. of second United Nations Internat. Conf. on the Peaceful Uses of Atomic Eng., P/1710 (1958).

15. Harris, D. R., "Stochastic Fluctuations in a Power Reactor," WAPD-TM-190 (1958).

16. Cohn, C. E., "A Simplified Theory of Pile Noise," Nuclear Sci. and Eng., 7, 472 (1960).

17. Cohn, C. E., "Determination of Reactor Kinetic Parameters by Pile Noise Analysis," Nuclear Sci. and Eng., 5, 331 (1959).

18. Luckow, W. K., "The Evaluation of Nuclear Reactor Parameters from Measurements of Neutron Statistics," University of Michigan, Ph. D. Thesis, (1958).

19. Griffin, C. W., Lundholm, J. G., Jr., "Measurement of the SRE and KEWB Prompt Neutron Lifetime Using Random Noise and Reactor Oscillator Techniques," NAA-SR-3765 (1959).

20. Cummins, J. D., "Frequency Spectrum of Calder Hall Reactor Noise," AEEW - M - 19, Harwell (1960).

21. Balcomb, J. D., Demuth, H. B., Gyftopolous, E. P., "A Crosscorrelation Method for Measuring the Impulse Response of Reactor Systems," Nuclear Science and Eng., 11, 159 (1961).

22. Rajagopal, V., "Determination of Reactor Transfer Functions by Statistical Correlation Methods," Nuclear Science and Eng., 12, 218 (1962).

23. McCulloch, D. B., "The Absolute Measurement of the Effective Delayed Neutron Fraction in the Fast Reactor Zephyr," AERE R/M 176 (1958).

24. Kendall, D. G., "On the Generalized 'Birth-and-Death' Process," Ann. of Math Statistics, XIX, No. 1, 1 (1948).

25. Hurwitz, H., Jr., "Derivation and Integration of the Pile Kinetic Equations," Nucleonics, 5, No. 1, 61 (1949).

26. Henry, A. F., "The Application of Reactor Kinetics to the Analysis of Experiments," Nuclear Sci. and Eng., 3, 52 (1958).

27. Schultz, M. A., Control of Nuclear Reactors and Power Plants, second ed., McGraw-Hill, New York (1961).

28. Lanning, J. H., Jr., Battin, R. H., Random Processes in Automatic Control, McGraw-Hill, New York (1956).

29. Davenport, W. B., Root, W. L., An Introduction to the Theory of Random Signals and Noise, McGraw-Hill, New York (1958).

30. Blackman, R. B., Tukey, J. W., The Measurement of Power Spectra, Dover Pub., New York (1958).

31. Cramer, H., Mathematical Methods of Statistics, 8th print., Princeton University Press, Princeton (1958).

32. Toppel, B. J., "Sources of Error in Reactivity Determinations by Means of Asymptotic Period Measurements," Nuclear Science and Eng., 5, 88 (1959).

33. Moore, K. V., Tables of Reactivity vs. Period for U-235, Pu-239, and U-233, IDO-16485 (1958).

34. Harris, D. R., "The Sampling Estimate of the Parameter Variance / Mean in Reactor Fluctuation Measurements," WAPD-TM-157 (1958).

35. Van Deusen, B. D., "Analog Computation of Autocovariance Functions and Power Spectra," Chrysler Corp., Detroit, Analog Computation Div. 62-01 (1962).

36. Bendat, J. S., Principles and Applications of Random Noise Theory, Wiley and Sons, New York (1958).

37. Grenander, U., Rosenblatt, M., Statistical Analysis of Stationary Time Series, Wiley and Sons, New York (1957).

38. Keepin, G. R., Wimett, T. F., Zeigler, R. K., "Delayed Neutrons from Fissionable Isotopes of Uranium, Plutonium and Thorium," LA-2118 (1957).

39. Skinner, R. E., Cohen, E. R., "Reduced Delayed Neutron Group Representations," Nuclear Science and Eng., 5, 291 (1959).

40. Weinberg, A., Schweinler, H., "Theory of Oscillating Absorber in a Chain Reacting Pile," Physical Review, 74, 851 (1948).

APPENDICES

APPENDIX A

A SURFACE WHOSE PARTIALLY EXPOSED AREA VARIES SINUSOIDALLY WITH ANGULAR FREQUENCY AND APPLICATION

Consider a flat, fixed, semicircular area and an arbitrarily shaped, symmetric flat surface rotating about the midpoint, P, of the diagonal of the semicircle. Using an arbitrary shape, S, as illustrated in Figure D.1, where $R(\theta)$ is the radial distance from P to the boundary of S, for that portion of S which is outside of the semicircle, as a function of the angle measured with respect to any straight line through P, such as L, in a clockwise direction.

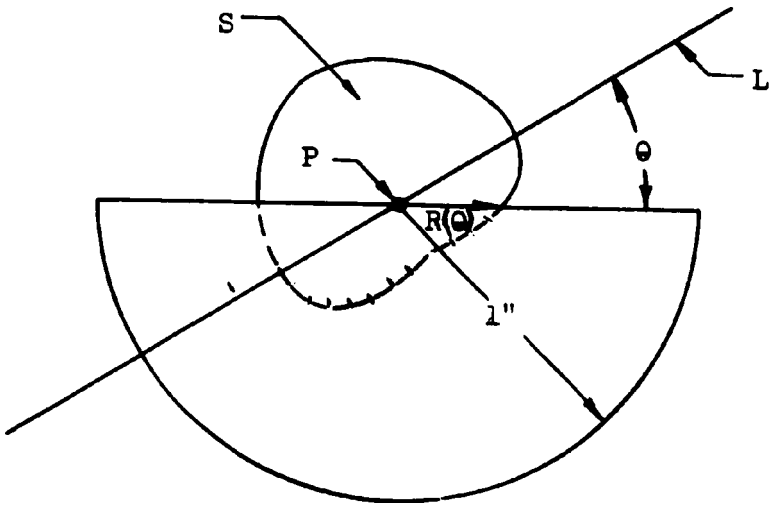


Figure A.1. Explanation of Disk Notation and Geometry.

The fraction of the total area of S which is outside the semicircle may be designated $A(\theta)$, and in general,

$$A(\theta) = \int_{\theta' = \theta}^{\theta' = \theta+\pi} \int_{r=0}^{R(\theta')} r(\theta')\, dr\, d\theta' \qquad (A.1)$$

It is necessary to find the form of $R(\theta)$ which will give a sinusoidally varying exposed area, i.e.

$$A(\theta) = K_1 + K_2 \sin \theta \qquad (A.2)$$

Integrating the general expression with respect to r,

$$A(\theta) = \frac{1}{2} \int_{\theta}^{\theta+\pi} R^2(\theta')\, d\theta' \qquad (A.3)$$

It is clear that the only function $\xi(\theta') = R^2(\theta')$ which will integrate to give $(K_1 + K_2 \sin \theta)$ is of the form $(K_3 + K_4 \cos \theta)$. This may be shown to be true by direct substitution. Thus,

$$R(\theta) = [K_3 + K_4 \cos \theta]^{1/2} \qquad (A.4)$$

Applying this result to an oscillating plate for the FNR, in a fuel channel, let $R_{min.} = R(0) = 0"$, $R_{max.} = R(\pi) = 1"$, giving $K_3 = 1/2$ sq. in. and $K_4 = -1/2$ sq. in.

The shape of the exposed plate is approximately as follows, being symmetric about the $\theta = 0°$ line. Where $R(30°) = 0.067$, $R(60°) = 0.5$, $R(90°) = 0.707$, $R(120°) = 0.866$, $R(150°) = 0.966$, $R(180°) = 1.0$.

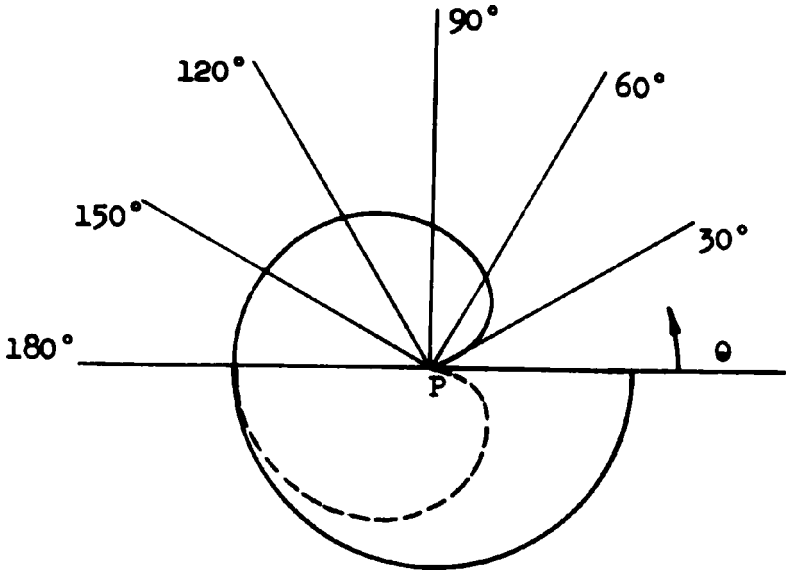


Figure A.2. Shape of Exposed Surface.

If the semicircular area is black to thermal neutrons, the rotation of the S plate should result in an absorption of neutrons which is approximately proportional to the exposed area for a flat neutron flux.

The shape used in the reactor oscillator was determined by (A.4). The author is indebted to Dr. Pawlicki of Argonne for suggesting (A.1).

APPENDIX B

NEUTRON-NEUTRON AND REACTIVITY-NEUTRON TRANSFER FUNCTIONS

When investigating the reactor response to a periodic reactivity driving function superimposed on the inherent fluctuations of the system, does the same transfer function describe both effects? In other words, can the noise fluctuations be thought of as arising from stochastic fluctuations about the mean effective multiplication constant or as fluctuations in the number of neutrons due to an external source.[6]

Writing the usual kinetic equations,

$$N_{,t} = \frac{k(1 - \beta) - 1}{\ell} N + \sum_i \lambda_i C_i + S \qquad (B.1)$$

$$C_{i,t} = \frac{k\beta_i}{\ell} N - \lambda_i C_i \qquad (B.2)$$

Linearize by setting $k = k_o + \delta k$, $N = N_o + \delta N$, $C_i = C_{io} + \delta C_i$, $S = S_o + \delta S$, $N_{o,t} = C_{io,t} = 0$. Neglect second order terms in δ to obtain,

$$\delta N_{,t} = \frac{(1 - \beta)}{\ell} (N_o \delta k + k_o \delta N) - \frac{\delta N}{\ell} + \sum_i \lambda_i \delta C_i + \delta S \qquad (B.3)$$

$$\delta C_{i,t} = \frac{\beta_i}{\ell} (k_o \delta N + \delta k\, N_o) - \lambda_i \delta C_i \qquad (B.4)$$

Taking the LaPlace transform, $\mathcal{L}\{f(t)\} = \overline{f}(p)$ setting initial conditions to zero, and substituting (B.4) into (B.3),

$$\overline{\delta N}\, p\ell\left[1 + \frac{(1 - k_o)}{S\ell} + \frac{k_o}{\ell} \sum_j \beta_i \Big/ (p + \lambda_i)\right] =$$

$$N_o \overline{\delta k}\left[1 - p \sum_i \beta_i \Big/ (p + \lambda_i)\right] + \overline{\delta S} \qquad (B.5)$$

For the reactivity-neutron transfer function, let $\overline{\overline{\delta S}} \rightarrow 0$, giving,

$$\frac{\overline{\overline{\delta N}}}{\overline{\overline{\delta k}}} = \frac{N_o[1 - p \sum_i \beta_i/(p + \lambda_i)]}{\ell p[1 + \frac{(1 - k_o)}{p\ell} + \frac{k_o}{\ell} \sum_i \beta_i/(p + \lambda_i)]} \qquad (B.6)$$

and for the neutron-neutron transfer function let $\overline{\delta k} \rightarrow 0$, giving,

$$\frac{\overline{\delta N}}{\overline{\delta S}} = N_o/[\ell p\{1 + \frac{(1 - k_o)}{\ell} + \frac{k_o}{\ell} \sum_i \beta_i/p + \lambda_i\}] \qquad (B.7)$$

If k is set equal to unity in (B.2), which introduces negligible error for small changes in k, (B.6) and (B.7) become identical.

APPENDIX C

FLUX HARMONICS DUE TO SMALL SINUSOIDAL CHANGES IN REACTIVITY

The contribution of harmonics to the neutron population for a small sinusoidal reactivity change can be determined in a direct manner. Writing the kinetic equations,

$$N_{,t} = \frac{-\delta k - \beta}{\ell} N + \sum_i \lambda_i C_i + S \tag{C.1}$$

$$C_{i,t} = \frac{\beta_i N}{\ell} - \lambda_i C_i \tag{C.2}$$

Let

$$\begin{aligned} \delta k &= \delta k_o \pm \delta k_1 e^{j\omega t} \\ N &= N_o + N_1 e^{j\omega(t + \theta_1)} + N_2 e^{2j\omega(t + \theta_2)} + \cdots \\ C_i &= C_{io} + C_{i1} e^{j\omega(t + \gamma_1)} + \cdots \end{aligned} \tag{C.3}$$

Substitute (C.3) into (C.1) and (C.2), and equate the coefficients of equal powers of the exponentials. The general terms are

$$N_m (mj\omega)\, e^{mj\omega\theta_m} = \frac{N_m}{\ell} e^{mj\omega\theta_m} (-\beta - \delta k_o) + N_{m-1} \frac{\delta k_1}{\ell} e^{(m-1)j\omega\theta_{m-1}} + \sum_i \lambda_i C_{im} e^{mj\omega\gamma_m} \tag{C.4}$$

and

$$C_{im}\, mj\omega\, e^{mj\omega\gamma_m} = \frac{\beta_i}{\ell} N_m e^{mj\omega\theta_m} - \lambda_i C_{im} e^{mj\omega\gamma_m} \tag{C.5}$$

Substituting for C_{im} from (C.5) into (C.4) gives, for $m = 0$, $N_o = S\ell / \delta k_o$ as expected. In general,

$$N_m e^{mj\omega\theta_m} = \delta k_1 N_{m-1} e^{(m-1)j\omega\theta_{m-1}} \Big/ \left[mj\omega + \beta + \delta k_o - \sum_i \frac{\lambda_i \beta_i}{(mj\omega + \lambda_i)} \right] \tag{C.6}$$

Substituting into the r.h.s. of (C.6) for values of m - i, i = 1,2, ..., m-1 gives,

$$N_m\, e^{mj\omega\theta_m} = N_o(\delta k_1)^m \Big/ \prod_{k=1}^{m} B_k \qquad (C.7)$$

where

$$B_k = kj\omega + \beta + \delta k_o - \sum_i \frac{\lambda_i \beta_i}{(kj\omega + \lambda_i)} \qquad (C.8)$$

The magnitudes of the harmonics are,

$$N_m = N_o(\delta k_1)^m \Big/ \prod_{k=1}^{m} B_k \quad . \qquad (C.9)$$

In a classic paper[40], the spatial dependence of the perturbed neutron flux due to a reactivity oscillation is considered.

APPENDIX D

THE EFFECT OF A SINUSOIDAL FUNCTION, SUPERIMPOSED ON THE FLUCTUATION DATA FROM THE REACTOR, ON THE CALCULATED RATIO OF THE VARIANCE TO MEAN NUMBER OF DETECTIONS AS A FUNCTION OF DETECTION TIME

Consider a magnetic tape which gives an instantaneous count rate represented by the continuous variable $g(t)$. A scaler sums the pulses occurring during a preset time, T, and then displays the result of the summation for a time, P, which is fixed, before starting another summation. The initial summing position on the tape occurs at time, t_o. Figure D.1 illustrates the procedure,

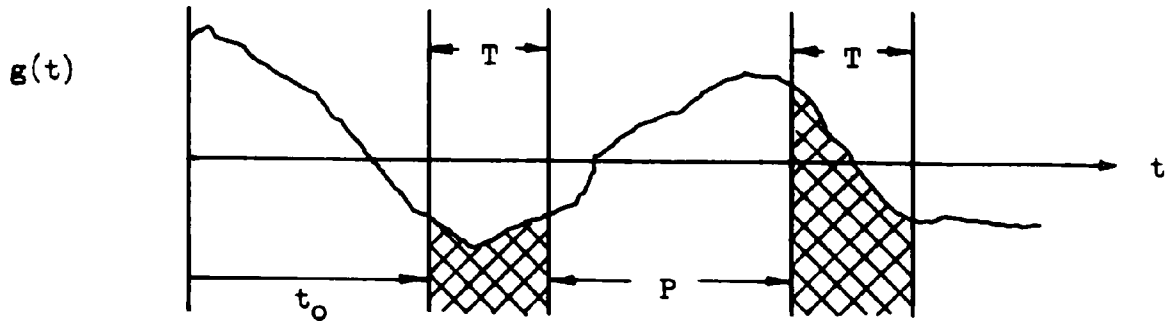


Figure D.1. Data Reduction Schematic.

where the cross-hatched areas indicate summation.

For a stationary process, let,

$$g(t) = A + \eta(t) + a \sin \omega t \qquad (D.1)$$

where A is the constant mean level, $\eta(t)$ represents noise fluctuation about the mean, and a $(\sin \omega t)$ represents the effect of a periodic forcing function. Define $Z_n(T)$ to be the number of counts displayed after the n'th counting interval of duration, T.

$$Z_n(T) = \int_{t_o+(n-1)(T+P)}^{t_o+(n-1)P+nT} g(t)\, dt \qquad (D.2)$$

Evaluating the integral,

$$\begin{aligned} Z_n(T) = {} & AT - \frac{a}{\omega} \cos \omega[t_o + nT + (n-1)P] \\ & + \frac{a}{\omega} \cos \omega[t_o + (n-1)(T+P)] \\ & + \bar{g}[t_o + (n-1)P + nT] - \bar{g}[t_o + (n-1)(T+P)] \end{aligned} \qquad (D.3)$$

If the quantity $(T + P) \neq$ [n] x [frequency of the periodic function], for n = 1, 2, ..., then all portions of the periodic function are used as starting points for pulse summation as the number of summations, N, goes to infinity. Thus, the inclusion of t_o is immaterial and may be omitted. Since $\bar{g} = 0$, and $\overline{\sin \omega t} = 0$,

$$\bar{Z}(T) = \frac{1}{N} \sum_{n=1}^{N} Z_n(t) = AT \; . \qquad (D.4)$$

Note g is composed of two independent parts, that due to normal reactor noise, R(t), and any effect caused by the periodic function, S(t).

$$\overline{g(t)} = \overline{R(t) + S(t)} = \bar{R} + \bar{S} = 0 \qquad (D.5)$$

The sample variance, σ_s^2 , is,

$$\sigma_s^2(T) = \overline{[Z_n(T) - Z(T)]^2} \qquad (D.6)$$

Equation (D.6) can be written compactly as,

$$\sigma_s^2(T) = \overline{[\Delta \cos + \Delta g]^2} \qquad (D.7)$$

where,

$$\Delta \cos = \frac{a}{\omega} \left[\cos \omega\{(n - 1)(T + P)\} - \cos \omega\{n(T + P) - P\}\right] \qquad (D.8)$$

and,

$$\Delta\zeta = \zeta[n(T + P) - P] - \zeta[(n - 1)(T + P)]. \qquad (D.9)$$

Since the cosine terms are assumed independent of the ζ terms,

$$\overline{\Delta \cos \Delta\zeta} = \overline{\Delta \cos}\ \overline{\Delta\zeta} = \overline{\Delta \cos}\ (0) = 0,$$

(D.7) becomes,

$$\sigma_s^2 = \overline{\Delta \cos^2} + \overline{\Delta\zeta^2} \qquad (D.10)$$

Evaluate the terms on the r.h.s. of (A.10).

$$\overline{\Delta \cos^2} = \overline{-2\left(\frac{a}{\omega}\right)^2 \cos \omega[n(T + P) - P] \cos \omega[(n - 1)(T + P)]}$$

$$+ \overline{\left(\frac{a}{\omega}\right)^2 [\cos^2 \omega(n[T + P] - P) + \cos^2 \omega(n - 1)(T + P)]} \qquad (D.11)$$

The mean value of a periodic function, $b(T + P)$, in the limit as $N \longrightarrow \infty$, is

$$\frac{\omega}{2\pi} \int_0^{2\pi/\omega} b(T + P)\, d(T + P) \qquad (D.12)$$

Performing the necessary integrations, using the trigonometric relation for $\cos(\alpha + \beta)$ and the orthogonality property of sine and cosine, find,

$$\overline{\Delta \cos^2} = \left(\frac{a}{\omega}\right)^2 (1 - \cos \omega T) \qquad (D.13)$$

Using (D.5),

$$\overline{\Delta\zeta^2} = \overline{\Delta R^2 + \Delta S^2 + 2\Delta R \Delta S} \qquad (D.14)$$

but, $\overline{\Delta R \Delta S} = (\overline{\Delta R})(\overline{\Delta S}) = 0$. Thus, assuming that the form of $\overline{\Delta S^2}$ is the same as $\overline{\Delta R^2}$, as a first approximation, we find the ratio of the variance to the

mean for the counting interval T is,

$$\frac{\sigma^2}{\bar{Z}}(T) = \frac{1}{\bar{Z}} \left(\frac{a}{\omega}\right)^2 [1 - \cos \omega T] + \left(\frac{\sigma^2}{\bar{Z}}\right)_{NOISE} \qquad (D.15)$$

The magnitude of "a" in (D.15) was investigated by evaluating the point kinetic equations using six delay groups and a representative source strength, on the nuclear engineering department's analog computer. For $\delta k = 0.00015 \sin \omega t$, a prompt lifetime = 10^{-4} seconds, an average $k_{eff} = 0.997$, and a frequency of 0.25 c.p.s., $\frac{a}{\bar{Z}}$ was about 3%. Thus the maximum practical contribution of the oscillator to $\frac{\sigma^2}{\bar{Z}}$ for $\cos \omega T = -1$, and $\bar{Z} = 2500$ c.p.s. is about 1.8. For a frequency of 10 c.p.s., $a/\bar{Z} = 0.46\%$, giving a contribution of about 0.00003. Considering deviations in $(\sigma^2/\bar{Z})_{NOISE}$ due to the low power level, the effect of the oscillator can not be seen in Figures 5.1 - 5.5.

APPENDIX E

A DERIVATION OF THE RELATIONSHIP BETWEEN THE RATIO OF THE VARIANCE TO THE MEAN OF THE DETECTIONS AS A FUNCTION OF COUNTING TIME AND THE AUTOCOVARIANCE FUNCTION

The autocovariance function of the observed neutron population was defined by (2.77), (2.79) and (2.81) to be:

$$\psi^{o}_{ob}(\tau) = \overline{\alpha(t)\,\alpha(t+\tau)} - \bar{\alpha}^2 \tag{E.1}$$

Let $\tau = t_2 - t_1$,

$$\psi^{o}_{ob}(t_2 - t_1) = \overline{\alpha(t)\,\alpha(t + t_2 - t_1)} - \bar{\alpha}^2 \tag{E.2}$$

change the dummy variable t to $t - t_2$,

$$\psi^{o}_{ob} = \overline{\alpha(t - t_2)\,\alpha(t - t_1)} - \bar{\alpha}^2 \tag{E.3}$$

Integrate (E.3) over t_1, $0 \le t_1 \le t_2$,

$$\int_0^{t_2} \psi^{o}_{ob}\, dt_1 = \overline{\alpha(t - t_2) \int_0^{t_2} \alpha(t - t_1)\, dt_1} - \bar{\alpha}^2 t_2 \tag{E.4}$$

or,

$$\int_0^{t_2} \psi^{o}_{ob}\, dt_1 = -\overline{\alpha(t - t_2) \int_t^{t-t_2} \alpha(t')\, dt'} - \bar{\alpha}^2 t_2 \tag{E.5}$$

$$\int_0^{t_2} \psi^{o}_{ob}\, dt_1 = -\overline{\alpha(t - t_2)[Z(t - t_2) - Z(t)]} - \bar{\alpha}^2 t_2 \tag{E.6}$$

Integrate over t_2, $0 \le t_2 \le \tau$, and changing variables as in (E.5) gives,

$$\int_0^{\tau}\int_0^{t_2} \psi^{o}_{ob}\, dt_1 dt_2 = \int_t^{t-\tau} \alpha(t')\, Z(t')\, dt' - Z(t) \int_t^{t-\tau} \alpha(t')\, dt' - \frac{\bar{Z}^2}{2} \tag{E.7}$$

Evaluating the first integral on the r.h.s. of (E.7) by identifying $\alpha(t')\,dt' = dZ(t')$, (E.7) becomes:

$$\int_0^{\tau}\int_0^{t_2} \psi^{o}_{ob}\, dt_1 dt_2 = \frac{\overline{Z^2(t-\tau)}}{2} + \frac{\overline{Z^2(t)}}{2} - \overline{Z(t)\,Z(t-\tau)} - \frac{\overline{Z}^2}{2} \qquad (E.8)$$

Recall the basic definition of $\overline{Z^2(\tau)}$,

$$\overline{Z^2(\tau)} = \lim_{T\to\infty} \frac{1}{2T} \int_{-T}^{T} \left[\int_{t-\tau}^{t} \alpha(t')\,dt'\right]^2 dt \qquad (E.9)$$

or,

$$\overline{Z^2(\tau)} = \overline{[Z(t) - Z(t-\tau)]^2} \qquad (E.10)$$

or,

$$\overline{Z^2(\tau)} = \overline{Z^2(t) - 2Z(t)\,Z(t-\tau) + Z^2(t-\tau)} \qquad (E.11)$$

However, since

$$\overline{Z^2(t-\tau)} = \lim_{T\to\infty} \frac{1}{2T} \int_{-T}^{T} Z^2(t-\tau)\,dt \qquad (E.12)$$

and, with a change of variable,

$$\overline{Z^2(t'')} = \lim_{T\to\infty} \frac{1}{2T} \int_{-T+\tau}^{T-\tau} Z^2(t'')\,dt'' \qquad (E.13)$$

one sees that,

$$\overline{Z^2(t)} = \overline{Z^2(t-\tau)} \qquad (E.14)$$

Substituting (E.14) into (E.11),

$$\overline{Z^2(\tau)} = \overline{2Z^2(t) - 2Z(t)\,Z(t-\tau)} \qquad (E.15)$$

Substituting (E.15) into (E.8) gives,

$$\frac{\overline{Z^2(\tau)} - \overline{Z(\tau)}^2}{\overline{Z}(\tau)} = \frac{2}{\overline{Z}(\tau)} \int_0^{\tau}\int_0^{t_2} \psi^{o}_{ob}\, dt_1 dt_2 \qquad (E.16)$$

which is the result quoted in (2.88).

APPENDIX F

REDUCED PULSE DATA

I - NOISE

Number of Gates	Mean	Variance/Mean	Gate Length (Seconds)
804	2.5286	1.3348	.001
168	7.3809	2.6591	.003
696	26.2112	4.4256	.010
288	50.8159	6.0204	.020
264	75.2273	6.3572	.030
468	88.9957	7.0993	.035
252	104.8333	8.2606	.040
300	123.6767	9.6275	.050
672	130.3542	8.1519	.050
276	151.4203	8.8379	.060
252	183.0039	7.6893	.070
636	192.8491	8.4268	.075
132	208.4924	9.6623	.080
192	229.7031	8.2452	.090
1440	257.7396	9.3350	.100
768	284.1354	8.7899	.110
600	309.0300	9.1078	.120
300	334.9033	9.8386	.130
648	364.8056	9.2445	.140
1356	386.9381	9.9524	.150
684	413.7412	8.9666	.160
636	438.2563	8.7662	.170
216	464.3379	8.0269	.180
672	459.9435	8.0481	.180
336	490.9583	9.1592	.190
564	488.0816	8.2235	.190
1284	515.0327	10.6589	.200
1284	646.8364	15.8497	.250
228	662.4079	18.8500	.250
216	652.6528	24.5800	.250
600	642.4917	12.3766	.250
1272	774.2209	10.5542	.300
264	812.6894	17.5724	.310
588	804.9915	15.2979	.310
600	837.7967	14.6686	.320
156	850.9487	20.4500	.320
144	864.3542	15.1175	.330
600	859.3233	14.4602	.330
600	889.2817	12.2253	.340
1092	900.9817	11.0241	.350
588	930.2704	12.5730	.360
564	959.8706	11.3714	.370
480	982.7938	10.2368	.380
552	1011.7917	11.1789	.390

I - NOISE

Number of Gates	Mean	Variance/Mean	Gate Length (Seconds)
1164	1027.0747	10.4657	.400
1116	1162.3745	10.6243	.450
960	1288.7458	10.8592	.500
912	1312.5230	10.6521	.510
984	1332.1829	9.9529	.520
852	1352.3145	10.2969	.530
1032	1378.2558	10.0477	.540
936	1416.6453	11.2129	.550
1020	1438.5098	10.9183	.560
1236	1469.8924	10.5272	.570
1032	1485.3246	9.6417	.580
1044	1508.6351	9.9581	.590
804	1543.8395	11.0037	.600
816	1673.5980	10.8071	.650
900	1801.3033	10.3343	.700
972	1930.0709	10.8199	.750
900	2053.2144	11.2198	.800
504	2184.1448	10.1899	.850
528	2187.9961	11.3180	.850
780	2314.3949	11.0736	.900
960	2445.7791	11.6876	.950
1020	2573.7392	11.1177	1.000
852	2830.9742	11.2129	1.100
744	3093.3226	11.5756	1.200
564	3337.2447	12.2286	1.300
564	3592.0745	12.6444	1.400
588	3861.5374	13.2293	1.500
768	3989.7630	12.7880	1.550
516	4101.6395	12.5296	1.600
324	4372.9969	13.0621	1.700
468	4361.6923	13.6934	1.700
336	4631.3690	12.2629	1.800
492	4622.4695	12.8840	1.800
324	4894.0956	13.6278	1.900
444	4876.1779	12.3096	1.900
456	5145.4605	12.5956	2.000
672	5275.8571	12.8478	2.050
300	5650.1899	12.2136	2.200
264	6431.1136	13.1745	2.500
192	7003.0521	48.0358	2.700
264	6937.4810	14.8475	2.700
228	7201.1096	149.5932	2.700
300	7769.9666	41.7125	3.000
120	8175.5166	231.8251	3.000
216	7986.9398	132.2187	3.000
228	8290.6184	34.2505	3.200
240	8346.5291	59.8971	3.200
240	8300.2749	38.8366	3.200
228	9100.5789	33.2269	3.500

I - NOISE

Number of Gates	Mean	Variance/Mean	Gate Length (Seconds)
204	9076.4901	31.5502	3.500
216	9062.7545	23.8910	3.500
144	9531.8680	20.3234	3.700
276	9548.9384	18.5318	3.700
132	9612.5529	31.6085	3.700
204	10308.0147	19.1199	4.000
180	10298.0055	16.4777	4.000
96	10225.9063	18.0948	4.000
84	10741.7856	16.2794	4.200
192	11573.1094	15.3619	4.500
144	12151.0347	16.3536	4.700
144	12832.7568	19.7296	5.000
288	12882.3923	15.7037	5.000
144	13609.1597	19.1299	5.300
132	14105.2196	17.5417	5.500
156	14617.5641	19.8225	5.700
144	15440.8750	18.5249	6.000
132	15930.9393	21.5625	6.200
120	16712.5166	22.8648	6.500
144	17221.9165	17.6537	6.700
132	17976.0454	18.6407	7.000
132	18794.3257	22.8983	7.300
96	19339.9478	19.7598	7.500
120	21882.3582	23.7165	8.500
168	23190.3154	22.2998	9.000
144	24429.2568	25.8109	9.500
84	25658.0117	24.7849	9.999

I - 1/2 cps

Number of Gates	Mean	Variance/Mean	Gate Length (Seconds)
348	2.5575	1.4625	.001
756	5.5661	3.3594	.003
468	24.9081	4.1211	.010
324	48.8673	5.9448	.020
288	48.0659	6.9108	.020
612	86.8938	7.7099	.035
264	101.7234	8.4905	.040
552	125.5417	8.8503	.050
264	147.8409	8.0422	.060
576	186.9323	8.5291	.075
1008	247.9554	8.4676	.100
1032	373.2442	8.9139	.150
1104	497.3315	8.8721	.200
984	624.0671	10.6256	.250
924	747.6071	9.3241	.300
1020	872.7618	10.5001	.350
996	990.4337	9.4415	.400
1020	1112.9706	10.3784	.450
1032	1239.8072	10.2760	.500
1104	1362.5634	9.8701	.550
792	1417.6667	10.5698	.570
1032	1489.0271	10.7460	.600
1044	1617.5268	10.3666	.650
1032	1731.2248	10.5024	.700
564	1855.2464	9.4756	.750
840	1853.8286	15.8024	.750
816	1987.5490	10.6602	.800
444	2112.2252	12.9256	.850
512	2116.6699	11.2714	.850
504	2103.3809	12.2742	.850
468	2245.5043	11.0576	.900
984	2235.6921	10.6395	.900
924	2359.4307	11.4586	0.950
492	2483.2337	10.6837	1.000
840	2479.3952	13.5654	1.000
900	2721.6878	11.0974	1.100
564	2980.1489	11.4734	1.200
816	2976.7328	12.1027	1.200
504	3221.9365	11.1807	1.300
612	3480.7745	11.6419	1.400
564	3719.6064	11.0933	1.500
720	3850.1208	11.6659	1.550
252	3975.6746	10.1789	1.600
504	3962.1349	13.3403	1.600
540	4218.3203	11.4070	1.700
324	4334.7963	13.1394	1.750
492	4468.5386	12.3721	1.800
468	4708.7414	12.5664	1.900
480	4850.2667	12.6898	1.950
672	5087.9523	12.6533	2.050

I - 1/2 cps (con't)

Number of Gates	Mean	Variance/Mean	Gate Length (Seconds)
168	5214.5238	14.1174	2.100
120	5437.9749	10.1737	2.200
120	5661.5000	12.2449	2.300
96	5882.0104	16.7015	2.400
96	6172.1771	12.9137	2.500
120	6434.6749	15.6576	2.600
120	6737.9166	33.4455	2.700
96	7026.8958	67.5129	2.800
132	7161.7954	12.7676	2.900
360	7442.9333	268.9948	3.000
492	7600.1524	99.5456	3.000
120	7617.7916	144.5249	3.100
96	8109.4479	111.4181	3.200
120	8539.2333	47.0732	3.400
228	8870.2719	56.1627	3.500
240	9111.9417	44.6847	3.600
108	9243.1574	27.2026	3.700
108	9536.2315	33.6265	3.800
120	9768.2500	36.7857	3.900
240	9988.0458	18.3369	4.000
372	10080.9086	31.3499	4.000
204	10210.7255	15.3172	4.100
144	10445.9513	14.1098	4.200
156	10696.3333	11.8085	4.300
156	10923.9614	13.6481	4.400
156	11154.3013	16.2812	4.500
144	11382.6250	15.4421	4.600
204	11670.3774	15.0878	4.700
180	11907.9221	16.1200	4.800
96	12172.9479	15.9029	4.900
192	12395.8594	13.3693	5.000
168	12541.6845	15.2351	5.050
156	12666.4038	16.9235	5.100
84	12960.9523	10.3460	5.200
96	13224.7916	19.2406	5.300
108	13359.0000	14.9829	5.400
168	13633.0892	15.3488	5.500
168	13909.4283	15.0567	5.600
72	13846.5277	20.5153	5.600
108	14143.3981	20.7513	5.700
156	14387.6282	15.2998	5.800
156	14697.7756	14.4239	5.900
276	14902.6558	16.0134	6.000
180	17344.4331	14.4547	7.000
72	17404.9443	14.8652	7.000
312	19859.0576	16.0279	8.000
348	22350.3103	16.7285	9.000
84	24782.1189	14.7431	9.999

I - 10 cps

Number of Gates	Mean	Variance/Mean	Gate Length (Seconds)
264	2.5341	1.5930	.001
216	10.0741	2.4317	.004
108	14.4074	3.4925	.005
216	14.8241	3.6902	.006
348	17.6581	3.3898	.007
384	20.5104	4.6639	.008
768	25.2305	4.4105	.010
1044	50.0249	5.7574	.020
792	74.1906	7.4306	.030
720	98.7264	7.6476	.040
696	122.2514	8.5489	.050
768	144.9887	8.3705	.060
744	173.2917	9.2634	.070
816	245.9129	8.5356	.100
1140	269.7114	9.3046	.110
1152	295.3004	9.3885	.120
1104	320.8569	9.3391	.130
780	348.7526	9.2919	.140
840	396.1357	8.7412	.160
840	416.9583	9.1396	.170
684	443.6784	10.0488	.180
1104	469.3795	9.4843	.190
864	493.1840	9.3705	.200
300	514.5833	8.3419	.210
240	513.4708	9.9105	.210
228	540.7412	10.3316	.220
312	538.6731	10.1563	.220
276	570.7029	9.9059	.230
288	565.9271	9.1233	.230
240	589.6917	11.4119	.240
300	592.1867	9.0560	.240
264	614.9924	8.2895	.250
276	617.0615	9.9922	.250
288	639.6007	11.2534	.260
396	641.9192	10.8798	.260
144	663.5277	9.4533	.270
204	672.2696	15.5473	.270
252	699.3492	13.7133	.280
264	685.3068	10.4744	.280
264	716.7311	14.5298	.290
276	714.7862	11.4458	.290
864	748.5162	15.7243	.300
636	772.3616	17.7197	.310
540	807.8518	18.5152	.320
396	828.9899	16.0836	.330
600	849.8100	15.2600	.340
384	876.9583	15.5929	.350
540	895.2426	12.9321	.360
288	923.2431	13.9724	.370
588	942.8061	12.5602	.380
564	975.7287	11.6554	.390
780	992.8231	11.2021	.400

I - 10 cps (con't)

Number of Gates	Mean	Variance/Mean	Gate Length (Seconds)
264	1000.9166	10.6962	.410
264	1032.2879	10.5677	.420
252	1050.1349	16.4912	.430
192	1086.9375	10.8698	.440
204	1109.2304	11.2740	.450
108	1132.5555	9.0964	.460
252	1153.0278	9.6579	.470
240	1181.0208	10.8065	.480
264	1210.1666	10.8516	.490
804	1235.7699	12.2554	.500
1024	1231.0951	11.0627	.500
1104	1244.6295	10.0072	.510
1080	1278.8499	10.2750	.520
1068	1298.2780	10.8549	.530
1056	1323.7149	10.7237	.540
900	1341.3433	17.6338	.550
1056	1355.8504	10.1800	.550
1056	1373.3049	10.6291	.560
1056	1394.4706	10.5628	.570
1068	1418.4176	10.2616	.580
1104	1444.2789	13.9216	.590
924	1447.8171	10.1649	.590
1080	1469.9361	11.1348	.600

IV - NOISE

Number of Gates	Mean	Variance/Mean	Gate Length (Seconds)
636	22.1085	3.6495	.010
324	44.1852	5.9579	.020
288	66.3125	7.5299	.030
300	85.0633	7.9682	.040
300	110.1267	9.4882	.050
360	130.6000	11.4124	.060
228	173.2851	8.2784	.080
264	195.5038	9.1912	.090
636	217.7389	9.4387	.100
264	432.3447	10.2874	.200
300	655.6167	14.1192	.300
252	882.5794	13.3869	.400
312	1080.6603	11.4842	.500
240	1307.2999	12.2989	.600
240	1521.4192	13.3573	.700
192	1740.7917	12.7811	.800
204	1958.9314	11.1705	.900
444	2159.1126	11.5230	1.000
216	2603.5093	12.6738	1.200
192	3253.1406	15.1422	1.500
144	3727.9375	15.3803	1.700
180	4342.0056	15.7652	2.000
156	4809.9294	15.7094	2.200
156	5443.5769	15.8856	2.500
132	5893.9545	13.0476	2.700
108	6521.4166	19.3046	3.000
120	6957.6083	20.3721	3.200
72	8179.6805	91.3717	3.700
108	8721.5925	25.1280	4.000
132	9151.3559	23.8029	4.200
108	9838.7684	20.8392	4.500
120	10296.1832	18.2746	4.700
96	10794.4895	21.1064	5.000
276	10881.1123	19.9194	5.000
180	11282.2888	23.8090	5.200
120	12019.7583	21.6415	5.500
120	12291.3750	21.9664	5.700
108	13084.7592	18.9873	6.000
72	13446.6666	22.5866	6.200
144	14165.4930	22.4697	6.500
108	15189.0463	22.3564	7.000
96	15686.4895	19.8661	7.200
120	16248.5333	24.8209	7.500
96	17379.6875	23.6548	8.000
120	17776.1165	20.9011	8.200
96	18591.1875	23.8447	8.500
132	18988.1816	26.1574	8.700
84	19483.6069	27.8478	9.000
120	20016.4915	26.2015	9.200
108	20660.5554	29.1204	9.500
108	21106.3332	27.2830	9.700
72	21743.5415	25.4216	9.999

V - NOISE

Number of Gates	Mean	Variance/Mean	Gate Length (Seconds)
456	21.3750	3.7734	.010
576	41.7413	6.2687	.020
348	63.4081	6.2869	.030
312	84.3045	6.8431	.040
252	105.6349	7.1761	.050
312	129.8526	8.3349	.060
324	141.5586	7.6584	.070
312	170.9711	9.0092	.080
276	188.7282	12.0381	.090
528	212.8523	8.2496	.100
228	426.5088	8.8731	.200
288	641.8750	15.3330	.300
276	860.8732	16.2483	.400
228	1064.0789	9.9086	.500
228	1277.1272	8.4580	.600
228	1482.1491	8.9461	.700
192	1699.2239	10.0743	.800
168	1921.3452	12.5920	.900
276	2125.7681	10.9550	1.000
204	2532.2647	10.6021	1.200
192	3169.0416	12.7027	1.500
156	3601.6154	12.9646	1.700
156	4247.7692	9.9657	2.000
168	4677.2380	11.9778	2.200
132	5322.3408	9.8543	2.500
168	5764.9464	12.6656	2.700
132	6363.2196	10.9111	3.000
72	6871.7500	12.0229	3.200
168	7485.8511	60.8032	3.500
156	8019.7500	92.1183	3.700
120	8540.6000	41.3043	4.000
120	8938.0499	14.2662	4.200
108	9621.0739	16.6371	4.500
96	10017.8437	16.5414	4.700
84	10621.4285	17.4601	5.000
192	11041.4219	15.1779	5.200
144	11667.7013	16.2718	5.500
120	12130.1333	15.7279	5.700
144	12703.9513	15.8583	6.000
120	13114.1832	14.5680	6.200
108	13867.4722	16.1715	6.500
132	14231.8484	15.9859	6.700
144	14891.7083	15.0345	7.000
120	15294.5999	16.0573	7.200
168	15972.3750	15.9556	7.500
132	16365.6515	16.8197	7.700
84	16996.5952	14.0974	8.000
108	17464.3239	14.9948	8.200
120	18059.0915	17.1308	8.500

V - NOISE

Number of Gates	Mean	Variance/Mean	Gate Length (Seconds)
108	18574.0183	17.2161	8.700
108	19108.1943	17.6358	9.000
108	19327.5647	30.7306	9.200
120	20081.1082	15.7528	9.500
108	20558.8518	17.0679	9.700

MISCELLANEOUS RUNS

	Run	Gates	Mean	Variance/Mean	Gate Length (Seconds)
I.	1817 rpm	372	2440.5779	10.8787	1.000
II.	Noise	456	2002.4890	11.1758	1.000
II.	$\frac{712}{480}$ cps	420	1774.2929	12.8476	1.000
II.	640 rpm	420	1709.8381	10.1892	1.000
II.	1915 rpm	384	1685.6693	11.7488	1.000

APPENDIX G

DIGITAL COMPUTER PROGRAMS

The following programs are included to show exactly how the computation in this thesis was accomplished. It is felt that such information would be helpful for future workers in this area of study. Both the FORTRAN and the MAD languages are used. These programs are written for the Michigan executive system and specifically the IBM-709.

Contents

		Page
1.	VAROMEAN - WESTERVELT Computes the ratio of the variance to mean for a given gate length	142
2.	ROOT 6 Computes the 7 roots of the 6 delay group inhour equation	143
3.	ROOT 2 Computes the 3 roots of the 2 delay group inhour equation	145
4.	CORR 6 Computes the 6 group autocorrelation function, given the roots of the inhour equations	146
5.	TWO GROUP Computes the effective 2 group delay constants from 6 group data using the method of Skinner and Cohen	151
6.	TWO GROUP COEFFICIENTS Computes the coefficients needed to calculate the 2 group autocorrelation function	152
7.	CORRELATION 7 Computes the 2 group autocorrelation function given the roots of the 2 group inhour equation and the results of program 6	154
8.	TRANSFER 6 Computes the 6 group transfer function in d.b., phase angle and power spectral density for a white noise input	155

```
$    COMPILE FORTRAN, PRINT OBJECT, EXECUTE, DUMP, PUNCH OBJECT,I/O DUMP
C    COMPUTES VARIANCE ,VA, TO MEAN,EM, RATIO, V, FOR A COUNTING INTERVAL
C     T.    100 VALUES OF T ARE ALLOWED, AND 1500 DATA POINTS FOR EACH T.
C      ALSO, COMPUTES THE MODIFIED RESULT RHO = V - 1.0, AND THE WEIGHT
C     OF EACH CALCULATED V BY, OMEGA WHICH IS DEFINED AS  THE INVERSE
C     OF TWICE THE VARIANCE OF EACH INDIVIDUAL V.  I USED HOURIS FOR
C   THE FORMULATION OF OMEGA.  THE OBSERVATION NUMBER, TIME, VAR/MEAN - 1.0
C     AND WEIGHT OF EACH DATA POINT ARE PUNCHED OUT READY FOR WESTERVELTS REGRESS
C     ION PROGRAM
C   IF NO = 1, PROGRAM WILL NOT PUNCH OUT RESULTS
      DIMENSION A(1500) , B(1500), C(1500), T(100), V(100), VA(100),
     XEM(100), N(100), RHO(100), OMEGA(100)  ,OBS(101)
      WRITE OUTPUT TAPE  6,5
    5 FORMAT (53H1 THE NAME OF THIS PROGRAM IS VARMEAN-WESTERVELT      )
      READ INPUT TAPE  7,4, NO
    4 FORMAT (I1)
      READ INPUT TAPE 7,8, M, (T(I), I=1,M)
    8 FORMAT (I3/(12F6.3))
      OBS(1)= 0.0
   50 DO   12     I=1,M
      READ INPUT TAPE 7,1,  Z, NI,  (A(IDAT),  IDAT=1,NI)
    1 FORMAT (F4.0,I4/(12F6.0))
      N(I)=NI
      OBS(I+1) = OBS(I) + 1.0
      B(1)= A(1)
      C(1)= A(1)*A(1)
      DO  2     J=2,NI
      B(J)= B(J-1) + A(J)
      A(J)=  A(J)*A(J)
      C(J)= C(J-1) + A(J)
    2 CONTINUE
      VA(I)=  (Z*C(NI)  - B(NI) * B(NI))/  (Z*(Z-1.0))
      EM(I)= B(NI)/Z
      V(I)=  VA(I)/EM(I)
      RHO(I) = V(I) - 1.0
      OMEGA(I) = 1.0/ ( (4.0/Z) *V(I)*V(I)+  (1.0 + V(I))/ (2.0*EM(I)*OBS
     X)
      WRITE OUTPUT TAPE 6,3, (N(I), VA(I), EM(I), T(I), V(I),OMEGA(I)
    3 FORMAT  ( 8HO  N      VARIANCE           MEAN          TIME         VAR
     X/MEAN                OMEGA          /(I10,2F15.3,F10.3,F20.6,F20.8)
   12 CONTINUE
      IF (NO-1)     20,50,20
   20 PUNCH 30, (OBS(I+1), T(I), RHO(I), OMEGA(I), I=1,M)
   30 FORMAT (F5.0, F10.3, F20.6, F20.8)
      END
```

```
$     COMPILE FORTRAN, PRINT OBJECT, EXECUTE, DUMP, PUNCH OBJECT,I/O DUMP
C     PROGRAM NAME IS ROOT 6
      DIMENSION   D(6), BE(6),  A(16),  R(14)
C     INHOUR EQUATION WRITTEN ORIGINALLY AS
C     0.0 = -(K-1.0)/(BETA*K) + R*TIME/(BETA*K) + (R/BETA)  X  SUM OVER BETA(I)/
C     (R +B(I))     FROM I=1, 6
C     AND IS THEN MANIPULATED TO PUT IN THE FORM
C     A(1)*R**7 + A(3)*R**6 + A(5)*R**5 + A(7)*R**4 + A(9)*R**3 + A(11)*R**2 +
C     A(13)*R**1  + A(15)    = 0.0
C     THIS PROGRAM COMPUTES THE A(I)S AND THEN THE ROOTS OF THE LATTER EQUATION US
C     NG THE SUBROUTINE ZER2
C     NOTATION   NEUTRON LIFETIME = TIME, MULTIPLICATION CONSTANT = EFFMUL
C     LAMBDAS = D(I), BETAS = BE(I),,
C     A(ODD)  = THE REAL PART OF THE COEFFICIENTS OF THE SEVENTH ORDER EQUATION.
C     A(EVEN)= IMAGINARY PART OF THE COEFFS, SHOULD BE ZERO
C     SIMILARLY, R(ODD)  = THE REAL  PART OF THE ROOT, WHICH SHOULD ALSO BE
C     THE ONLY PART
C     THE H IN FORMAT 5 SHOWS THAT RZER IS WORKING PROPERLY IF H= I
      DO  10     I= 2, 16,2
   10 A(I) =      0.0
      DO  12    I=2,14,2
   12 R(I) = 0.0
    1 WRITE OUTPUT TAPE  6,9
    9 FORMAT (25H1 PROGRAM NAME IS ROOT6     )
      READ INPUT TAPE 7,2, TIME, EFFMUL,(D(I), I=1,6),(BE(I),I=1,6)
    2 FORMAT (2F10.6/6F10.5/6F10.7)
      WRITE OUTPUT TAPE  6,11, TIME, EFFMUL, (D(I),I=1,6),(BE(I),I=1,6)
   11 FORMAT (15HO LIFETIME =   F10.6,  20HO MULTIPLICATION CONSTANT =
     X F10.6/ 12HO LAMBDAS =   6F10.5/ 10HO BETAS =   6F10.7)
      BT = 0.0
      BT = 0.0
      DO  3     I=1,6
      BT = BT + D(I)
    3 BT = BT + BE(I)
      A(1) = TIME/ (EFFMUL*BT)
      GAMMA = -(EFFMUL-1.0) / (EFFMUL*BT) + 1.0
      A(3) = A(1) * DT + GAMMA
      H = D(1)*D(3)+D(2)*D(3) + D(1)*D(2) + (D(1) + D(2) + D(3))*D(4)
     X  + (DT - D(5) - D(6)) *D(5)
      E = D(1)*D(3) + D(2)*D(3) +D(1)*D(2) +(D(1) +D(2)+D(3))*D(4)
      HF = (D(1)*D(3) + D(2)*D(3)+D(1)*D(2),*D(4) + D(1)*D(2)*D(3)
      C = D(1)*D(2)*D(3)
      DD = D(1) + D(2) + D(3) + D(4)
      P1 = -BE(1)*D(1)/BT
      P2 = -BE(2)*D(2)/BT
      P3 = -BE(3)*D(3)/BT
      P4 = -BE(4)*D(4)/BT
      P5 = -BE(5)*D(5)/BT
      P6 = -BE(6)*D(6)/BT
      A(5) = A(1)*(E+DD*D(5) + (DD+D(5)) *D(6)) + GAMMA*BT + P1 + P2 +
     X     P3 + P4 + P5 + P6
      A(7) = A(1) *(HF+E*D(5) + H*D(6)) + GAMMA*(H+ (DD+D(5))*D(6)) + P1
     X    *(DT-D(1)) + P2*(DT - D(2)) + P3*(DT - D(3)) + P4*(DT - D(4)) +
     X  P5 * (DT-D(5)) + P6*(DT-D(6))
      HJ = C*D(4) + HF*D(5)
      HI = HF + E*D(5)
      Q = D(2)*D(3) + (D(2)+D(3))*D(4) + (D(2)+D(3)+D(4))*D(5)
      HA6 = D(1)*D(3) +(D(1)+D(3))*D(4)+(D(1)+D(4)+D(3))*D(5)
      W = D(1)*D(2) +(D(1) +D(2))*D(4)+(D(1)+D(2)+D(4))*D(5)
```

```
      B = (D(1)+D(2))*D(3) + D(1)*D(2)
      Z = B + (D(1) + D(2)+D(3))*D(5)
      A(9) = A(1)*(HJ + HJ*D(6)) + GAMMA*(HJ+HH*D(6)) + P1*(G+(DT-D(1)-
     X   D(6))*D(6)) +P2*(HA6 +(DT - D(2) -D(6))*D(6)) +P3*(W+(DT-D(3)-D
     X(6))*D(6)) +P4*(Z+(D(1)*D(2)*D(3)*D(5))*D(6))+P5*(E +(DT-D(5)-D(6
     X))*D(6)) +P6*H
      HA1 =  C + ((D(1)*D(2))*D(3) + D(1)*D(2))*D(5)
      HA3 = D(1)*D(3)+(D(1)+D(3))*D(4)
      HA4 = D(1)*D(3)*D(4)
      R = D(2)*D(3)*D(4) + (D(2)*D(3)+(D(2)+D(3))*D(4))*D(5)
      HA7 = HA4 + HA3 *D(5)
      X = D(1)*D(2)*D(4) +(D(1)*D(2)+(D(1)+D(2))*D(4))*D(5)
      A(11) = A(1)*(C*D(4)*D(5)*HJ*D(6)) + GAMMA*(HJ+HH*D(6)) + P1*(X+G+
     X D(6)) + P2*(HA7+HA6*D(6)) + P3*(X+W*D(6)) +P4*(HA1 +Z*D(6)) + P5*
     X   (HF + E*D(6)) +P6*HH
      HH = D(2)*D(3)*D(4)
      U = D(1)*D(2)*D(4)
      A(13) = A(1)*C*D(4)*D(5)*D(6)    + GAMMA*(C*D(4)*D(5)    +HJ*D(6)) +
     X   P1*(HH*D(5) + R*D(6))  +P2*(HA4*D(5) +HA7*D(6)) + P3*(U*D(5) +
     X  X*D(6))  +P4*(C*D(5)  +HA1*D(6)) + P5*(G*D(4) +HF*D(6)) + P6 *
     X  HJ
      A(15) = GAMMA*C*D(4)*D(5)*D(6)    + P1 *HH*D(5)*D(6)  +P2*HA4*D(5)
     X*D(6)    +P3*U*D(5)*D(6)  + P4*C*D(5)*D(6)  +  P5*C*D(4)*D(6)
     X      +P6*C*D(4)*D(5)
      M = ZERZ(Y , A,R)
      WRITE OUTPUT TAPE  6,5,(A(I), I=1,15,2),(R(I),I=1,14)  , M
    5 FORMAT(7HNO COEFFICIENTS OF THE SEVENTH ORDER EQUATION ARE (A(I),A
     X(3),....A(15))        /8E14.7/114HO THE ROOTS OF THE 6 GROUP INNOV
     XN EQUATION ARE (R(1),R(2),...,R(14)) WHERE R(2),R(4),...R(14) SHOU
     XLD BE 9ERO)         /6E20.7/6E20.7/2E20.7/62HO IF M IS UNITY, ROOT
     XSUBROUTINE IS WORKING PROPERLY   M =          I5)
      PUNCH 30, (R(I),I=1,13,2)
   30 FORMAT (7F10.5)
      GO TO 1
      END
```

```
$  COMPILE MAD, PRINT OBJECT, PUNCH OBJECT, EXECUTE, DUMP, I/O DUMP
          DIMENSION   A(10),D(10),BETA(10),R(10)
         R   PROGRAM NAME IS ROOT 2
         R  THIS PROGRAM COMPUTES THE ROOTV, R(I), OF THE TWO DELAY
         R   GROUP INHOUR EQUATION, IN THE FORM  A(0)*Y**3 + A(4)*Y
         R   + A(6)  =  0.0
         R   NOTE THAT A(EVEN) CORRESPONDS TO AN IMAGINARY COEFFICIENT
         R   AS   FAR AS THE ROOT SUBROUTINE IS CONCERNED.
         R  SIMILARLY,  R(EVEN) SHOULD ALL BE ZERO AS A TEST ON THE
         R   SUBROUTINE, SINCE A(EVEN) = 0.0
         R   NOTATION    MULTIPLICATION CONSTANT = GEN, PROMPT
         R   LIFETIME = TAU,  LAMBDAS = D(I),  BETAS = BETA(I)
QQ0002    READ FORMAT QQ0003, GEN,TAU, D(1),D(2), BETA(1), BETA(2)
          VECTOR VALUES     QQ0003  = $ 2F10.7/2F10.5/2F10.7    *$
          WRITE BCD   TAPE  6      ,     QQ0008
          VECTOR VALUES     QQ0008  = $ 27HI NAME OF PROGRAM IS ROOTZ
         1      *$
          EXECUTE       ZERO.(A(0),...,A(10))
          EXECUTE ZERO.( R(0),...,R(10) )
          PRINT FORMAT  QQ0009,GEN,TAU,D(1),D(2),BETA(1),BETA(2)
          VECTOR VALUES     QQ0009  = $ 28HO MULTIPLICATION CONSTANT =
         1 F10.7,19HO LIFETIME =  F10.7/14HO LAMBDAS ARE  2F10.5/12HO B
         1ETAS ARE  2F10.7  *$
          A(0)=TAU/GEN
          A(2)=(1.0-GEN)/GEN+A(0)*(D(1)+D(2))+BETA(1)+BETA(2)
          A(4)=(1.0-GEN)/GEN*(D(1)+D(2))+A(0)*D(1)*D(2)+BETA(1)*D(2)+BE
         1TA(2)*D(1)
          A(6)=(1.0-GEN)/GEN*D(1)*D(2)
         R   INTO ROOT SUBROUTINE
         R
          N=ZER2 .(   3,A,R)
          PRINT FORMAT QQ0013,  A(0),A(2),A(4),A(6),R(0),...,R(5),N
          VECTOR VALUES     QQ0013  = $ 14HOCOEFFICIENTS  4E20.7/18HO R
         1OOTS OF INHOUR  /6E18.7/63HO IF N EQUALS 1 ROOT SUBROUTINE IS
         1 WORKING PROPERLY       N =      I3    *$
          TRANSFER TO QQ0002
          INTEGER N
QQ0001    END OF PROGRAM
```

```
$ COMPILE MAD, PRINT OBJECT, PUNCH OBJECT, EXECUTE, DUMP, I/O DUMP
R   PROGRAM NAME IS CORRELATION 6
R   FOR 6 DELAY GROUPS, PROGRAM SETS THE REAL PART OF THE
R TRANSFER FN = SUM (J=1,7) OF THE REAL PART OF AA(J)/
R    (IW -R(J)), WHERE R(J) IS THE JTH ROOT OF THE INHOUR EQ.
R THESE 7 EQS ARE SOLVED EXPLICITLY FOR THE 7 AA(J)'S WHICH ARE
R  USED TO COMPUTE A G(J).  THEN USING THE R(J), AA(J), AND G(
R  J), THE AUTOCOVARIANCE FN IS COMPUTED.  THE FIRST TIME USED
R  SHOULD BE ZERO FOR NORMALIZATION
R    JTIME = NUMBER OF DELAY TIMES USED
R    TT(J) = THE DELAY TIMES, READ IN AS DATA
  PRINT FORMAT TAPP
  VECTOR VALUES TAPP =$ 33H1 PROGRAM NAME IS CORRELATION 6    *$
R    THE ADJUSTERS MAY BE SET TO UNITY.  HOWEVER, THEY ARE
R    USEFUL IN ADJUSTING THE VALUES OF THE C(J,I) MATRIX,
R    I USED VALUES OF 100 AND 1000  TO KEEP AS MANY SIGNIFICANT
R    DECIMAL PLACES AS POSSIBLE.
  READ FORMAT TAP, JTIME, TT(1),...,TT(JTIME)
  VECTOR VALUES  TAP=$  I3/ (7F10.4)  *$
  READ FORMAT ADJK, F(1),...,F(7)
  VECTOR VALUES ADJK =$ 7F10.1  *$
  PRINT FORMAT ADJS  , F(1),...,F(7)
  VECTOR VALUES ADJS  =$29H  THE MATRIX ADJUSTERS ARE        /7
1F10.1    *$
Q1
  READ FORMAT DATA, GEN, TAU, POP, D(1),...,D(6), BETA(1),...,BETA(
16)
  VECTOR VALUES DATA =$2F10.7/  E20.8/ 6F10.5/ 6F10.7*$
  DIMENSION  R(10),YY(2**10), B(10), BETA(10), BB(10), G(10),
1  PIECE(10), C(49,DES), F(10), T(10), AA(10) ,ERROR(10)
  VECTOR VALUES DES= 2,1,7
  INTEGER  DES, I, J,      JTIME, JJJ, KKK
  READ FORMAT TAPE, R(1),...,R(7)
  VECTOR VALUES TAPE =$ 7F10.5    *$
  PRINT FORMAT OUT, GEN, TAU, POP, D(1),...,D(6), BETA(1),...,BETA(
16),R(1),...,R(7)
  VECTOR VALUES OUT  =$ 26HO MULTIPLICATION FACTOR =   F10.7,
1  19HO LIFETIME =   E10.3, 18HO NEUTRON LEVEL =  E20.5/
2 14HO LAMBDAS ARE   6F15.5/ 12HO BETAS ARE    6F15.7/36HO ROO
3TS OF THE INHOUR EQUATION ARE    /7F14.5    *$
  FIRST = 1.0
  W = -R(1)
  CM = GEN/TAU
   CT= (1.0- GEN)/TAU
R  LOOP TO Q50 COMPUTES REAL PART OF TRANS FN EVALUATED
R  AT ANGULAR FREQS = MINUS ROOTS OF INHOUR
  THROUGH Q50, FOR J=1,1,J.G.7
  B0(0) = 0.0
  SNAP=0.0
  C0=0.0
  WW= W*W
R  LOOP TO Q50 COMPUTES TERMS IN TRANS FN
  THROUGH Q50, FOR I=1,1,I.G.6
  SNAP = BETA(I)/(WW+D(I)*D(I) )
  B0(I)=       B0(I-1)  + SNAP
  C0 = C0 + SNAP*D(I)
Q50
  CONTINUE
  T-J)  = POP/TAU* ((1.0-WW*B0(6) )*(CT+CM*WW*B0(6)) -WW*C0*(
11.0+CM*C0 )) /(( CT+CM*WW*B0(6)) *(CT+CM*WW*B0(6)) +WW*(1.0
2 +CM*C0)*(1.0+CM*C0))*F(J)
```

```
      PRINT RESULTS W, Y(J)
      W=   -R(J+1)
Q60   CONTINUE
C  CALC THE COEFFS OF THE UNKNOWNS, STORE IN C(J,K)
      THROUGH Q75, FOR J=1,1,J+6,7
       W =   -R(J)
        WW= W*W
      THROUGH Q70, FOR I=1,1,I+6,7
      C(J,I)  = -R(I)/(R(I)*R(I)  +WW) *F(J)
Q70   CONTINUE
Q75   CONTINUE
      PRINT RESULTS   C(1,1)...C(7,7)
      X2 = C(2,2) - C(2,1)*C(1,2)/C(1,1)
      Y = T(2) - C(2,1)*T(1)/C(1,1)
      Y2 = C(2,1)*C(1,3)/C(1,1) - C(2,3)
      Z2= C(2,1)*C(1,4)/C(1,1)- C(2,4)
      PRINT RESULTS     X2,Y,Y2,Z2
      M2= C(2,1)*C(1,5)/C(1,1) - C(2,5)
      P2= C(2,1)*C(1,6)/C(1,1)- C(2,6)
      Q2=  C(2,1)*C(1,7)/C( 1,1)  - C(2,7)
      PRINT RESULTS     M2,P2,Q2
      R3 = C(3,2) - C(3,1)*C(1,2)/C(1,1)
      X3= -C(3,1)*C(1,3 )/C(1,1) +R3*(Y2       )/X2   + C(3,3)
      B3 = T(3) -C( 3,1)*T(1)/C(1,1)  -R3*Y/X2
      C3 = C(3,1)*C(1,4)/C(1,1) - R3*(Z2       )/X2   - C(3,4)
      PRINT RESULTS     R3,X3,B3,C3
      D3= C(3,1)*C(1,5)/C(1,1) -R3*(M2       )/X2 -C(3,5)
      E3= C (3,1)*C(1,6)/C(1,1) - R3*(P2       )/X2 - C(3,6)
      F3=C(3,1)*C(1,7)/C(1,1) -R3*(Q2       )/X2 -C(3,7)
      J3  = C(4,2)/X2
      PRINT RESULTS     D3,E3,F3,J3
       G4=  C(4,1)*C(1,2)/(C(1,1)*X2)
      J4= C(4,2)*Y2/( X2*X3)
       XYZ  = C(4,1)*T(1)/C(1,1)  + J3*Y  + C(4,3)*B3/X3  -G4*Y
     1  -C(4,1)*C(1,3)*B3   /(C(1,1)*X3)  +J4*B3-G4*Y2*B3/X3
        XYZ1=   -C(4,1)*C(1,3)/(C(1,1)*X3)
       XYZ2=   -G4*Y2/X3
       XYZ3=   -C(4,1)  / C(1,1)
        XYZ4=   C(4,3)/X3
       PRINT RESULTS G4,J4, XYZ, XYZ1
       PRINT RESULTS  XYZ2, XYZ3, XYZ4
       G= XYZ1*C3 + J4*C3 + XYZ2*C3 + XYZ3*C(1,4) + J3*Z2 +
     1   XYZ4*C3  + C(4,4)  - G4*Z2
       G6= XYZ1*D3 +J4*D3 +XYZ2*D3 + XYZ3*C(1,5) +J3*M2 +XYZ4*D3
     1   + C(4,5)   -G4*M2
       G7= XYZ1*E3  + J4*E3  + XYZ2*E3  + XYZ3*C(1,6) + J3*P2
     1    + XYZ4*E3   + C(4,6)   - G4*P2
       G8=  XYZ1*F3 + J4*F3 +XYZ2*F3 + XYZ3*C(1,7) + J3*Q2 +
     1   XYZ4*F3  +C(4,7)   - G4*Q2
       PRINT RESULTS     G,G6,G7,G8
        YY= T(4) - XYZ
       K1= C(5,1)*C(1,2)/(C(1,1)*X2  )
       K=   C(5,1)/C(1,1)
       K3= C(5,2)/X2
       PRINT RESULTS     YY,K1,K,K3
       K4= C(5,4)/G
       B5 = K*T(1) - K1*Y- K*C(1,4)*YY/G  +Y*K3  +YY*K4
       B6= -K1*Y2  -K*C(1,3) +C(5,3) + Y2*K3
```

```
      B7= -K1*Z2    +K3*Z2
      PRINT RESULTS     K4,B5,B6,B7
      B8= -K1*W2 +K*C(1,4)*G6/G -K*C(1,5)+ K3*W2 -K4*G6 + C(5,5)
      B9= -K1*P2+K*C(1,4)*G7/G -K*C(1,6) +K3*P2 -K4*G7 + C(5,6)
      BZ= -K1*QZ +K*C(1,4)*G8/G - K*C(1,7) +K3*QZ-K4*G8+C(5,7)
      D= B6/X3
      PRINT RESULTS      B8,B9,BZ, D
      D2=    B7/G
      D1= B6*C3/(X3*G)
      D4= B5 +D*B3 +D1*YY + YY*D2
      D5 =-G6*D1 + D*D3 -D2*G6 +B8
      D6= -D1*G7 -D2 *G7 +D*E3 + B9
       PRINT RESULTS  D2,D1,D4,D5,D6
      B8= C(6,1)/C(1,1)
      B81= -B8*C( 1,2)/X2
      D7= -D1*G8 +D*F3 -G8*D2   + B2
      B82= B81* Y2/X3
      PRINT RESULTS      B81,D7,B82,B8
      B83=  -B81* C(1,3)/X3
        B84=  C(6,2)  /X2
      B85=  B84*Y2/X3
      B86= C(6,3)/X3
      PRINT RESULTS      B83,B84,B85,B86
      CC1= B8*T(1) + B81*Y +B82*B3+B83*B3 +B84*Y +B85*B3 +B86*B3
      CC2= B82*C3 +B81*Z2 +B83*C3+ B85*C3 - B81*C(1,4) +B84*Z2
     1+    B86* C3    +C(6,4)
      CC3=  B82*D3  + B81*W2  +B83*D3 -B81*C(1,5) + B85*D3 + B84*W2
     1     +B86*D3     + C(6,5)
      CC4= B82*E3  +B81*P2 +B83*E3 -B81*C(1,6) +B85*E3 +B84*P2
     1    +B86*E3  +C(6,6)
      PRINT RESULTS      CC1,CC2,CC3,CC4
      CC5= B82*F3 +B81*Q2 + B83*F3 -B81*C(1,7) + B85*F3 +B84*Q2
     1     +B86*F3    +C(6,7)
      CC6=  CC2/G
      CC9= -CC6*G6   + CC3
      CC7= -CC6*G7    +CC4
      PRINT RESULTS      CC5,CC6,CC7,CC9
      CC8= -CC6*G8    +CC5
      DD1=  CC9/ D5
      DD2=    T(6)-CC1 - CC6*YY-DD1*(T(5)-D4)
      DD3= -DD1*D6    +CC7
      PRINT RESULTS      CC8,DD1,DD2,DD4
      DD4= -DD1*D7     +CC8
      DD8=  C(7,1)/C(1,1)
      DD5= - C(7,1)*C(1,2)/(C(1,1)*X2)
      DD6= DD5*Y2/X3
      PRINT RESULTS      DD4,DD8,DD5,DD6
      DD7= -C(7,1)*C(1,3)/(C(1,1)*X3)
      EE= C(7,2)/X2
      DD9= C(7,2)*Y2/(X2*X3)
      EE1= C(7,3)/X3
      PRINT RESULTS      DD7,EE,DD9,EE1
      EE2 =  DD8*T(1) +DD5*Y + DD6*B3+ DD7*B3 + EE*Y + DD9*B3
     1+ EE1*B3
      EE3=  DD6*C3 + DD5*Z2 +DD7*C3 -DD8*C(1,4)+ EE*Z2  +EE1*C3
     1     +DD9*C3    +C( 7,4)
      EE4= DD6*D3  +DD5 *W2 +DD7*D3 -DD8*C(1,5) + EE1*D3  +C(7,5)
     1     +DD9*D3     +EE*W2
```

```
      EE5= DD6*E3 +DD5*P2 +DD7*E3-DD8*C(1,6) + DD9*E3 +EE*P2
     1  +EE1*E3     + C(7,6)
      PRINT RESULTS    EE2,EE3,EE4,EE5
      EE6= DD6*F3  +DD5*Q2 +DD7*F3 -DD8*C(1,7) +DD9*F3  +EE*Q2
     1    ++ EE1*F3  +C(7,7)
      EE7= EE3/G
      EE8= -EE7*G6/D5
      EE9= EE4/D5
      PRINT RESULTS     EE6,EE7,EE8,EE9
      FF = EE2 + EE7*YY +EE8*T(5) -     EE8*D4  + EE9*T(5) -EE9*D4
      FF1= -EE8*D6 -EE7*G7 -EE9*D6  + EE5
      FF2= -EE8*D7 - EE7*G8  -EE9*D7     + EE6
      PRINT RESULTS     FF,FF1,FF2
      A7 = (T(7)-FF-FF1*DD2/DD3)/ (FF2-FF1*DD4/DD3)
      A6= (DD2- DD4*A7)/DD3
      A5= (T(5) -D4 -D6*A6 - D7*A7)  /D5
      A4= ( YY       -G6*A5- G7*A6     - G8*A7)  /G
      A3=   (B3 +C3*A4 + D3*A5 + E3*A6 + F3*A7)  /X3
      A2=  (Y + A3*Y2 +A4*Z2 +A5*H2  +A6*P2 + A7*Q2)  /X2
      A1=  (T(1) -C(1,2)*A2 -C(1,3)*A3 -C(1,4)*A4 - C(1,5)*A5
     1    -C(1,6)*A6  -C(1,7)*A7 )         /C(1,1)
      AA(1)= A1
      AA(2) = A2
      AA(3)= A3
      AA(4)= A4
      AA(5)= A5
      AA(6)= A6
      AA(7)= A7
      PRINT RESULTS     AA(1),...,AA(7)
      THROUGH CHECK, FOR JJJ= 1,1,JJJ.G.7
      TRIAL = 0.0
      THROUGH ADD,    FORKKK=1,1, KKK.G.7
      TRIAL = TRIAL + C(JJJ, KKK)*        AA(KKK)
ADD   CONTINUE
      ERROR(JJJ) = TRIAL - T(      JJJ)
      PRINT RESULTS   ERROR(JJJ)
CHECK  CONTINUE
R    ERROR(J) ARE ZERO IF THE SOLUUION IS EXACT
R  LOOP TO Q100 COMPUTES THE G(J)
      THROUGH Q100, FOR J=1,1,J.G.7
      ZUM =0.0
      THROUGH Q90, FOR I=1,1,I.G.7
      ZUM = ZUM - AA(I)/( R(J) + R(I) )
Q90   CONTINUE
      G(J) = ZUM
Q100  CONTINUE
      PRINT RESULTS     G(1),...,G(7)
R NOW TO COMPUTE THE AUTOCOVARIANCE FN
R LOOP TO Q160 VARIES THE TIME, WHICH HAS BEEN READ IN
      THROUGH Q160, FOR J=1,1,J.G. JTIME
      ZUMT = 0.0
      THROUGH Q150, FOR I=1,1,I.G.7
      PIECE(I)= AA(I)*      G(I)*EXP.(R(I)*TT(J))  /FIRST
      ZUMT = ZUMT+  PIECE(I)
Q150  CONTINUE
       COR= ZUMT
      WHENEVER(TT(J)-0.0009) .GE     .0.0, TRANSFER TO Q157
      FIRST = COR
```

```
0157        PRINT FORMAT ANS, CORR,TTT(J)
            VECTOR VALUES ANS =S 33HO THE AUTOCORRELATION FUNCTION IS
           I EZU.8, IZH  AT TIME =    F10.4, 10H  SECONDS    =S
0160        CONTINUE
            TRANSFER TO 01
            END OF PROGRAM
```

```
$  COMPILE MAD, PRINT OBJECT, PUNCH OBJECT, EXECUTE, DUMP, I/O DUMP
          R  PROGRAM NAME IS TWO GROUP
          R  THE TWO GROUP PARAMETERS ARE CALCULATED FROM THE 6 GROUP
          R  DATA USING THE TECHNIQUE OF SKINNER  AND COHEN, NS AND E
          R   5,1959.
          R   NOTATION
          R   D(J) = LAMBDA(J)
          R   BETA(J) = BETA(J)
           DIMENSION      AB(10), BETA(6), D(6)
           INTEGER        J
GO         PRINT FORMAT COMET
           VECTOR VALUES COMET  = $29H1 PROGRAM NAME IS TWO GROUP     *$
           READ FORMAT INPUT, D(1),,,D(6), BETA(1),,,BETA(6)
           VECTOR VALUES INPUT =$ 6F10.5/6F10.7  *$
           PRINT FORMAT INPUTA ,D(1),,,D(6),BETA(1),,,BETA(6)
           VECTOR VALUES INPUTA =$14H LAMBDAS ARE    6F10.5/12H BETAS AR
          1E    6F10.7   *$
           ALPH2 = 0.0
           ALP1 = 0.0
           ALPH1 = 0.0
           BETAS = 0.0
           THROUGH LOOP1, FOR J=1,1,J.G.6
LOOP1      BETAS = BETAS + BETA(J)
           THROUGH LOOP2, FOR J=1,1,J.G.6
           AB(J) = BETA(J) /BETAS
           ALP1 = ALP1  + AB(J)*D(J)
           ALPH1 = ALPH1 + AB(J)/D(J)
           ALPH2 = ALPH2 + AB(J)/(D(J)*D(J))
LOOP2      CONTINUE
           PRINT RESULTS ALP1, ALPH1, ALPH2
           B = (ALP1*ALPH2  - ALPH1)/(2.0*(ALPH2-ALPH1*ALPH1))
           C = (ALP1*ALPH1  -1.0)/(ALPH2 - ALP*1*ALPH1)
           ROOT = SQRT.(B*B-C)
          R   LAMB1 AND LAMB2 ARE THE 2 GROUP LAMBDAS
            LAMB1=   B- ROOT
           LAMB2=  B+ROOT
           INNER = (ALPH1*C-B)/ROOT
          R   A1 AND A2 ARE THE RELATIVE ABUNDANCES OF THE FIRST AND
          R   SECOND  DELAY GROUPS
           A1 = 0.5*(1.0 + INNER)
           A2= 0.5*(1.0-INNER)
           PRINT RESULTS  A1, A2
          R   BET1 AND BET2 ARE THE EFFECTIVE TWO GROUP BETAS
           BET1 = A1*BETAS
           BET2 = A2*BETAS
           PRINT FORMAT RESULT, LAMB1,LAMB2,BET1,BET2
           VECTOR VALUES RESULT =$ 24H TWO GROUP LAMBDAS ARE    2E20.8/
          1  22H TWO GROUP BETAS ARE    2E20.8  *$
           TRANSFER TO GO
           END OF PROGRAM
```

```
$  COMPILE MAD, PRINT OBJECT, PUNCH OBJECT, EXECUTE, DUMP, I/O DUMP
R    PROGRAM COMPUTES THE A(1)...A(3) USED TO COMPUTE THE
R    THE AUTOCORRELATION FUNCTION IN CORR7
R    THE BETA(1) AND BETA(2) READ IN AS DATA ARE THE RELATIVE
R    ABUNDANCES NOT THE REAL BETAS
R  BETAT = SUM OF BETA(J) FOR J=1,6
OK    PRINT FORMAT NAME
      VECTOR VALUES NAME =$ 43HI PROGRAM NAME IS TWO GROUP COEFFECI
     1ENTS        *$
      READ FORMAT DATA,GEN, TAU, POP, D(1), D(2),BETA(1), BETA(2),
     1  R(1), R(2), R(3)    , BETAT
      VECTOR VALUES DATA =$ 3F15.8/2F10.5  /2F10.7 /3F10.5/F10.7*$
      PRINT FORMAT DATB ,GEN, TAU, POP, D(1), D(2), BETA(1), BETA(2
     1)         , R(1), R(2), R(3)
      VECTOR VALUES DATB =$17H K EFFECTIVE =      F15.8,14H LIFETIM
     1E =      F15.8, 19H NEUTRON LEVEL =      F15.8/
     2  13H LAMBDAS =      2F10.5/ 20H RELATIVE BETAS =      2F10.7
     3 /21H ROOTS OF INHOUR =      3F10.5    *$
R CALCULATE THE REAL PART OF THE TRANSFER FN FOR FREQS = -ROOT
R   S OF INHOUR
      BETA(1)= BETAT*BETA(1)
      BETA(2)= BETAT*BETA(2)
      PRINT RESULTS   BETA(1),BETA(2)
      CM = GEN/TAU
      CT = (1.0- GEN)/TAU
      W = -R(1)
      THROUGH REAL, FOR I=1,1,I.G.3
      BO(I)= 0.0
      CO = 0.0
      SNAP = 0.0
      WW = W*W
      THROUGH PART, FOR J =2,1,J.G.3
      ITT = J-1
      SNAP = BETA(ITT)/(WW+ D(ITT)*D(ITT) )
      BO(J) = BO(ITT) + SNAP
      CO = CO + SNAP*D(ITT)
PART  CONTINUE
      TIT)= POP/TAU * (1.0- WW*BO(3)) *(CT + CM*WW*BO(3)) *
     1WW*CO*( 1.0+      CM*CO)) /((  CT + CM*WW*BO(3))* (CT+CM*
     2 WW*BO(3))   +WW*(1.0 + CM*CO)  *(1.0+ CM*CO))
      PRINT RESULTS T(1)
      W = - R(I+1)
REAL   CONTINUE
R  CALCULATE COEFFS OF THE UNKNOWNS
      THROUGH COOF, FOR I=1,1,I.G.3
      THROUGH COOF, FOR J=1,1,J.G.3
      C(I,J)=  -R(J)/(R(J)*R(J) + R(I)*R(I)  )
      PRINT RESULTS C(I,J)
COOF  CONTINUE
      INTEGER I,J,TYPE
      DIMENSION    D(2), BETA(2), R(3), C(9,TYPE),BO(3), A(3) ,
     1       ERROR(3)      ,T(3)
       VECTOR VALUES TYPE = 2,1,3
R  SOLVE FOR THE UNKNOWNS DIRECTLY TO GET
       D= 1.0/C(1,1)
       E= C(1,2)/C(1,1)
      F= C(1,3)/C(1,1)
      G= C(2,1)*E  -C(2,2)
        H= C(2,1)*D
```

```
      JJ=     C(2,I)*F
    M= C(3,1)*D*T(1)
     K= (C(3,2) - E*C(3,1) )/G
     N= -T(2) + M*T(1)
     DIV=  C(3,1)*F  -C(3,3)  + K*JJ - K*C(2,3)
     A(3) = (-T(3)  + M+K*N)  /DIV
      A(2)=       ( -T(2)  +     H*T(1)  -JJ*A(3)+ C(2,3)*A(3))/G
     A(1)=       D*T(1)  - A(2)*E  - A(3)*F
    PRINT RESULTS   A(1), A(2), A(3)
     SOME = 0.0
       THROUGH CHEC1, FOR I=1,1,I.G.3
       THROUGH CHEC2, FOR J=1,1,J.G.3
      SOME = C(I,J)*A(J)  + SOME
CHEC2 CONTINUE
     ERROR(I)= SOME - T(I)
     SOME = 0.0
CHEC1 CONTINUE
     PRINT RESULTS ERROR(1)...ERROR(4)
   R   ERROR(J) ARE ZERO IF THE SOLUTION IS EXACT
     TRANSFER TO OK
    END OF PROGRAM
```

```
$ COMPILE MAP, PRINT OBJECT, PUNCH OBJECT, EXECUTE, DUMP, I/O DUMP
      R  PROGRAM NAME IS CORRELATION 7
      R  FOR TWO DELAY GROUPS, PROGRAM COMPUTES THE AUTOCORRELATION
      R       FN.  THE AA(J) FOUND BY SETTING THE REAL PART OF THE IN
      R  ANSPER FN TO THE USUAL SUM AND SOLVING EXPLICITLY FOR THE
      R   AA(J), J=1,3  ARE READ IN AS DATA.  THE AA(J) ARE COMPUTED
      R  IN THE PROGRAM CALLED TWO GROUP COEFFS
      R  THE FIRST TIME READ IN AS DATA SHOULD BE ZERO
      READ FORMAT TAP,JTIME,    TT(1),...,TT(JTIME)
      VECTOR VALUES TAP=$   I3/(7F10.4   )  $$
01    READ FORMAT DATA, AA(1),...,AA(3), R(1),...,R(3),GEN,TAU,POP
     1     , BETAT
      VECTOR VALUES DATA=$  3E20.8/3F10./3F10.6/F10.6  $$
      DIMENSION   R(10), YY(200), G(10), PIECE(10),Y(10), AA(10)
      INTEGER  I, J, JTIME
      PRINT FORMAT YAPP
      VECTOR VALUES YAPP=$ 33H1 PROGRAM NAME IS CORRELATION 7   $$
       PRINT RESULTS    GEN, TAU, BETAT
      PRINT RESULTS   AA(1),...,AA(3)
      PRINT RESULTS   R(1),...,R(3)
      FIRST = 1.0
      R  LOOP TO 0100 COMPUTES THE G(J)
      THROUGH 0100, FOR J=1,1,J.G.3
      ZUM =0.0
      THROUGH 090, FOR I=1,1,I.G.3
      ZUM = ZUM + AA(I)/( R(J) + R(I) )
090   CONTINUE
      G(J) = ZUM
0100  CONTINUE
      PRINT RESULTS    G(1),...,G(3)
      R NOW TO COMPUTE THE AUTOCOVARIANCE FN
      R LOOP TO 0150 VARIES THE TIME, WHICH HAS BEEN READ IN
      THROUGH 0160, FOR J=1,1,J.G. JTIME
      ZUMT = 0.0
      THROUGH 0150, FOR I=1,1,I.G.3
      PIECE(I)= AA(I)*     G(I)*EXP.(R(I)*TT(J))   /FIRST
      ZUMT = ZUMT+  PIECE(I)
0150  CONTINUE
       COR= ZUMT
      WHENEVER(TT(J)=0.0000) ,OR     .0.0, TRANSFER TO 0157
      FIRST = COR
0157  PRINT FORMAT ANS, COR,TT(J)
      VECTOR VALUES ANS =$ 33HO THE AUTOCORRELATION FUNCTION IS
     1 E20.8, 12H  AT TIME =     F10.4, 10H  SECONDS    $$
0160  CONTINUE
      TRANSFER TO 01
      END OF PROGRAM
```

```
$  COMPILE MAD, PRINT OBJECT, PUNCH OBJECT, EXECUTE, DUMP, I/O DUMP
R  PROGRAM NAME IS TRANSFER 6.  GIVES THE TRANSFER FUNCTION
R  IN DECIBELS NORMALIZED TO FREQ(1) IN CPS
R  OTHER FREQUENCIES READ IN    AS DATA IN THE FORM
R  FREQ(2)...FREQ(NTOP), CYCLES PER SECOND
R   ALSO COMPUTES A POWER SPECTRAL DENSITY FN, PSD, NORMALIZED
R  AT FREQ(1)
 DIMENSION    BETA(10),D(10),BO(10), PART(300) ,
2   TRANS(300), DECIB(300)   ,FREQ(300)
 INTEGER   NTOP, J, I
START
 PRINT FORMAT NAME
 VECTOR VALUES NAME =$  28HI PROGRAM NAME IS TRANSFER6      *$
 READ FORMAT DATA          ,GEN,TAU,D(1)...D(6), BETA(1)...
2  BETA(6), NTOP, FREQ(1)...FREQ(NTOP)
 VECTOR VALUES DATA =$ 2F10.7/6F10.5/6F10.7/13/(6F10.4)*$
 PRINT FORMAT DATB,  GEN,TAU,D(1)...D(6),BETA(1)...BETA(6),
2   FREQ(1)
 VECTOR VALUES DATB =$ 26HO MULTIPLICATION FACTOR =   F10.7,15
2H    LIFETIME =   E10.3/11H LAMBDAS =   6F10.5/9H BETAS =
3  6F10.7/32H NORMALIZING FREQUENCY (CPS) =     F10.4*$
 CM = GEN/TAU
 CT = (1.0-GEN)/TAU
 PRINT FORMAT ANS
 VECTOR VALUES ANS =$ 18HO FREQUENCY(CPS)     , 21H
2DECIBELS      *$
 THROUGH LOOP, FOR J=1,1,J.G.NTOP
 W = 2.0*3.14159265*FREQ(J)
 WW = W*W
 BO(0) = 0.0
 SNAP = 0.0
 CO = 0.0
 THROUGH CALC , FOR I=1,1,I.G.6
 SNAP = BETA(I)/(WW + D(I)*D(I))
 BO(I) = BO(I-1)  + SNAP
CALC
 CO = CO +  SNAP*D(I)
 B = WW*BO(6)
 C = W*CO
 PART(J) =  ( (1.0-B)/TAU *(1.0-B)/TAU +C*C/(TAU*TAU))
2  /(  (CT+CM*B)*(CT +CM*B)  +(W+CM*C)*(W+CM*C)  )
 TRANS(J) = SQRT.(PART(J))
 PRINT RESULTS    B,C,PART(J),TRANS(J)
 DECIB(J) = 20.0*ELOG.(TRANS(J)/TRANS(1)) /2.303
 PRINT FORMAT RESULT, FREQ(J), DECIB(J)
 VECTOR VALUES RESULT =$F12.4,$18,E20.8 *$
  PSD = PART(J)/PART(1)
  PRINT RESULTS     PSD
  BBB=  W*CO
  AAA= 1.0-  WW*BO(6)
   CCC=  CT+  CM*WW*BO(6)
   DDD=  W + CM*W*CO
  PHASE=  ATAN.( -(BBB*CCC + AAA*DDD)/(AAA*CCC-BBB*DDD) )
  PHASE = PHASE*180.0/ 3.14159265
 PRINT RESULTS   PHASE
LOOP
 CONTINUE
 TRANSFER TO START
 END OF PROGRAM
```